

AD-A074 571

AEROJET LIQUID ROCKET CO SACRAMENTO CA
JEFF(A) MIXED-FLOW MODEL FAN PERFORMANCE OPTIMIZATION.(U)
JUN 79 S A LORENC

F/G 13/10

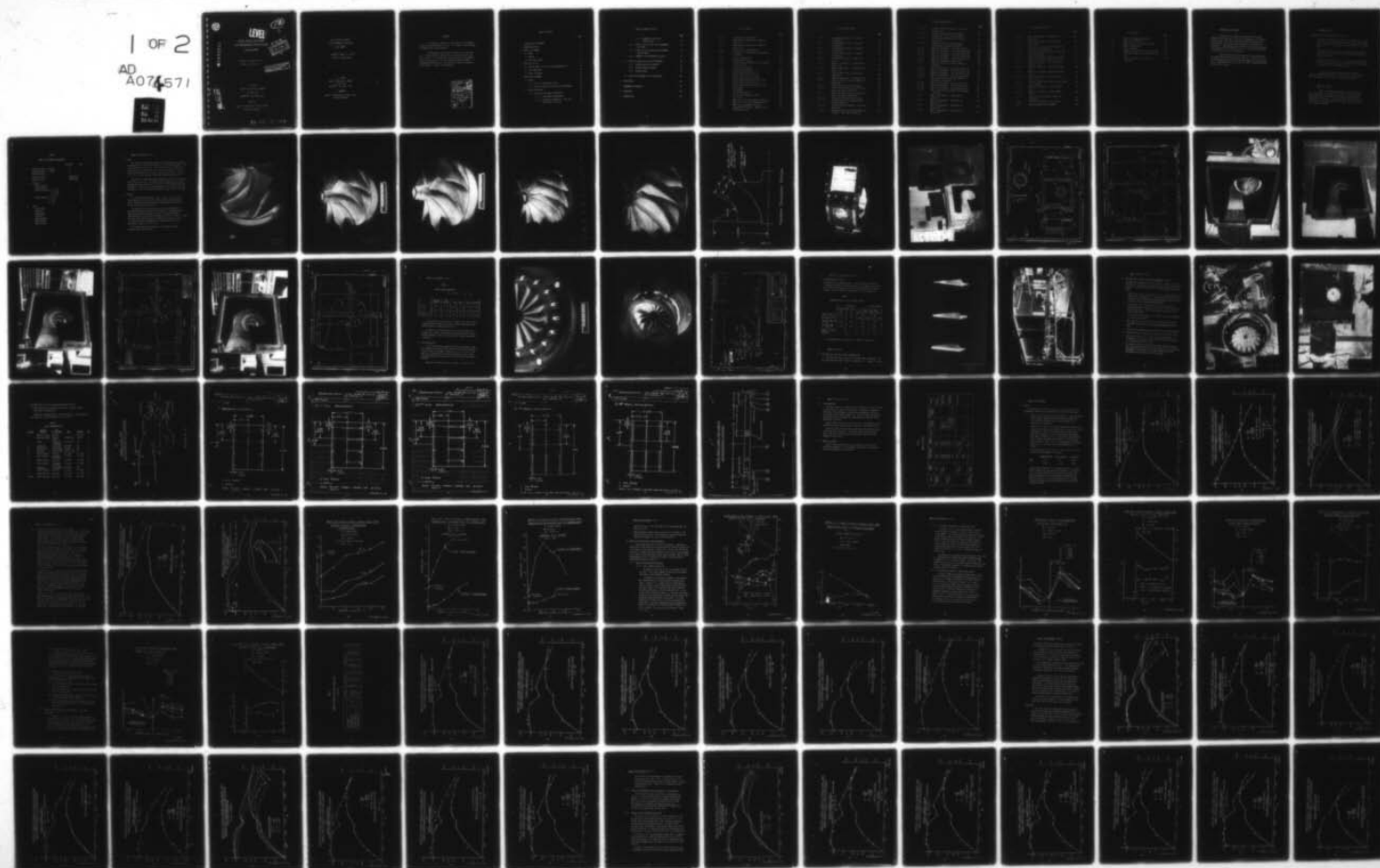
UNCLASSIFIED ALRC-FD9630-001

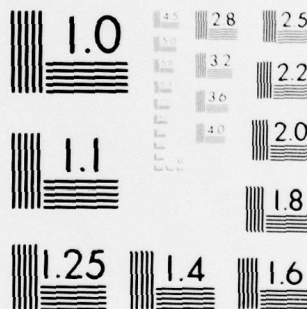
N00014-78-C-0441

NL

1 OF 2

AD
A074571





MICROCOPY RESOLUTION TEST CHART
NATIONAL BUREAU OF STANDARDS-1963-A



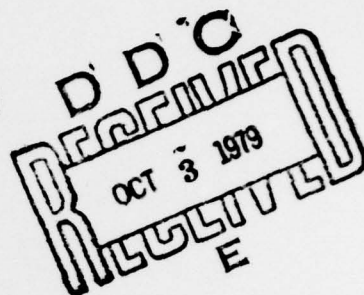
AD A074571

LEVEL

12

5

JEFF(A) MIXED-FLOW MODEL
FAN PERFORMANCE OPTIMIZATION
FINAL REPORT



CONTRACT: N00014-78-C-0441

REPORT NO. FD:9630:001

This document has been approved
for public release and sale; its
distribution is unlimited.

DDC FILE COPY

S. A. LORENC
AEROJET LIQUID ROCKET COMPANY
P.O. BOX 13222
SACRAMENTO, CALIFORNIA 95813

JUNE 1979

DAVID W. TAYLOR NAVAL SHIP R&D CENTER
BETHESDA, MARYLAND

79 09 17 009

6 JEFF(A) MIXED-FLOW MODEL
FAN PERFORMANCE OPTIMIZATION

9 FINAL REPORT

15 CONTRACT: N00014-78-C-0441

REPORT NO. FD-9630-001

14 ALRC-FD9630-001

10 S. A. LORENC
AEROJET LIQUID ROCKET COMPANY
P.O. BOX 13222
SACRAMENTO, CALIFORNIA 95813

12 120

11 JUNE 1979
DAVID W. TAYLOR NAVAL SHIP R&D CENTER
BETHESDA, MARYLAND

405 880

jos

FOREWORD

This report is submitted in fulfillment of the Statement of Work in Contract N00014-78-C-0441. The Technical Project Manager at DTNSRDC was Mr. George Wachnik.

The Aerodynamic Design and Data Analysis were performed by S. A. Lorenc who also prepared this report under the direction of K. G. Kirk. S. R. Finato was responsible for the Test Hardware Design and Procurement. He also performed the Model assembly, Instrumentation and Testing. The program was under the cognizance of Mr. Werner P. Luscher, Program Manager.

Accession For	
NTIS Grant	
DOC TAB	
Unannounced	
Justification <i>for the</i>	
<i>on file</i>	
By	
Distribution/	
Availability Codes	
Dist	Avail and/or special
<i>A</i>	

TABLE OF CONTENTS

	<u>PAGE</u>
1. INTRODUCTION AND SUMMARY	1
2. PROGRAM OBJECTIVES	2
3. MODEL TEST HARDWARE	3
3.1 ROTOR	4
3.2 HOUSING	4
3.3 INLET GUIDE VANES	5
4. MODEL TEST SET UP	25
4.1 DESCRIPTION OF TEST SET UP AND INSTRUMENTATION	28
4.2 TEST CONDITIONS	30
4.3 MODEL TEST MATRIX	39
5. MODEL FAN PERFORMANCE	41
5.1 ROTOR	41
5.1.1 EFFECT OF ROTOR BLADE LENGTH	41
5.1.2 EFFECT OF ROTOR EXIT WIDTH ON FAN PERFORMANCE	45
5.2 INLET GUIDE VANES	51
5.2.1 HUB-TO-TIP PRE WHIRL DISTRIBUTION	51
5.2.1.1 ROTOR INDUCED PREROTATION	51
5.2.1.2 PRE WHIRL DISTRIBUTION - FLAT IGV'S, IGV SETTING = 0° & $+20^{\circ}$	54

TABLE OF CONTENTS (CONT'D)

	<u>PAGE</u>
5.2.1.3 SUMMARY OF ROTOR INLET TRAVERSE DATA	54
5.2.2 EFFECT OF IGV SETTING ON FAN PERFORMANCE - FLAT VANES	59
5.2.3 EFFECT OF IGV SETTING ON FAN PERFORMANCE - TWISTED VANES	79
5.2.4 SUMMARY OF FAN PERFORMANCE WITH IGV'S	79
5.3 EFFECT OF HOUSING SIZE ON FAN PERFORMANCE	92
5.3.1 HOUSING AXIAL WIDTH INCREASE	92
5.3.2 HOUSING DIAMETER INCREASE	97
5.3.3 PLENUM HOUSING	97
5.4 PREDICTED PERFORMANCE OF THE OPTIMUM FAN	100
6. CONCLUSIONS	106
7. RECOMMENDED OPTIMUM FAN	107
8. REFERENCES	108
9. NOMENCLATURE	109

LIST OF FIGURES

		<u>PAGE</u>
3.1-1	Photograph of 8 Bladed Rotor	5
3.1-2	Photograph of 8 Bladed Rotor, Blade Cut- Back 0.5 IN	6
3.1-3	Photograph of 8 Bladed Rotor, Blade Cut- Back 1.0 IN	7
3.1-4	Photograph of 11 Bladed Rotor	8
3.1-5	Photograph of 11 Bladed Rotor Having Narrow Exit Width	9
3.1-6	Sketch of Narrow Rotor	10
3.2-1	Baseline Model Housing	11
3.2-2	Plenum Housing and Reference Volute Housing (A=13.6, B=5.58)	12
3.2-3	Plenum Housing Drawing	13
3.2-4	Reference Volute Housing	14
3.2-5	Volute Housing (A=13.6, B=6.67)	15
3.2-6	Volute Housing (A=13.6, B=7.76)	16
3.2-7	Volute Housing (A=15.10, B=5.58)	17
3.2-8	Volute Housing Drawing (A=15.10, B=5.58)	18
3.2-9	Volute Housing (A=16.60, B=5.58)	19
3.2-10	Volute Housing Drawing (A=16.60, B=5.58)	20
3.3-1	IGV Assembly	22
3.3-2	IGV Assembly	23
3.3-3	IGV Assembly Drawing	24
3.3-4	Inlet Vane Configurations Tested	26
4.1-1	Test Set Up	27
4.1-2	Model Fan on Test Stand (Baseline Housing)	29
4.1-3	Model Fan on Test Stand (Plenum Housing)	30
4.1-4	Model Fan Instrumentation Location	32
4.1-5	Instrumentation Location - Model Fan Exit (Reference Housing)	33

LIST OF FIGURES (CONT'D)

		<u>PAGE</u>
4.1-6	Instrumentation Location - 1st Axial Configuration	34
4.1-7	Instrumentation Location - 2nd Axial Configuration	35
4.1-8	Instrumentation Location - 1st Radial Configuration	36
4.1-9	Instrumentation Location - 2nd Radial Configuration	37
4.1-10	Instrumentation Location - Model Test Set Up	38
5.1.1-1	Model Fan Performance - Leading Edge Cut Back 0.5 IN	42
5.1.1-2	Model Fan Performance - Leading Edge Cut Back 1.0 IN	43
5.1.1-3	Effect of Rotor Blade Cut Back on Fan Performance	44
5.1.2-1	Model Fan Performance - Narrow Rotor Exit	46
5.1.2-2	Effect of Rotor Exit Width on Model Fan Performance	47
5.1.2-3	Shroud Static Pressure Distribution	48
5.1.2-4	Static and Total Pressure Distribution at Rotor Exit, $\phi=0.42$, $N=6000$ rpm	49
5.1.2-5	Static and Total Pressure Distribution at Rotor Exit, $\phi=0.25$, $N=6000$ rpm	50
5.2.1.1-1	Rotor Inlet Flow Angles Distribution	52
5.2.1.1-2	Average Pre-whirl and Incidence Angles vs Flow Coefficient	53
5.2.1.2-1	Pre-whirl Angle Distribution - Thick IGV's Position 0°	55
5.2.1.2-2	Average Pre-whirl and Incidence Angles Distribution - Thick IGV's Position 0°	56

LIST OF FIGURES (CONT'D)

		<u>PAGE</u>
5.2.1.3-1	Pre-whirl Angle Distribution - Thick IGV's Position $+20^{\circ}$	57
5.2.1.3-2	Average Pre-whirl and Incidence Angles Distribution - Thick IGV's Position $+20^{\circ}$	58
5.2.1.4-1	Pre-whirl Angle Distribution - Thin IGV's Position 0°	60
5.2.1.4-2	Average Pre-whirl and Incidence Angles Distribution - Thin IGV's Position 0°	61
5.2.2-1	Model Fan Performance - Thick IGV Setting 0°	63
5.2.2-2	Model Fan Performance - Thick IGV Setting $+10^{\circ}$	64
5.2.2-3	Model Fan Performance - Thick IGV Setting $+20^{\circ}$	65
5.2.2-4	Model Fan Performance - Thick IGV Setting $+30^{\circ}$	66
5.2.2-5	Model Fan Performance - Thick IGV Setting $+40^{\circ}$	67
5.2.2-6	Model Fan Performance - Without IGV's	68
5.2.2-7	Effect of Positive IGV Setting on Model Fan Performance	70
5.2.2-8	Model Fan Performance - Thick IGV Setting -10°	71
5.2.2-9	Model Fan Performance - Thick IGV Setting -20°	72
5.2.2-10	Model Fan Performance - Thick IGV Setting -30°	73
5.2.2-11	Model Fan Performance - Thick IGV Setting -40°	74
5.2.2-12	Effect of Negative IGV Setting on Model Fan Performance - Thick Vanes	75
5.2.2-13	Model Fan Performance - Thin IGV Setting 0°	76
5.2.2-14	Model Fan Performance - Thin IGV Setting -20°	77
5.2.2-15	Model Fan Performance - Thin IGV Setting $+20^{\circ}$	78
5.2.2-16	Effect of IGV Setting on Model Fan Performance - Thin Vanes	80
5.2.3-1	Model Fan Performance - Twisted IGV Tip Setting 0°	81
5.2.3-2	Model Fan Performance - Twisted IGV Tip Setting $+10^{\circ}$	82
5.2.3-3	Model Fan Performance - Twisted IGV Tip Setting $+20^{\circ}$	83
5.2.3-4	Model Fan Performance - Twisted IGV Tip Setting $+30^{\circ}$	84

LIST OF FIGURES (CONT'D)

		PAGE
5.2.3-5	Model Fan Performance - Twisted IGV Tip Setting $+40^{\circ}$	85
5.2.3-6	Model Fan Performance - Twisted IGV Tip Setting $+50^{\circ}$	86
5.2.3-7	Effect of Positive IGV Setting of Model Fan Performance - Twisted Vanes	87
5.2.4-1	Model Fan Performance Comparison - Thick and Thin IGV Setting 0°	88
5.2.4-2	Model Fan Performance Comparison - Flat IGV Setting $+20^{\circ}$, Twisted IGV Tip Setting $+30^{\circ}$	89
5.3.1-1	Model Fan Performance - Reference Housing (B=5.58, A=13.6)	93
5.3.1-2	Model Fan Performance - Housing Axial Width B=6.67	94
5.3.1-3	Model Fan Performance - Housing Axial Width B=7.76	95
5.3.1-4	Model Fan Performance - Baseline Housing (B=5.58, A=13.6)	96
5.3.1-5	Effect of Housing Axial Width Increase on Model Fan Performance	98
5.3.2-1	Model Fan Performance - Housing Diameter A=15.1	99
5.3.2-2	Model Fan Performance - Housing Diameter A=16.6	100
5.3.2-3	Effect of Housing Diameter on Model Fan Performance	101
5.3.3-1	Model Fan Performance - Plenum Housing	103
5.4-1	Predicted Optimum Fan Performance	105

LIST OF TABLES

		<u>PAGE</u>
1	Model Test Hardware Requirements	3
2	Model Housing Dimensions	21
3	Characteristics of Inlet Vanes Tested	25
4	Model Instrumentation	31
5	Model Test Matrix	40
6	Summary of Model Rotor Inlet Traverse Data	62
7	Performance Comparison of Flat and Twisted IGV's	90
8	Effect of Housing Size on Model Fan Performance	102

1. INTRODUCTION AND SUMMARY

→ This Model Test Program was conducted under Contract N00014-78-C-0441 in order to improve the performance of the JEFF(A) Mixed-Flow Fan. Both rotor and housing changes were made to the existing model fan and tests were conducted in the ALRC Physics Laboratory. Rotor modifications consisted of varying blade length and narrowing the rotor width at the exit. Housing size was varied by changing axial and radial dimensions.

The sensitivity of fan performance to IGV positioning was also determined for both flat and twisted vanes. Finally, full size fan performance was predicted for the best combination of housing and rotor. Recommendations are also made for further improvement of the Mixed-Flow Fan concept. ↗

2. PROGRAM OBJECTIVES

The objectives of this program were as follows:

1. To improve performance of the previously demonstrated 1/6 scale Mixed-Flow Lift Fan Model to meet the Lift Systems Requirements and to be capable of absorbing the total available TF-40 Engine Power.
2. To evaluate the effect of fan housing modifications and rotor modifications on the Model Fan performance within the vehicle envelope constraints.
3. To evaluate the effectiveness of inlet guide vanes to increase the fan airflow capability above the baseline configuration and to improve the craft seakeeping capability.

These objectives were accomplished by modifying an existing mixed flow model rotor and baseline housing and conducting tests according to the test matrix discussed in this report.

3. MODEL TEST HARDWARE

Model test hardware requirements are listed in Table 1. The existing model fan components were used to the fullest extent possible and the new components were designed in house and sub-contracted for fabrication. The fan test setup did not require any modifications or additions other than the check out and calibration of all recording equipment.

TABLE 1

MODEL TEST HARDWARE REQUIREMENTS

		<u>EXISTING</u>	<u>NEW</u>
1.	Mixed-Flow Rotor - 8 Blades	X	
	Mixed-Flow Rotor - 11 Blades	X	
	Matching Shroud	X	
2.	Narrow Exit Rotor	X(Modified)	
	Matching Shroud	X(Modified)	
3.	Housing		
	Baseline Volute	X	
	Plenum Chamber		X
	Volute Axial Width B = 5.583		X
	B = 6.673		X
	B = 7.763		X
	Volute Diameter A = 13.6		X
	A = 15.1		X
	A = 16.6		X
4.	IGV's		
	Airfoil Vanes	X	
	Thin Vanes		X
	Twisted Vanes		X
	Inlet Bell		X
	Housing Adapter		X
	Shaft Spinner		X
	Shaft Tie Bolt		X

3. MODEL TEST HARDWARE (cont'd)

3.1 Rotor

The effect of rotor blade length on fan performance was evaluated by cutting back the blade leading edges on the eight bladed rotor. This was accomplished in two steps. First, the blade axial length was reduced by 0.5 in. and then by 1.0 in. which corresponds to a full size blade length reduction of 3.0 and 6.0 inches, respectively. Figures 3.1-1 to 3.1-3 show the eight bladed rotor before and after trim.

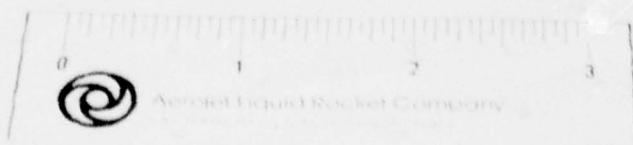
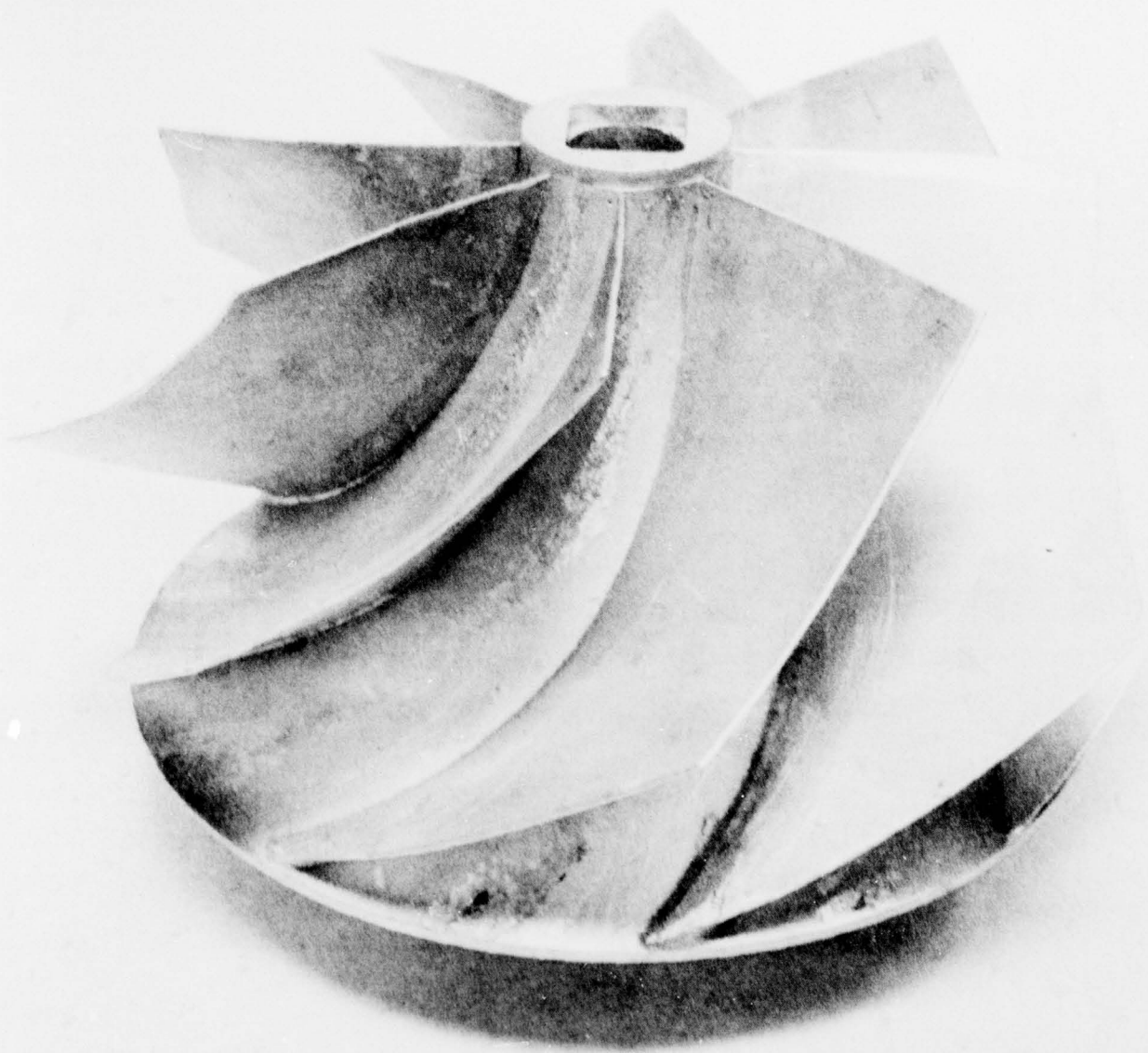
The present 11 bladed rotor was modified to reduce its exit width from 1.90 in. to 1.42 in. The reason for this change was to determine if the wake along the shroud could be reduced and thereby improving rotor performance. Figure 3.1-4 is the photograph of the original rotor and Figures 3.1-5 and 3.1-6 show the modified rotor with reduced exit width.

3.2 Housing

An existing model housing, shown in Figure 3.2-1, was used for evaluation of the rotor modifications and the inlet guide vanes tests. The narrow rotor exit required shroud modification and the IGV tests required a new inlet bell.

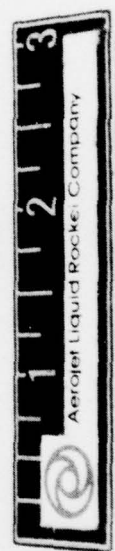
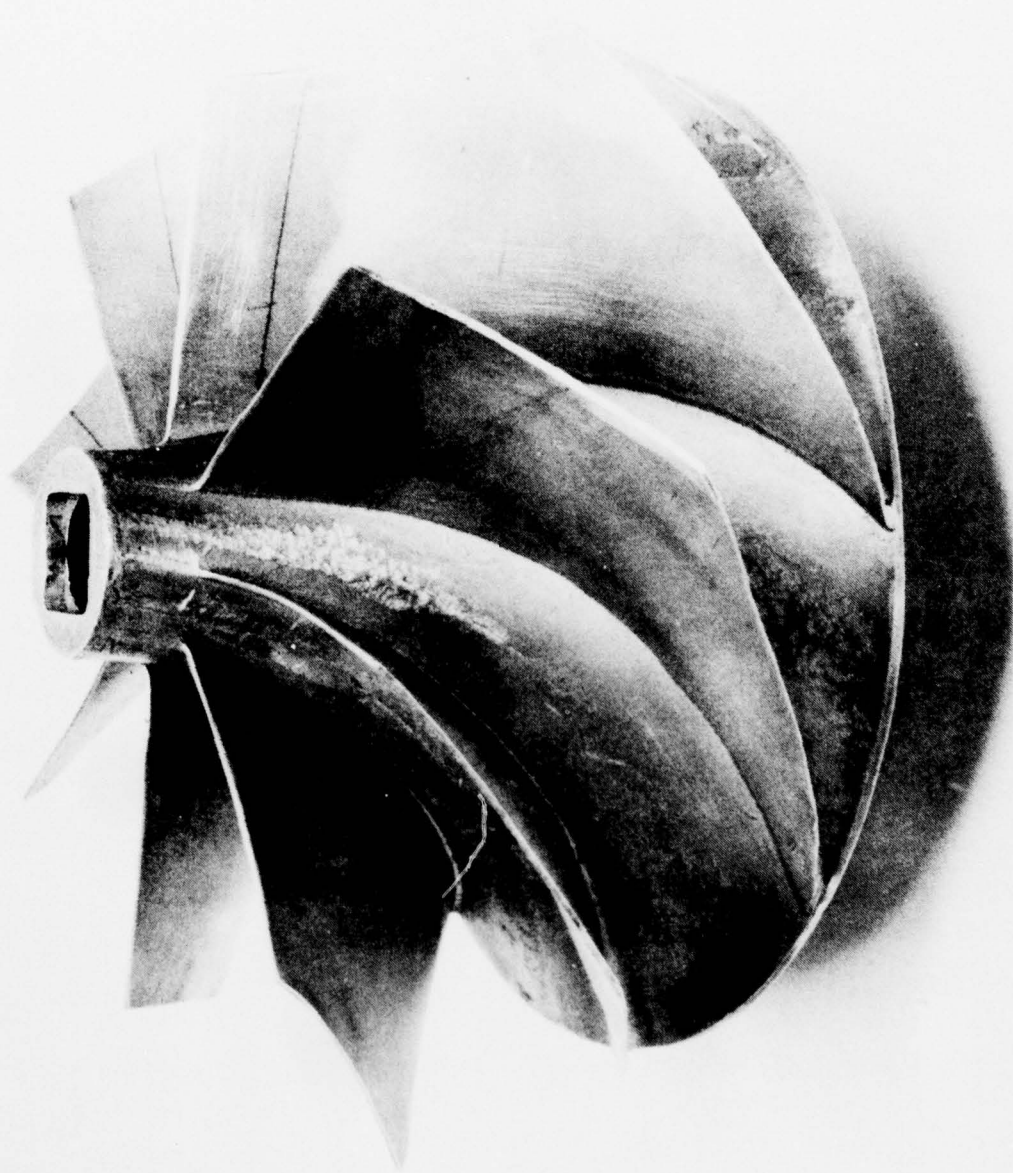
To evaluate the effect of housing size on fan performance, a new housing plenum was designed and constructed. Styrofoam inserts were placed inside the plenum box to vary axial width and volute inserts were used to vary radial dimensions. Figures 3.2-2 and 3.2-3 show the plenum box, reference volute and adapter box, Figures 3.2-4 to 3.2-6 show the axial configurations. Larger volute inserts are indicated in Figures 3.2-7 to 3.2-10.

All significant housing dimensions, including the volume parameter K , are given in Table 2.

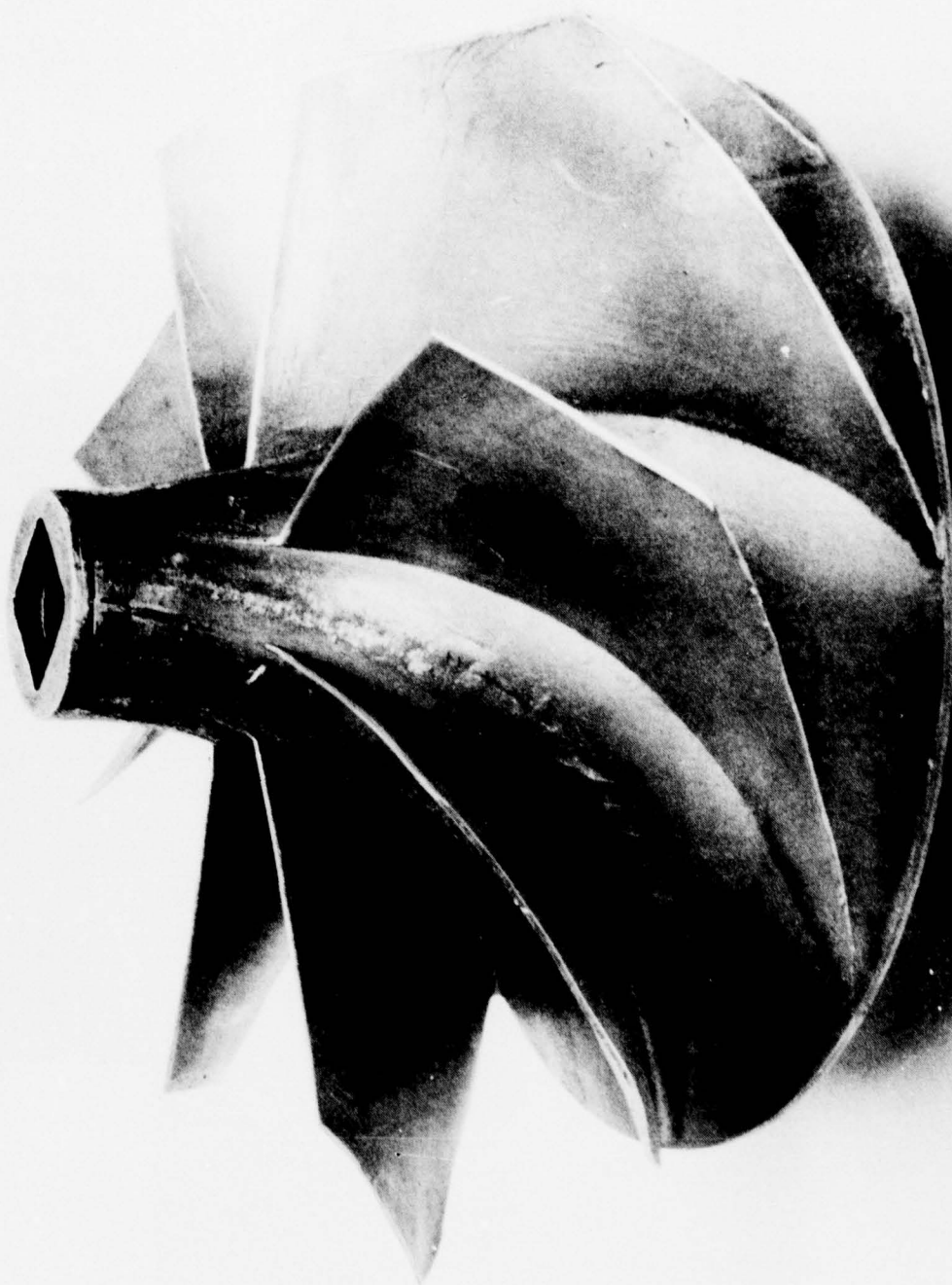


8 BLADED ROTOR

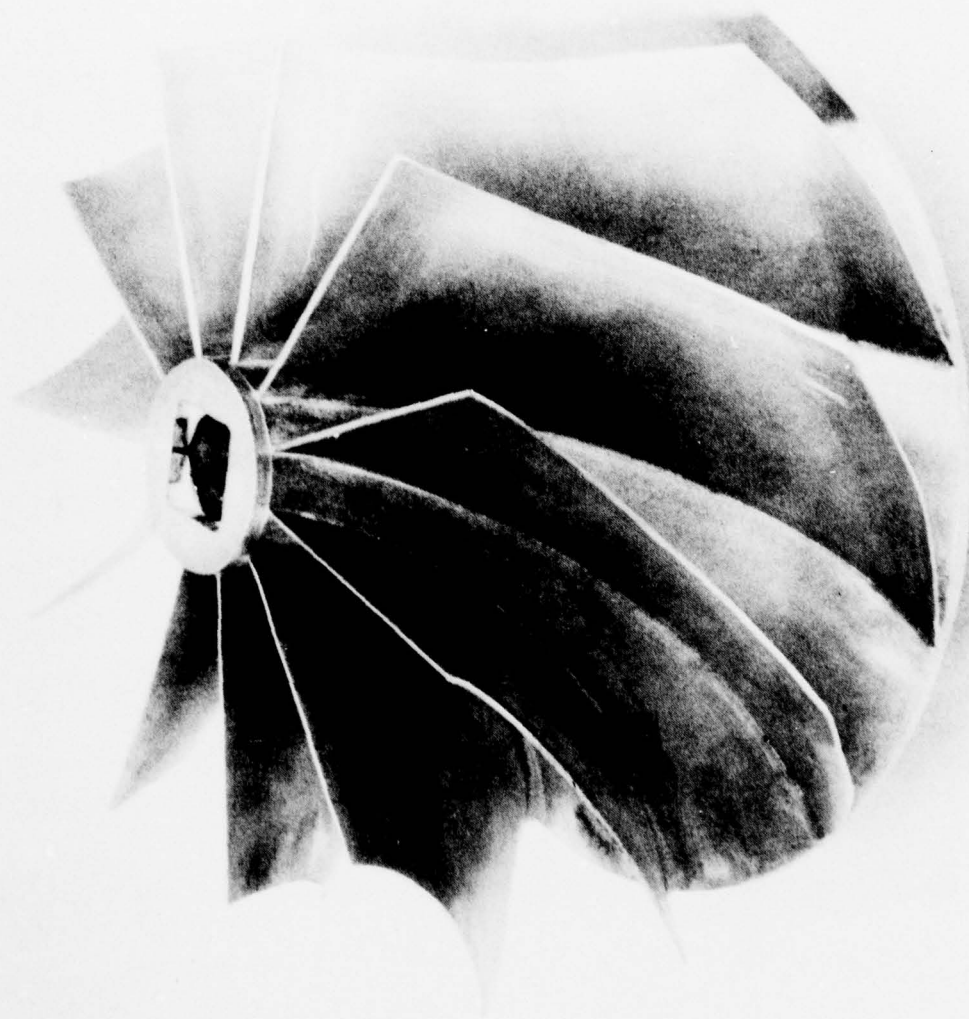
FIGURE 3.1-1



3 BLADED ROTOR
BLADE CUT BACK 0.5 IN
FIGURE 3.1-2



3 BLADED ROTOR
BLADE CUT BACK 1.0 IN
FIGURE 3.1-3

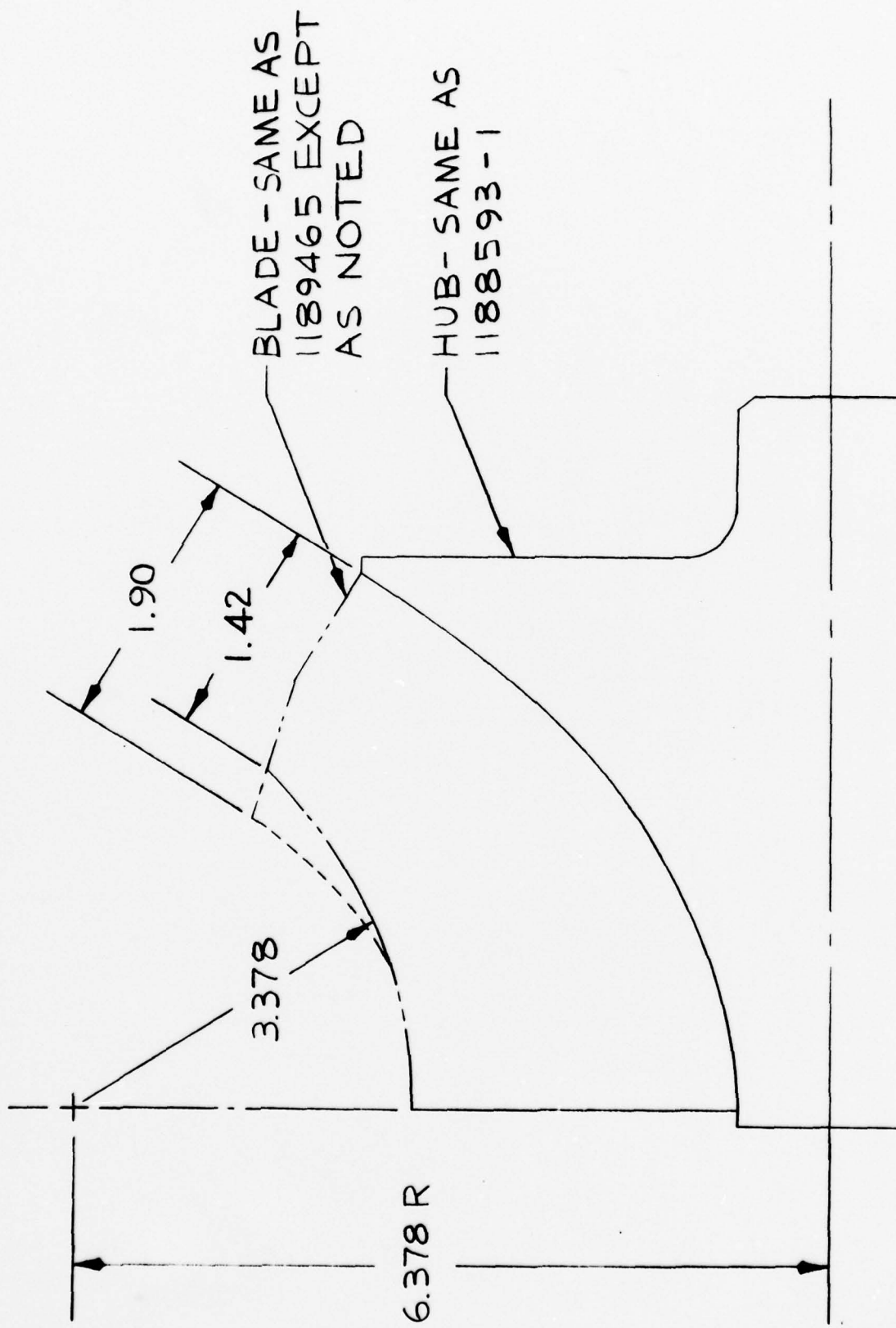


11 BLADED ROTOR
FIGURE 3.1-4

1 2 3 4 5 6 7 8 9 10 11 1FT



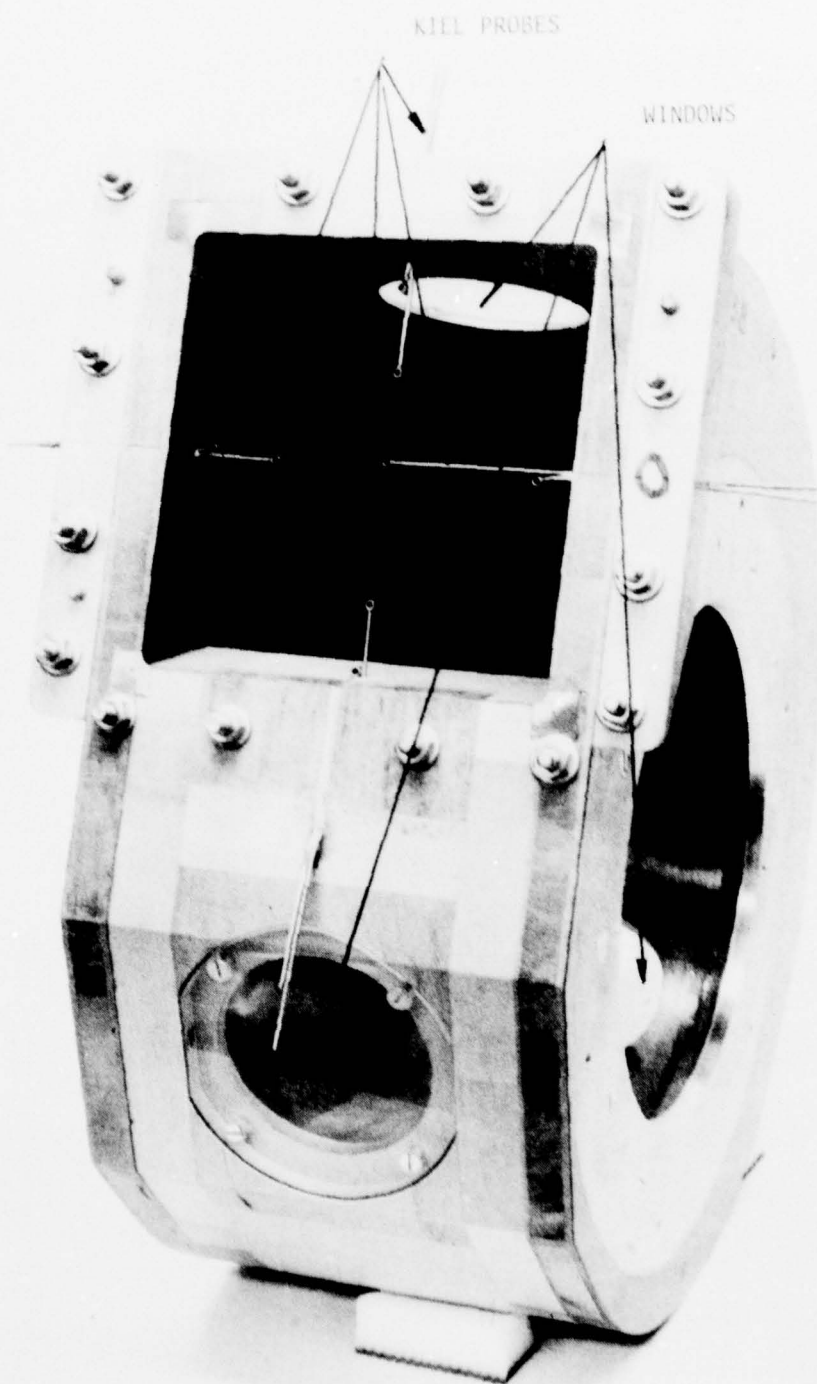
11 BLADED ROTOR
NARROW EXIT WIDTH
FIGURE 3.1-5

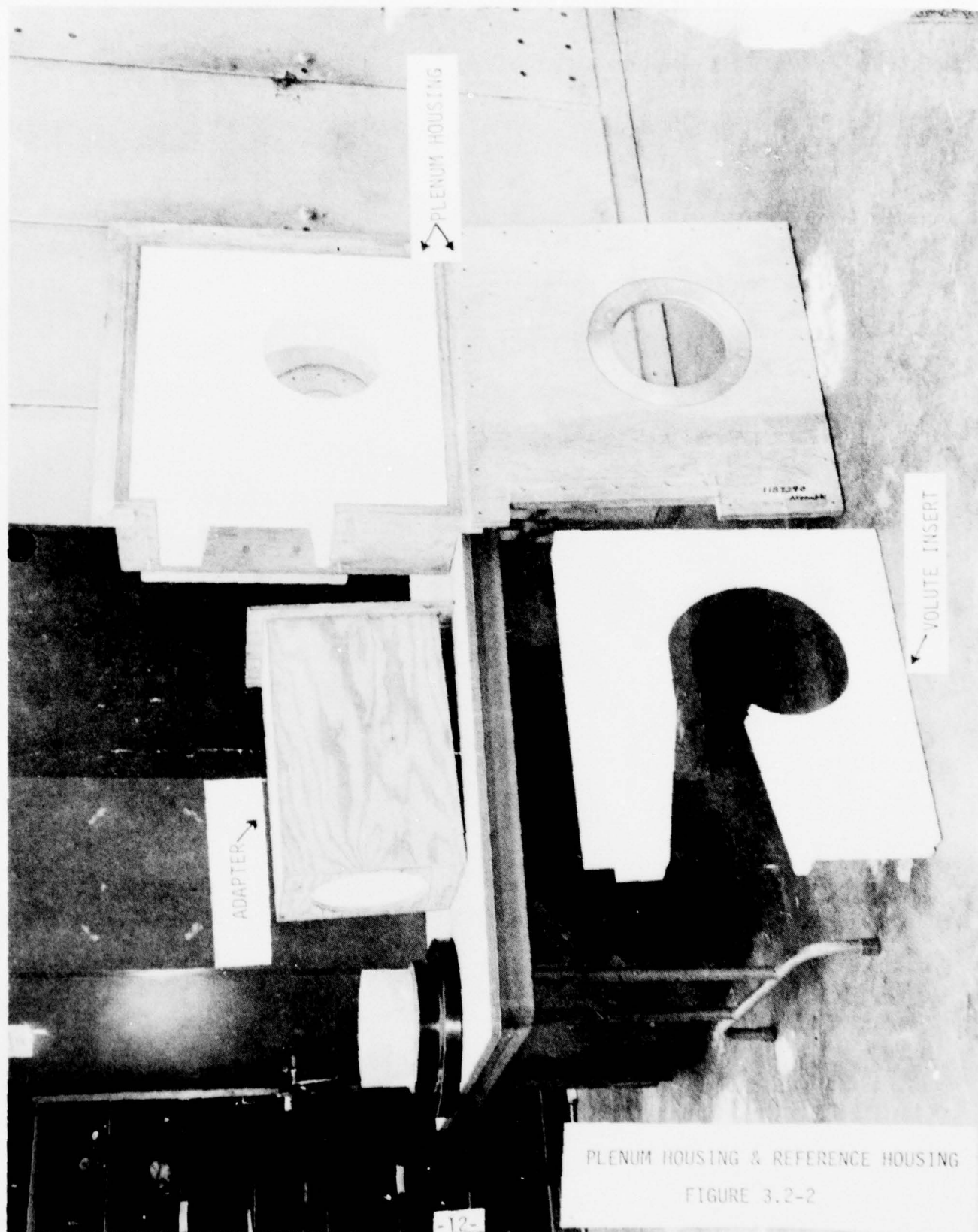


NARROW DISCHARGE ROTOR

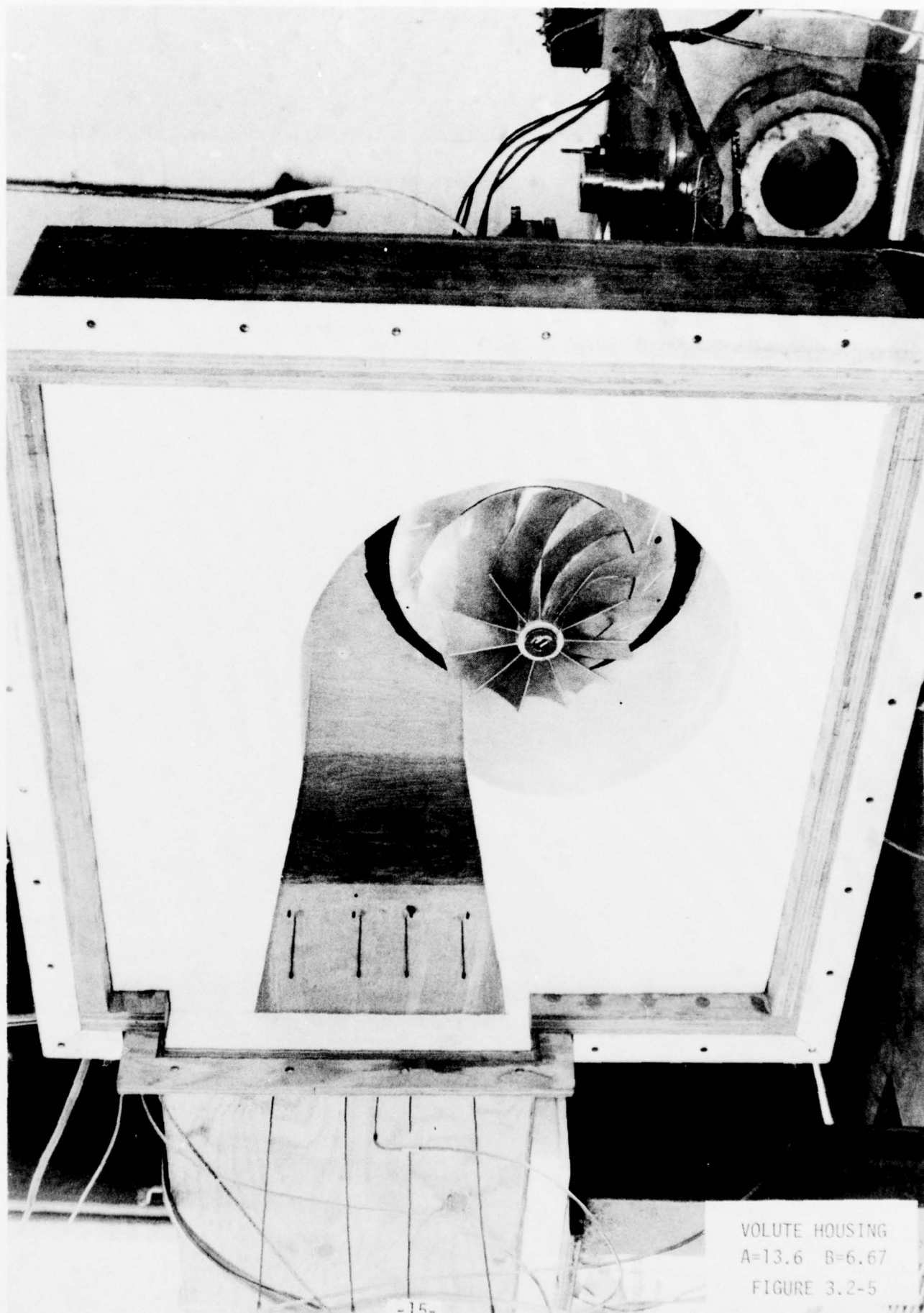
FIGURE 10

PHOTO 0177 SP 118

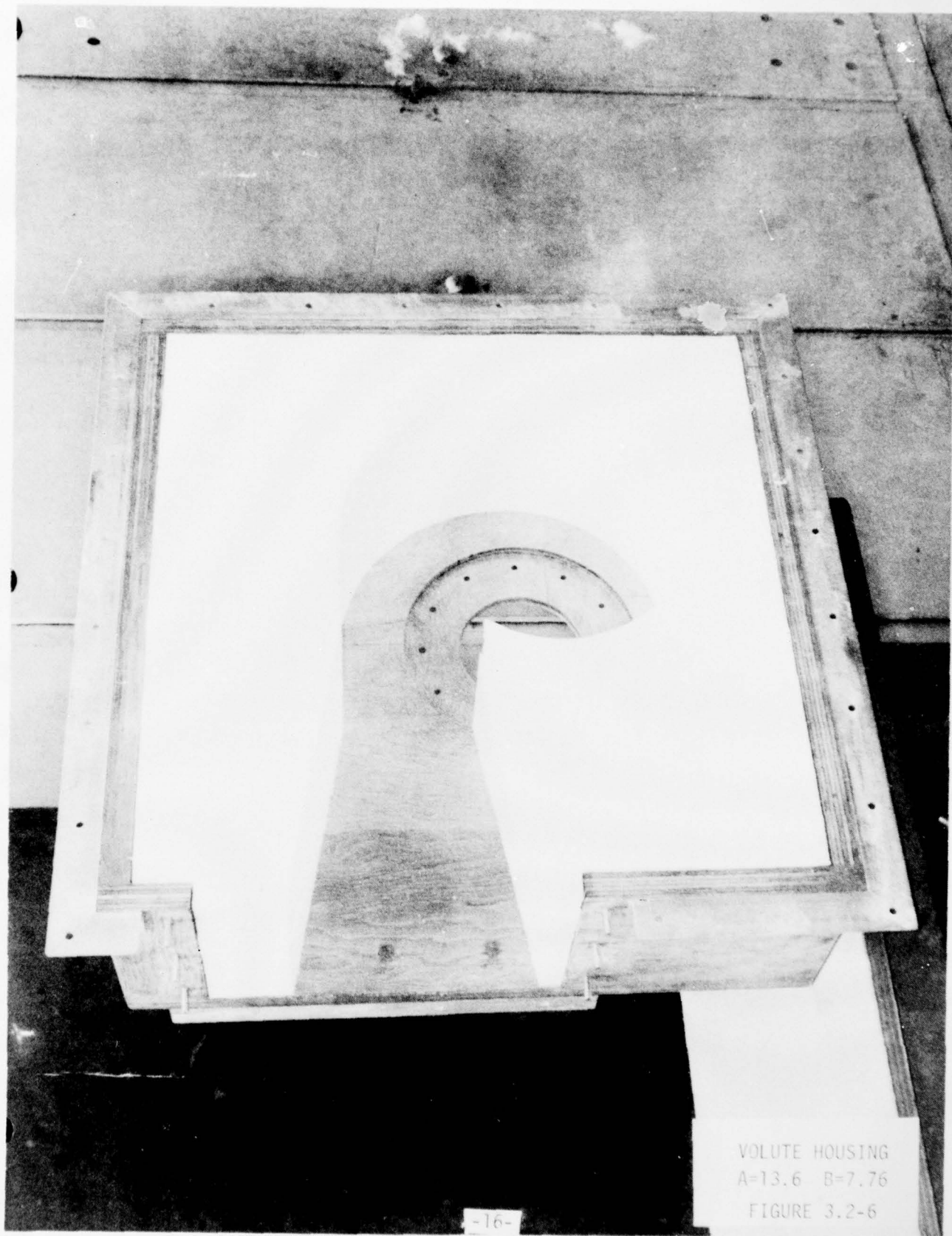








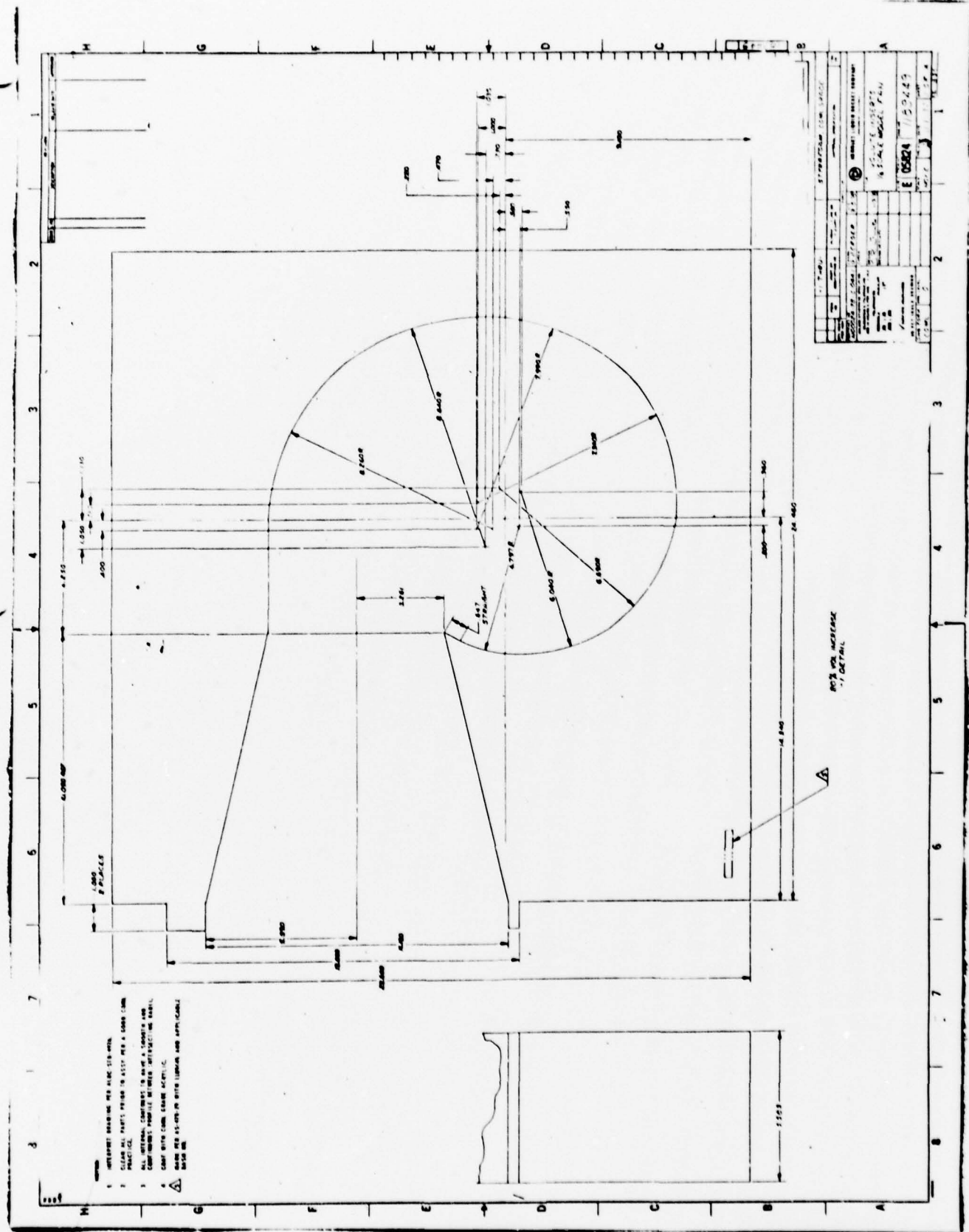
VOLUTE HOUSING
A=13.6 B=6.67
FIGURE 3.2-5

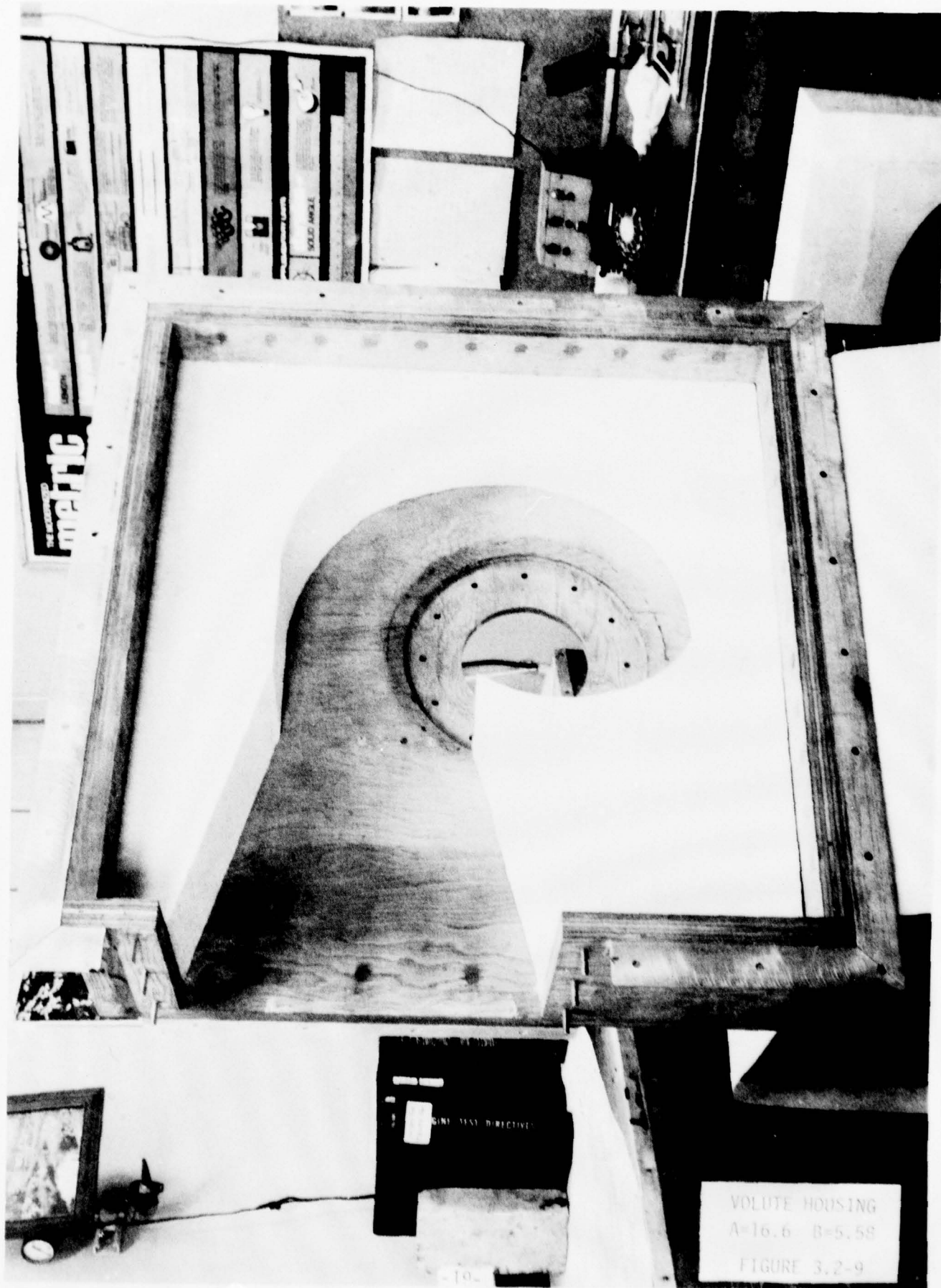


VOLUTE HOUSING
A=13.6 B=7.76
FIGURE 3.2-6



VOLUTE HOUSING
A-15.1 B-5.58
FIGURE 3.2-7





VOLUTE HOUSING

A=16.6 B=5.58

FIGURE 3.2-9

3. MODEL TEST HARDWARE (cont'd)

TABLE 2

MODEL HOUSING DIMENSIONS

$$\bar{D}_2 = 7.74 \text{ IN.} \quad b_2 = 1.90$$

	BASELINE HOUSING	NEW HOUSING	AXIAL WIDTH		VOLUTE DIAMETER	
B, IN	5.58	5.58	6.67	7.76	5.58	5.58
A, IN	13.60	13.60	13.60	13.60	15.10	16.60
$K = \frac{\pi B}{4b} \left(\frac{A}{D} \right)^2$	7.13	7.13	8.52	9.91	8.75	10.60

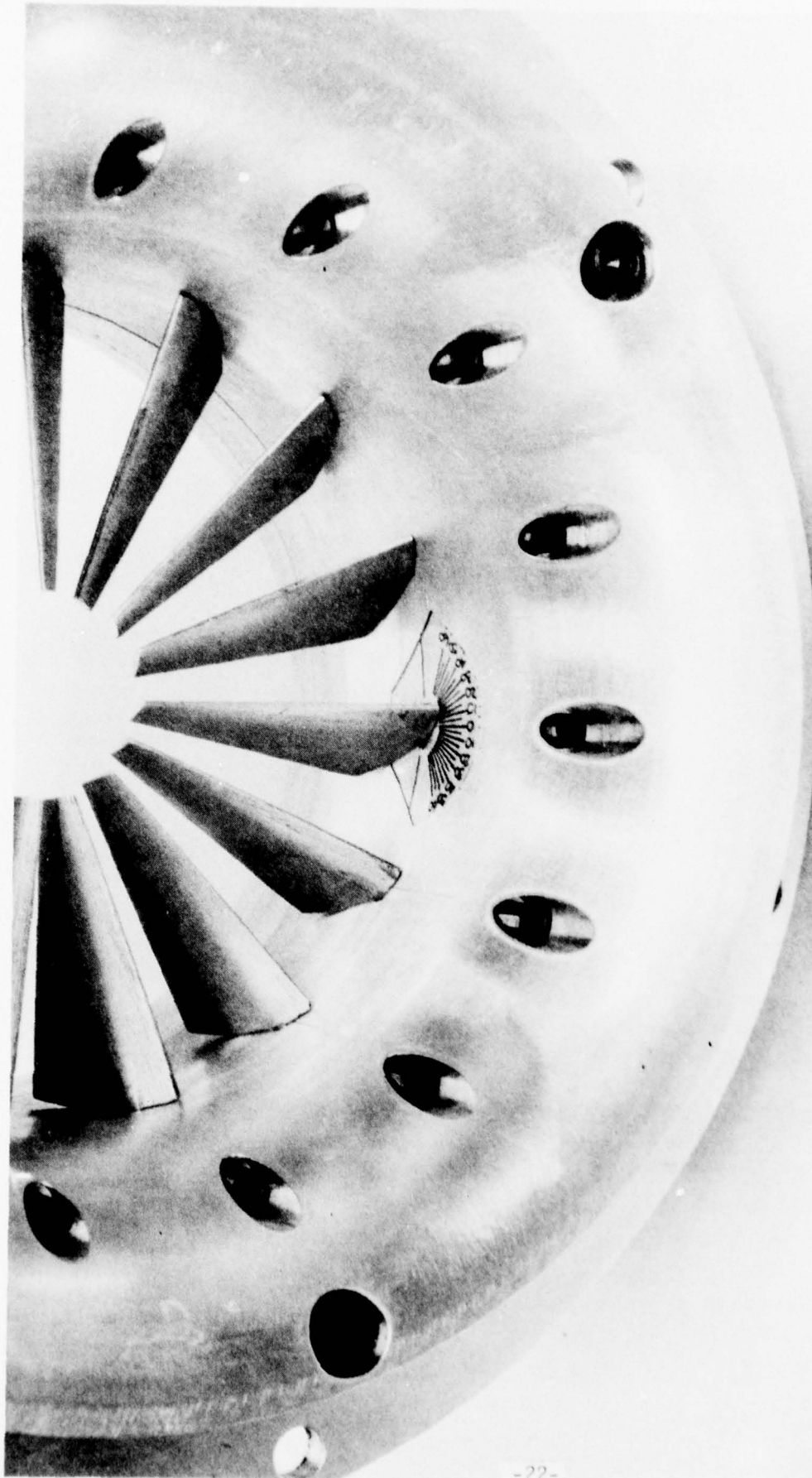
As the volute of the housing was changed, so was the diffuser, keeping diffuser length and area ratio constant and equal to the baseline diffuser length and area ratio.

To adapt this new housing to the test facility eight inch diameter duct system, a new adaptor box and inserts were required, having rectangular inlet cross-sections which change from housing to housing.

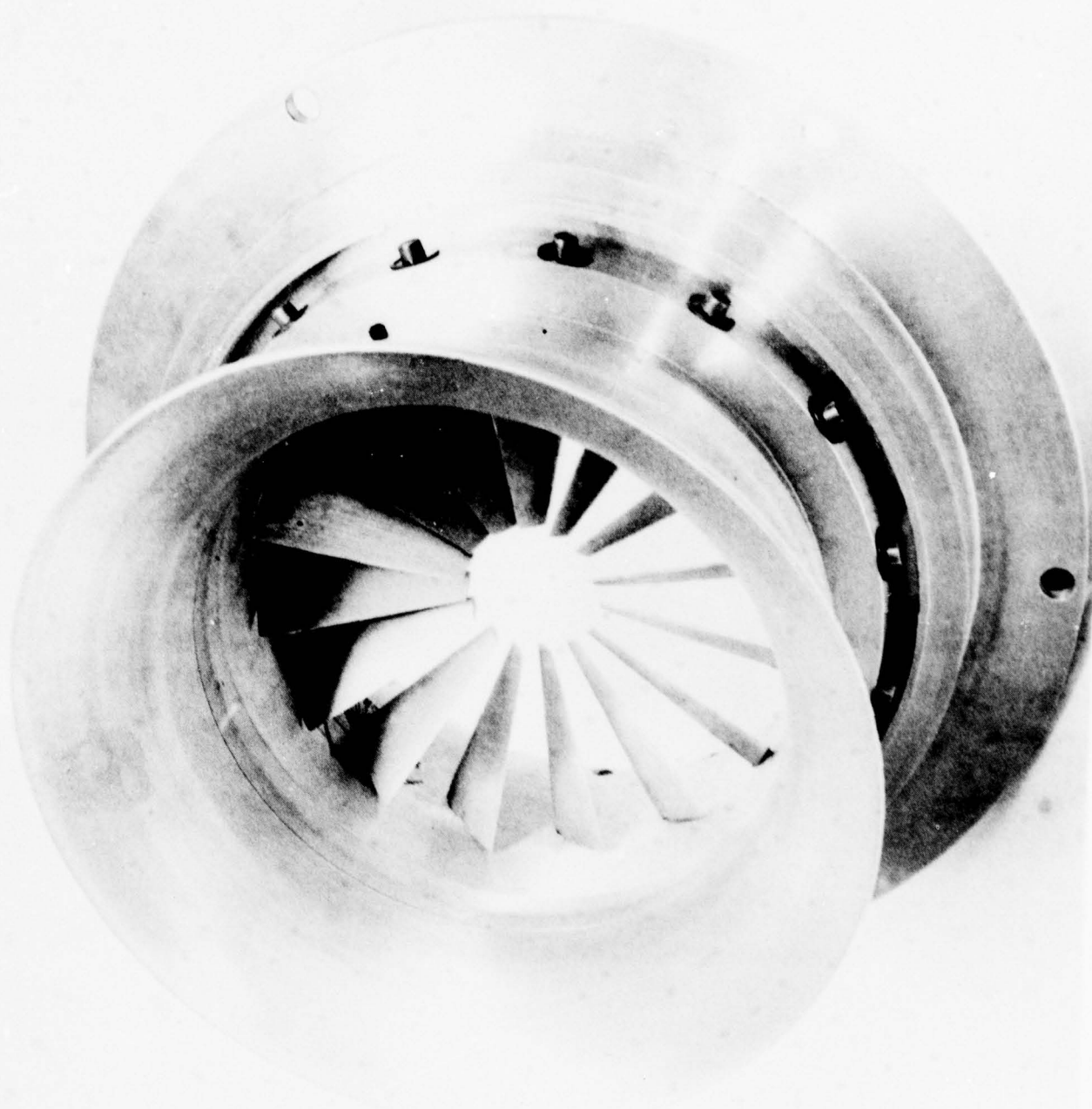
3.3 Inlet Guide Vanes

To test the fan model equipped with inlet guide vanes, a new IGV assembly was fabricated that includes an inlet bell, shroud and locking screws for the vanes (Figures 3.3-1, 3.3-2, 3.3-3). Each vane is set individually in the desired position, using a small protractor glued to the surface of the inlet bell, and is locked in position.

Three sets of inlet vanes were tested. The first set



IGV ASSEMBLY
FIGURE 3.3-1



IGV ASSEMBLY
FIGURE 3.3-2

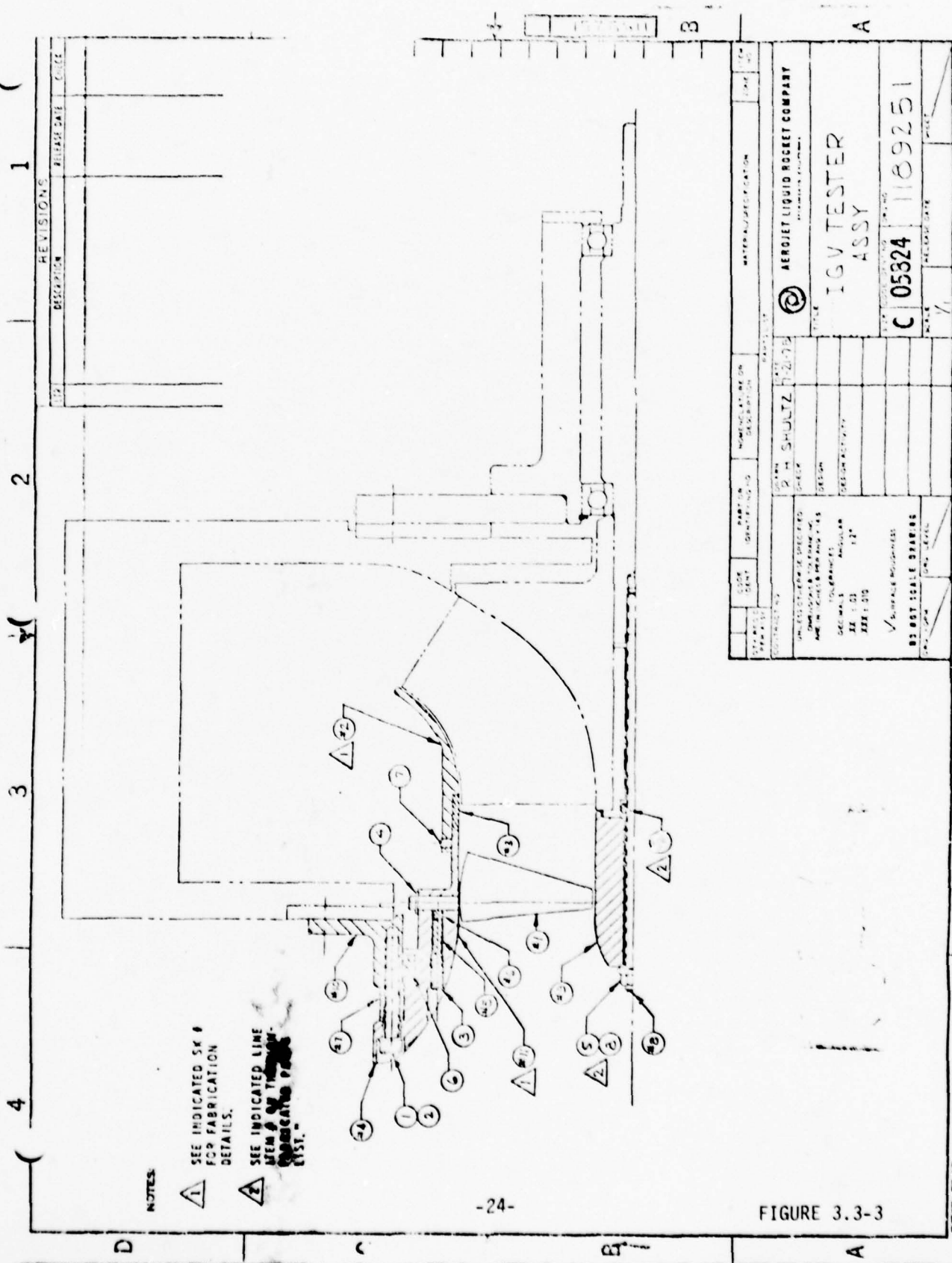


FIGURE 3.3-3

3. MODEL TEST HARDWARE (cont'd)

3.3 Inlet Guide Vanes (Cont'd)

consisted of 15 uncambered airfoils. The second set consisted of 15 constant thickness flat vanes and finally, the third set consisted of 15 constant thickness vanes with a 15° twist between the tip and the hub. Table 3 shows basic characteristics of all vanes used.

TABLE 3

CHARACTERISTICS OF THE INLET VANES TESTED

	FLAT VANES				TWISTED VANES	
	AIRFOIL VANES (THICK)		THIN VANES		THIN VANES	
	HUB	TIP	HUB	TIP	HUB	TIP
Max. Thickness, IN	0.08	0.22	0.04		0.04	
Thickness/Chord	0.25	0.18	0.125	0.033	0.125	0.033
Leading Edge Rad. IN	0.01	0.01	0.01		0.01	
Trailing Edge Rad., IN	0.005	0.005	0.005		0.005	
Number of Vanes	15		15		15	
Solidity	1.0		1.0		1.0	

The photograph of all three vanes is shown in Figure 3.3-4.

4. MODEL TEST SETUP

4.1 Description of Test Set Up and Instrumentation

The model tests were conducted in the ALRC Physics Laboratory. The test set up was described in detail in Reference (2). Figure 4.1-1 shows

TWISTED VANE



FLAT VANE



THICK AIRFOIL VANE



INLET VANE CONFIGURATION
TESTED

FIGURE 3.3-4

PHOTO 0227 SP 075

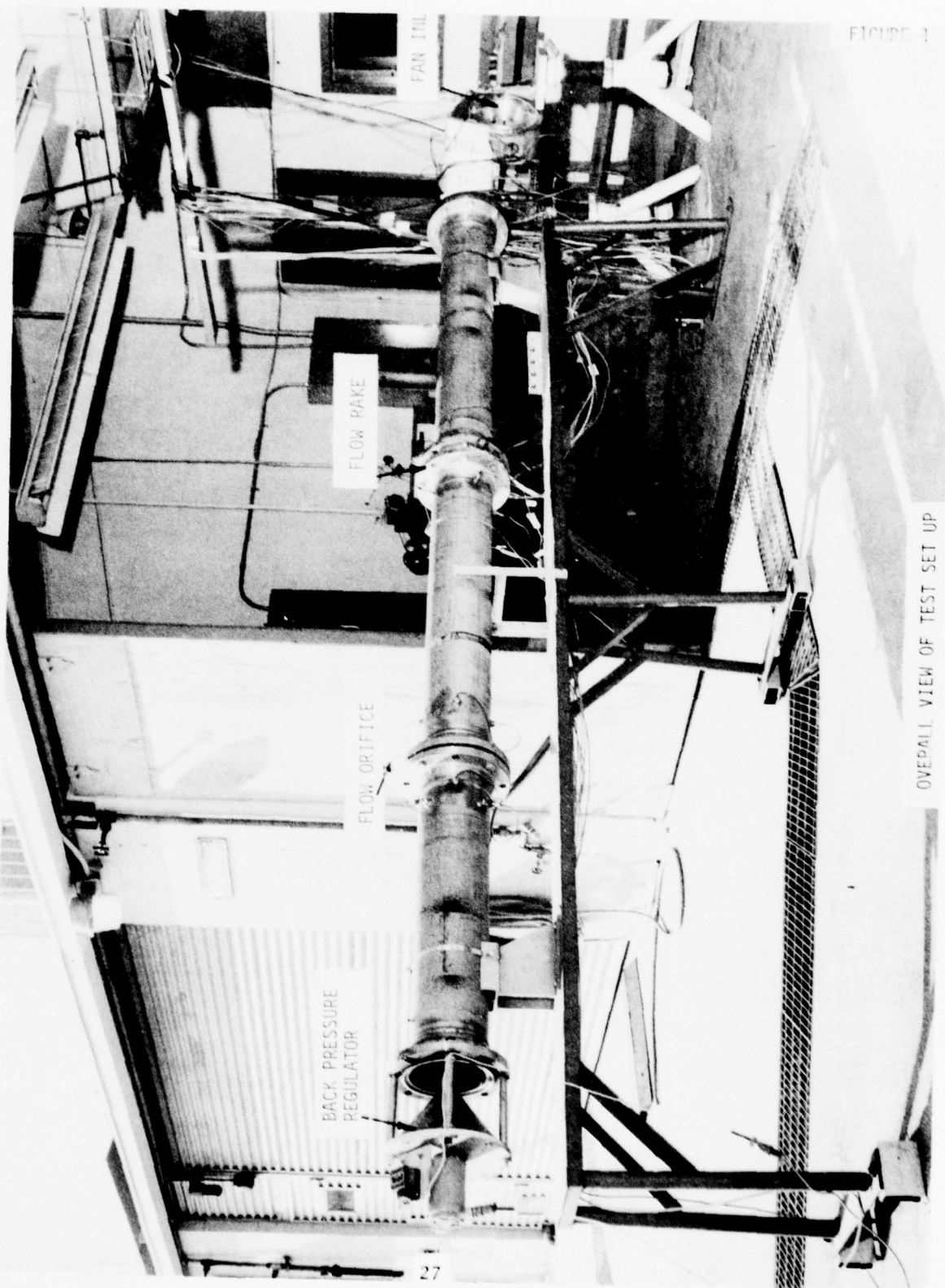


FIGURE 1

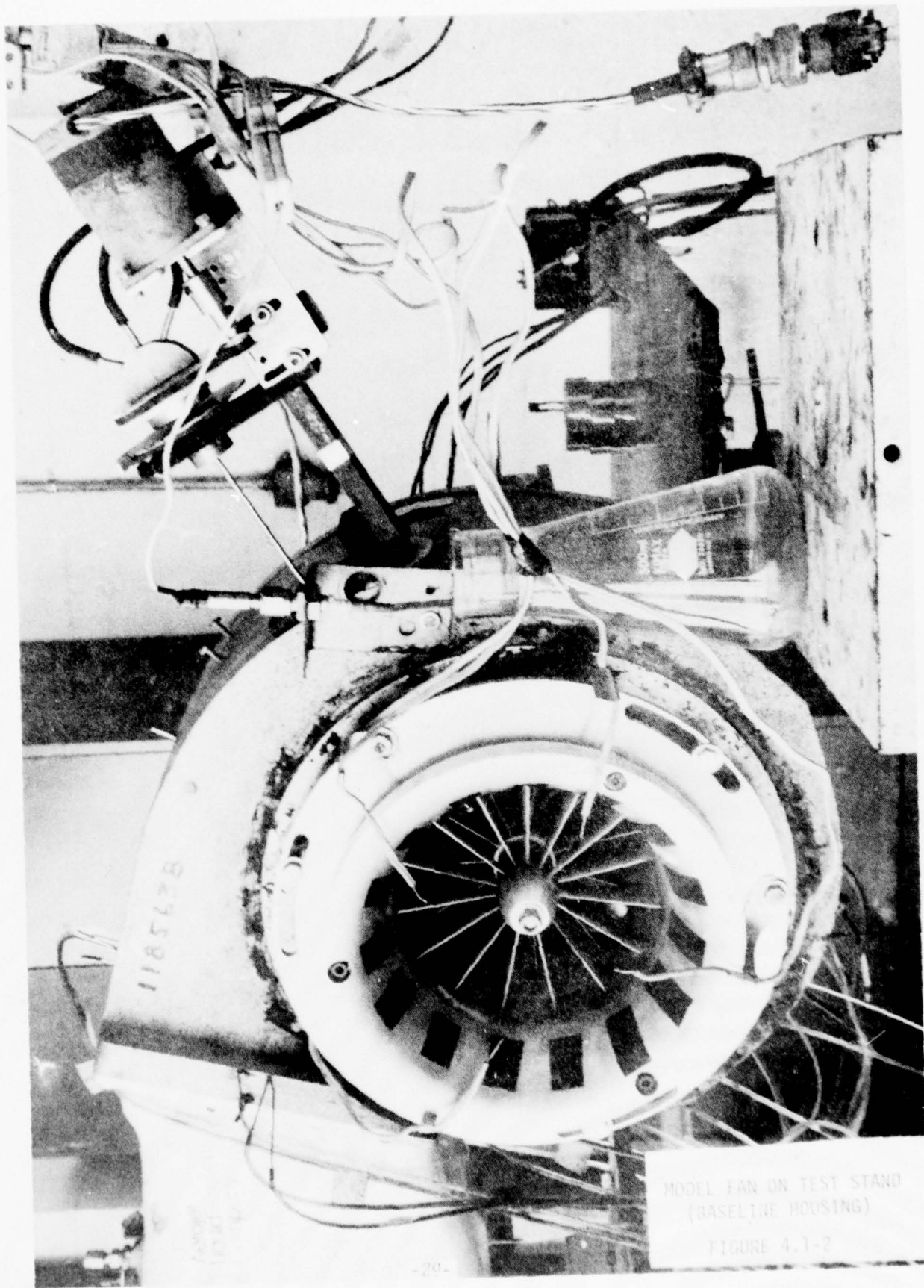
OVERALL VIEW OF TEST SET UP

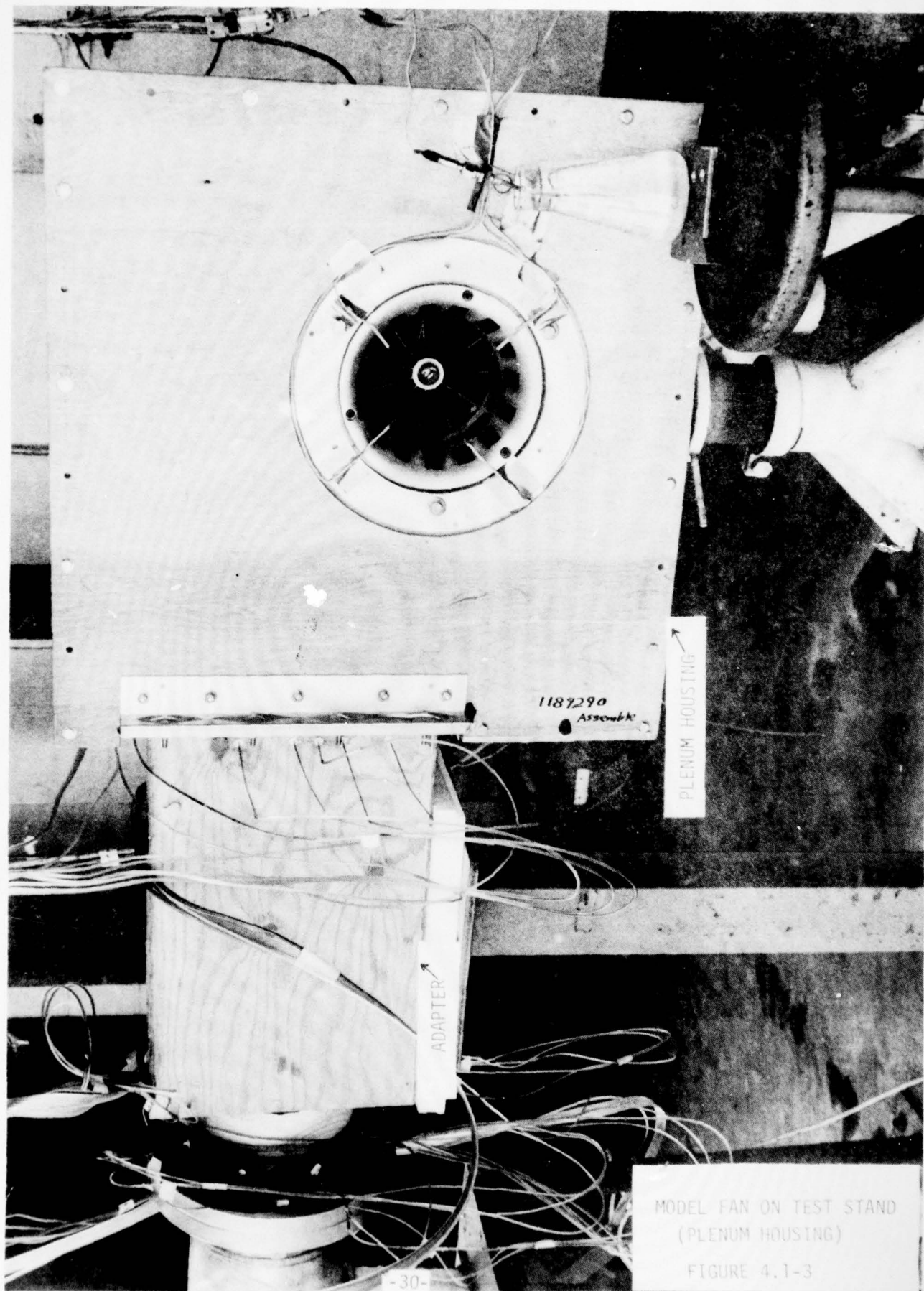
4. MODEL TEST SETUP (cont'd)

4.1 Description of Test Set Up and Instrumentation (Cont'd)

the model fan installed in the test facility. Figure 4.1-2 shows the model fan fitted with the baseline housing and IGV assembly while Figure 4.1-3 shows the installation of the new plenum housing and adapter.

1. Weight flow rate was measured by means of a standard ASME orifice installed in the exhaust duct. Four thermocouples were used to measure the orifice upstream temperature and wall taps were used to measure upstream and downstream pressures.
2. Fan pressure rise from ambient to fan exit was obtained by measuring barometric pressure at the inlet and total pressure at the diffuser outlet. Twelve Kiel probes were used for total pressure measurement.
3. The flow angle distribution at the rotor inlet was measured with a 3-element wedge probe.
4. Wall taps were provided to measure static pressure along the stationary shroud, rotor exit, housing discharge and diffuser exit.
5. The fan inlet temperature was measured with four CA thermocouples.
6. Rotational speed was measured by means of an electronic counter.
7. Torque was measured with a strain gage type torquemeter. The torquemeter was calibrated statically before and after the test run by applying weights on an arm.
8. All measured quantities except pressures were stored on magnetic tape, averaged and converted into engineering units. Air pressure measurements were connected to the water manometer board and photographed for data reduction on the computer.





4.1 Description of Test Set Up and Instrumentation (Cont'd)

9. Data reduction was performed by means of a computer program described in Reference (2).

Model test instrumentation is listed in Table 4. The instrumentation location is given in Figures 4.1.-4 to 4.1.-10.

TABLE 4
MODEL INSTRUMENTATION

<u>LOCATION</u>	<u>MEASURED QUANTITY</u>	<u>TYPE OF INSTRUMENT</u>	<u>RANGE</u>	<u>ACCURACY</u>	<u>QTY</u>
-	Ambient Pressure	Barometer	-	0.01" Hg	1
-	Rotational Speed	Electric Counter	0-12000 rpm	100 rpm	1
-	Torque	Calibrated Torquemeter	0-2.5 ft/lb	0.5%	1
0	Temperature	Thermocouple	30-120°F	2°F	4
0	Wet Bulb Temp.	Thermocouple	30-120°F	2°F	1
2	Flow Rake	Three Element	-30° to +30°	1°	1
4	Static Pressure	Wall Tap	0-1 psia	0.1" H ₂ O	2
5	Total Pressure	2 Element Kiel Probe	0-1 psia	0.1" H ₂ O	12
5	Static Pressure	Wall Tap	0-1 psia	0.1" H ₂ O	4
6	Total Pressure	2 Element Kiel Probe	0-1 psia	0.1" H ₂ O	12
7	Temperature	Thermocouple	30-120°F	2°F	4
8	Static Pressure	Wall Tap	0-1 psia	0.1" H ₂ O	4
9	Static Pressure	Wall Tap	0-1 psia	0.1" H ₂ O	4
Shroud	Static Pressure	Wall Tap	0-1 psia	0.1" H ₂ O	6

MODEL LIFT FAN
INSTRUMENTATION LOCATION

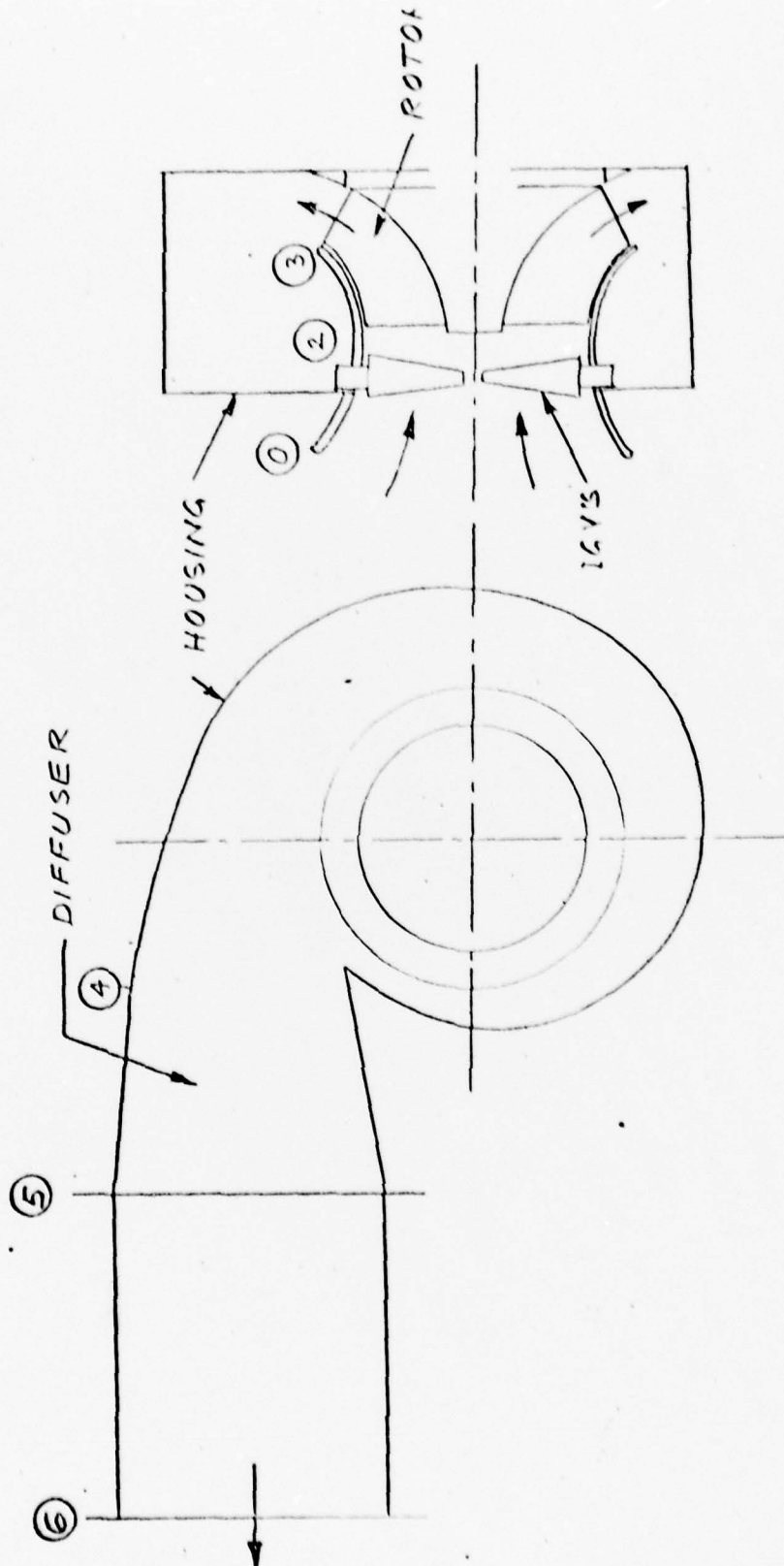


FIGURE 4.1-4.

SUBJECT

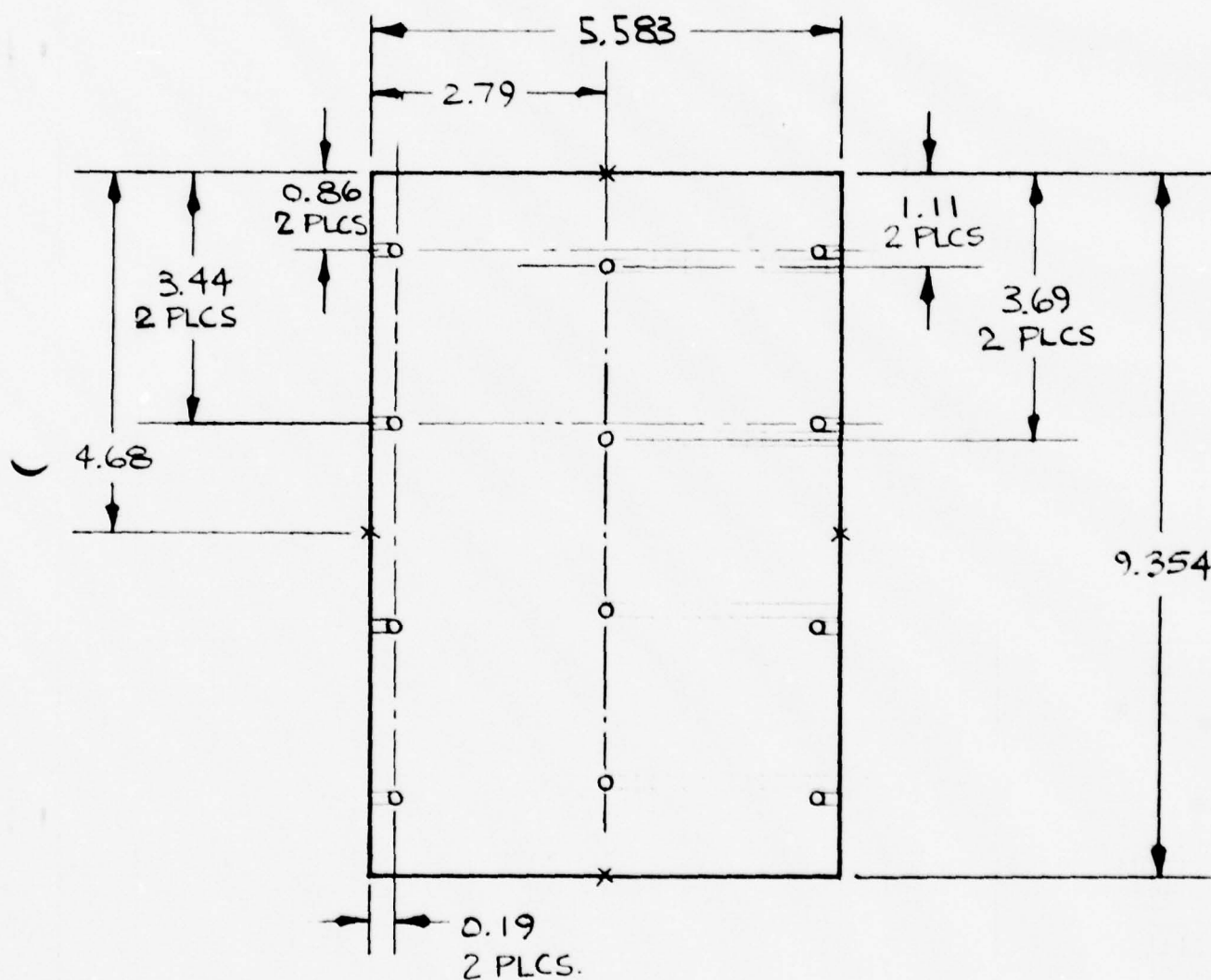
INSTRUMENTATION - KIEL PROBE POSITIONING
AT STATION 5DATE
3/12/79WORK ORDER
2288-01

BY S.R. FINATO

CHK BY

DATE

1) REFERENCE CONFIGURATION



O KIEL PROBE

X STATIC

NOTE: OFFSET PROBES IN CENTER ARE SETBACK
0.25 IN.

INSTRUMENTATION - KIEL PROBE POSITIONING AT STATION 5

PAGE 2 OF

DATE 3/12/79

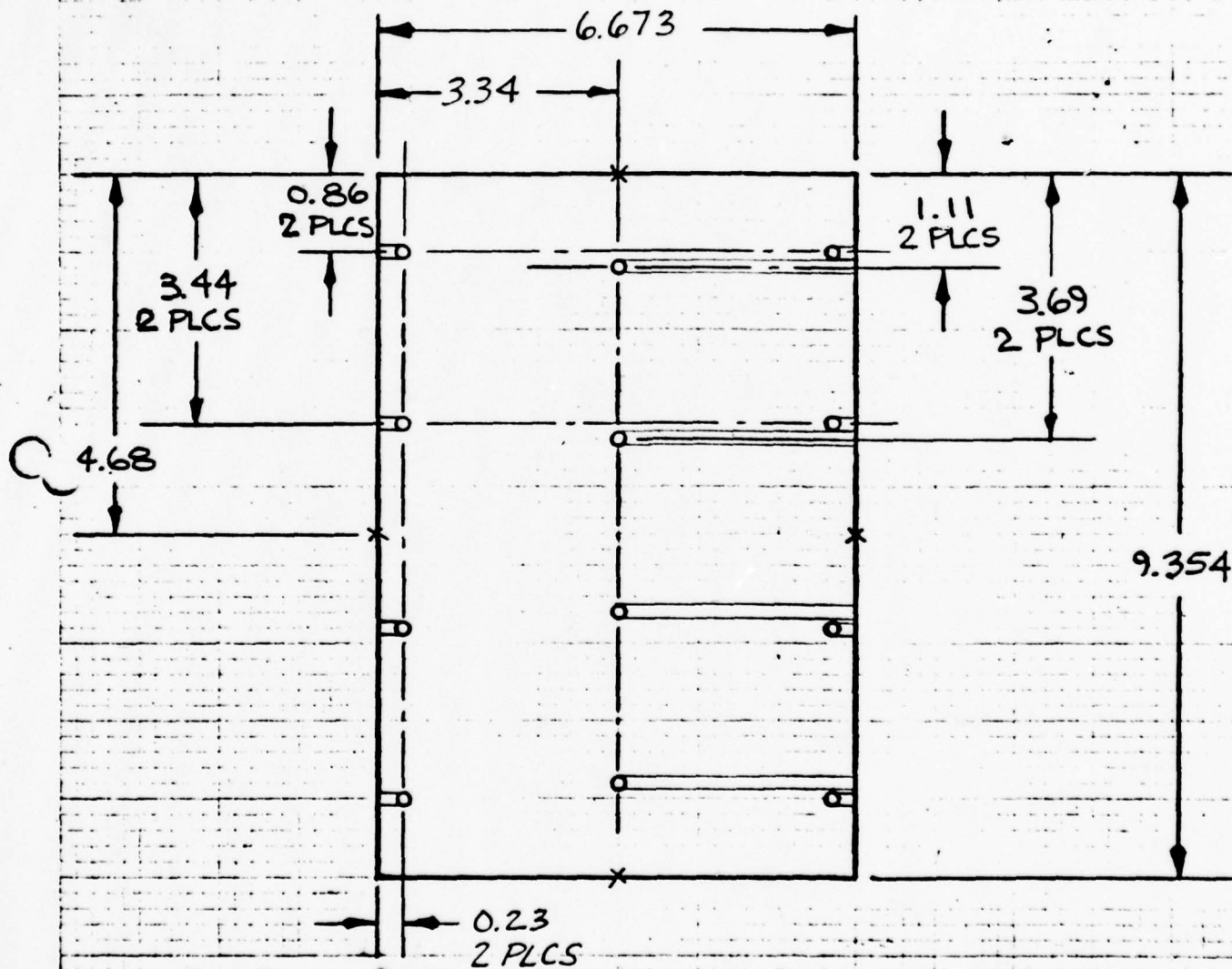
WORK ORDER 2288-01

SR. FINATO

CHK BY

DATE

2) 1ST AXIAL CONFIGURATION



o KIEL PROBE

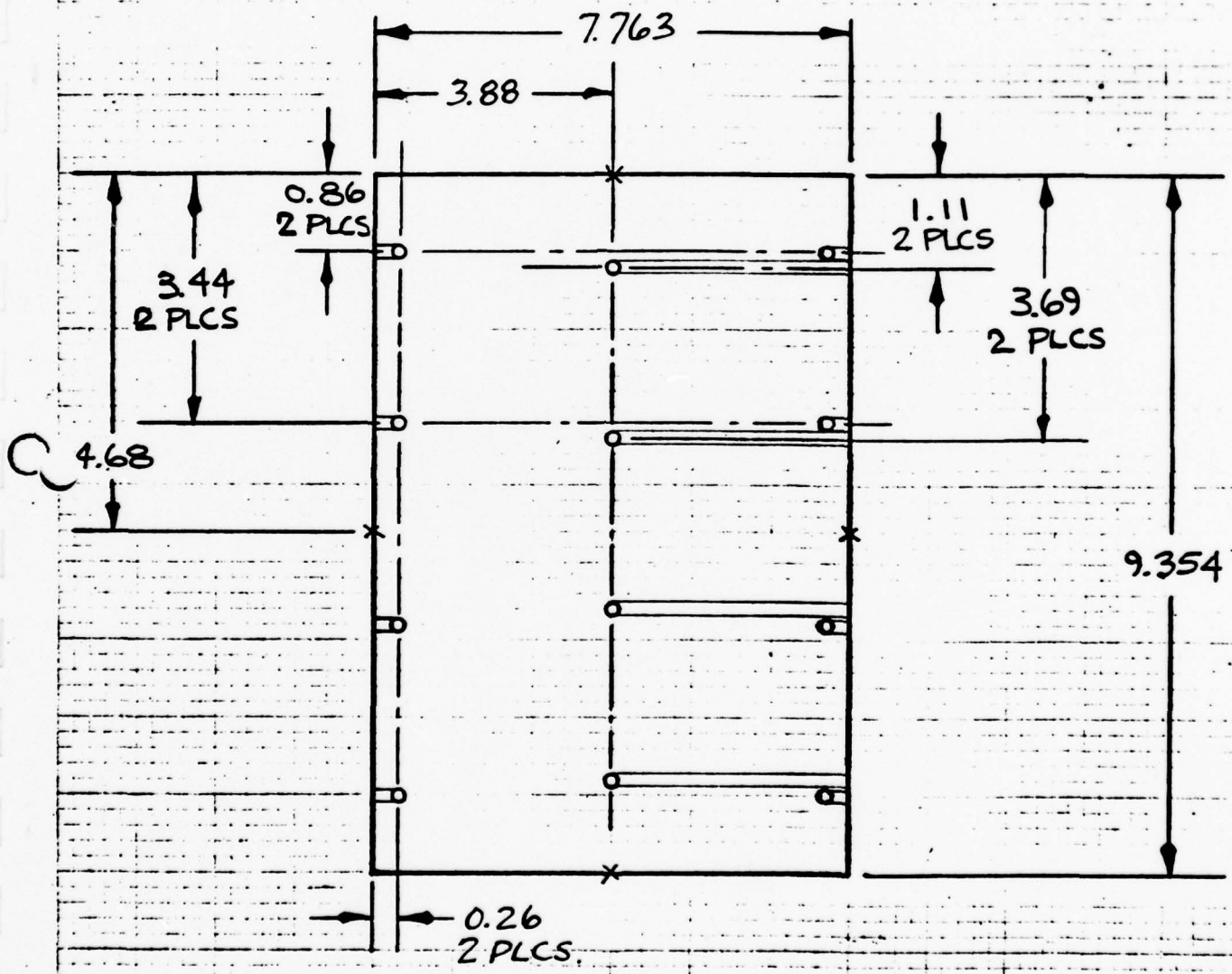
x STATIC

NOTE: OFFSET PROBES IN CENTER ARE SETBACK 0.25 IN.

FIGURE 4.1-5

SUBJ. INSTRUMENTATION - KIEL PROBE POSITIONING AT STATION 5		REPORT NO.	PAGE 3 OF
SR. FINATO		CHK. BY	DATE 3/12/79
			WORK ORDER 2288-01
			DATE

3) 2ND AXIAL CONFIGURATION



○ KIEL PROBE

× STATIC

NOTE: OFFSET PROBES IN CENTER ARE SETBACK 0.25 IN.

FIGURE 4.1-7

INSTRUMENTATION - KIEL PROBE POSITIONING
AT STATION 5

DATE 3/12/79

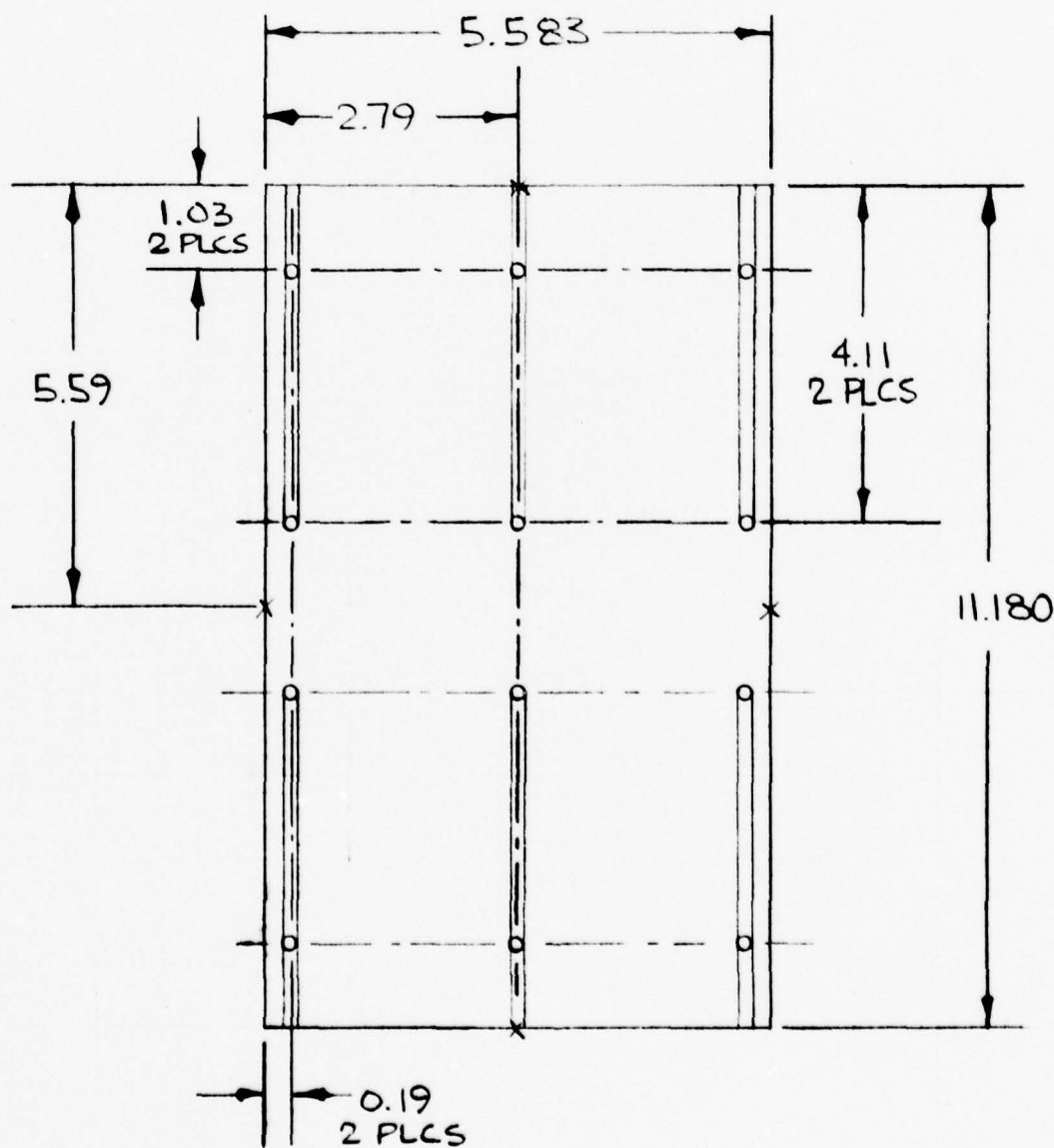
WORK ORDER 2288-01

BY S.R. FINATO

CHK BY

DATE

4) 1ST RADIAL CONFIGURATION

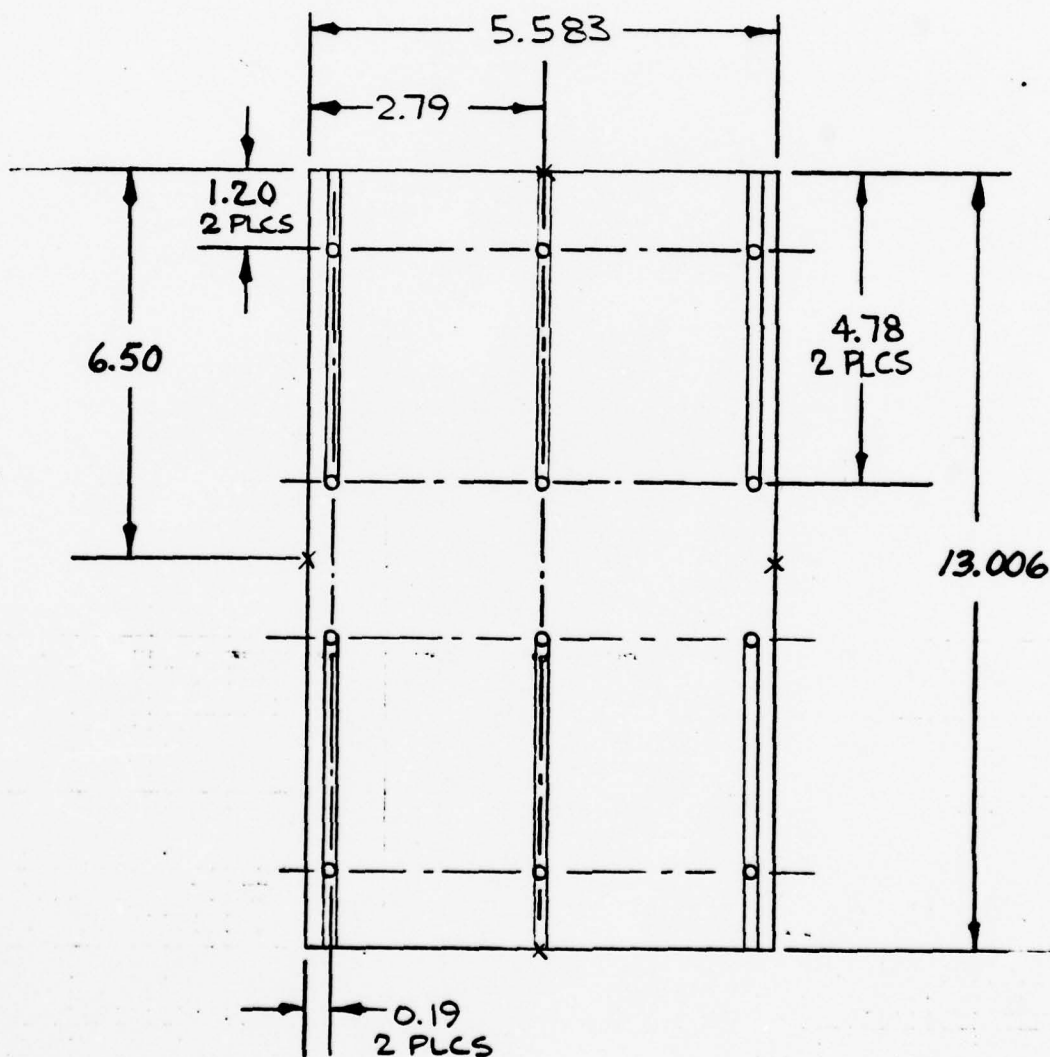


O KIEL PROBE

X STATIC

NOTE: SIX PROBES IN CENTER ARE SET BACK 0.25 IN.

SUBJECT		REPORT NO.	PAGE 5 OF
INSTRUMENTATION - KIEL PROBE POSITIONING AT STATION 5		DATE	3/12/79
BY S.R. FINATO		WORK ORDER	2288-01
CHK BY		DATE	

5) 2ND RADIAL CONFIGURATION

O KIEL PROBE

X STATIC

NOTE: SIX PROBES IN CENTER ARE SET BACK 0.25 IN.

JEFF (A) SCALE MODEL TEST SET UP

INSTRUMENTATION LOCATION

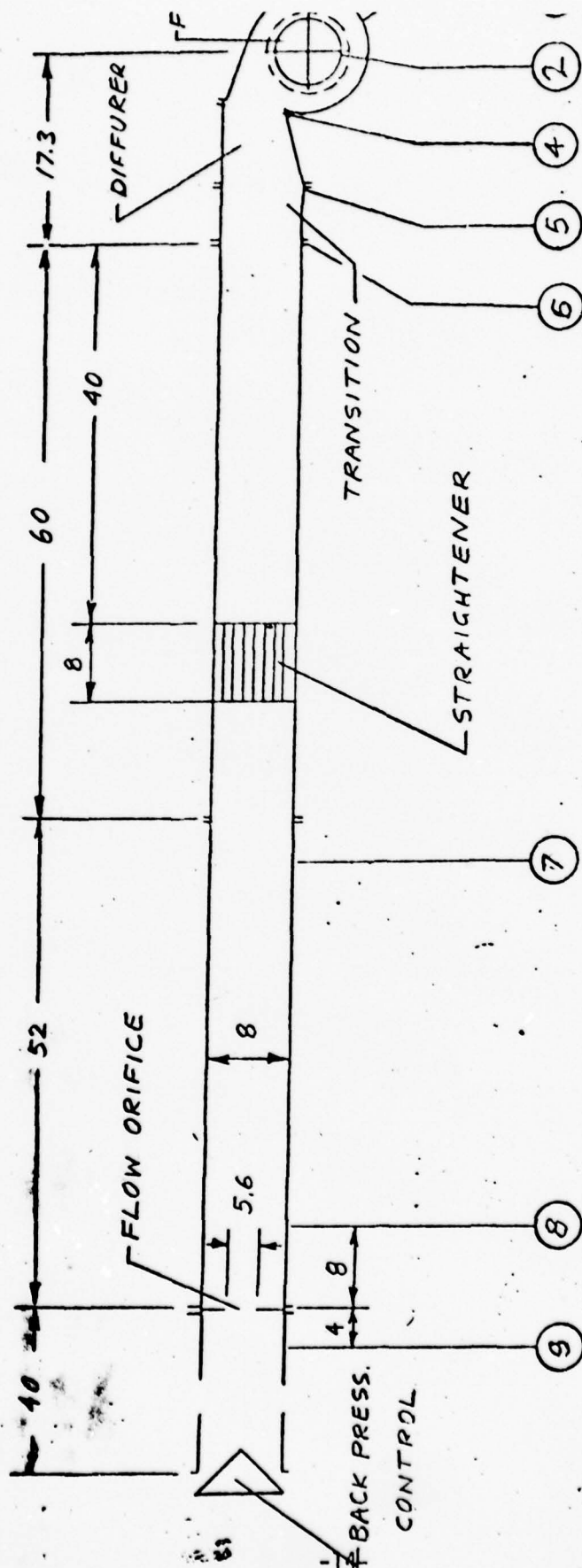


FIGURE 4.1-10

4. MODEL TEST SETUP (cont'd)

4.2 Test Conditions

All tests were run at 6000 rpm while varying the back pressure valve position from fully open to fully closed. In addition to measuring the overall fan performance, traverses were performed at the rotor inlet with a three element wedge probe. Pre-whirl angle distribution was determined first without inlet guide vanes and then with inlet guide vanes installed.

When testing the model with various housing configurations, it was necessary to change the Kiel probe locations at the diffuser exit.

Using test data, the model head coefficient, efficiency and flow coefficient were calculated. Traverse data were used to plot pre-whirl angle and incidence angle distributions at the rotor inlet between the hub and tip.

4.3 Model Test Matrix

Table 5 shows the matrix of tests conducted by varying rotor and housing parameters. Fan performance sensitivity to inlet guide vane positioning was also evaluated.

TABLE 5

MODEL TEST MATRIX

ROTOR	BLADE LENGTH	HOUSING VOLUTE AXIAL WIDTH	VOLUTE DIAMETER	PLENUM	FLAT IGV'S POSITION, DEGREES	TWISTED IGV'S POSITION, DEGREES	REMARKS
Baseline 8 Blades	-0.5 -1.0	5.58	13.6				Blade Cut Back
		5.58	13.6				
Baseline 11 Blades	Full Length	5.58	13.6		No IGV's 0° (Thick) +20° 0° (Thin)		Traverse at Rotor Inlet
		5.58	13.6				
		5.58	13.6				
		5.58	13.6		-40° to +40° (Thick) -20° to +40° (Thin)	+10° to +50°	Performance with IGV's
	Full Length	5.58	13.6				New Housing
		5.58	13.6				
		5.58	13.6				
		5.58	13.6				
Narrow Exit Rotor	Full Length	5.58	13.6				
		5.58	13.6				

5. MODEL FAN PERFORMANCE

5.1 Rotor

Using the baseline housing, the rotor was modified and the fan performance characteristics determined over the entire flow range.

5.1.1 Effect of Rotor Blade Length on Performance - Reduction of the rotor length is desirable to reduce the rotor weight and cost of fabrication, providing that the decrease in fan performance is acceptable.

Figures 5.1.1-1 and 5.1.1-2 show the model test results of the 8-bladed rotor having blade leading edges cut back 0.5" and 1.0" respectively. The effect of blade cut-back on efficiency and head coefficient is clearly illustrated in the summary plot shown in Figure 5.1.1-3. It can be seen that the blade cut-back reduces fan efficiency primarily in the high efficiency range ($\eta = 0.65 - 0.74$). The head reduction, although modest for 0.5" cut-back, is quite considerable for 1.0" cut-back.

At the maximum efficiency point ($\phi = 0.22$), the reduction of the model fan performance is as follows:

	<u>Original Blades</u>	<u>0.5" Cut-Back</u>	<u>1.0" Cut-Back</u>
η_{MAX}	0.74	0.71	0.68
ϕ	0.387	0.372	0.345

In conclusion, the effect of 0.5" blade cut-back is to reduce model fan peak efficiency and head by about 4%. A cut-back of 1.0" reduces peak efficiency by about 8% and head by 11%. These results apply to the 8-bladed rotor fitted into the baseline housing. It is to be expected that the 11-bladed rotor, having higher blade solidity, should be less sensitive to blade cut-back.

JEFF (A) SCALE MODEL MIXED-FLOW FAN
HEAD COEFFICIENT AND EFFICIENCY

vs
FLOW COEFFICIENT

BASED ON FAN EXIT PRESSURE

$\bar{D}_2 = 7.406$ IN

RUN 71

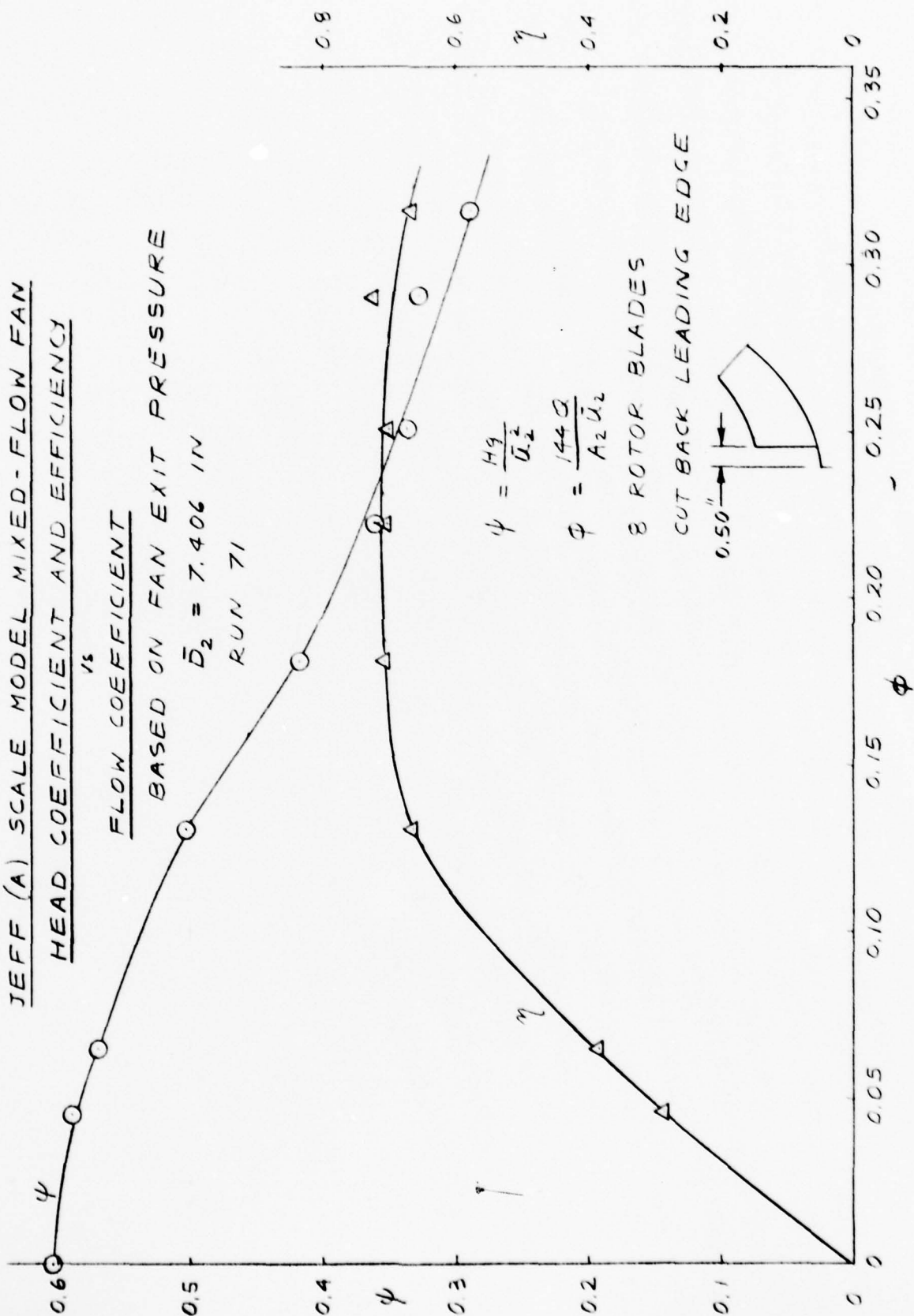


FIGURE 5.1.1-1

JEFF (A) SCALE MODEL MIXED-FLOW FAN
HEAD COEFFICIENT AND EFFICIENCY
 vs

FLOW COEFFICIENT

BASED ON FAN EXIT PRESSURE

$\bar{D}_2 = 7.406$ IN

RUN 72

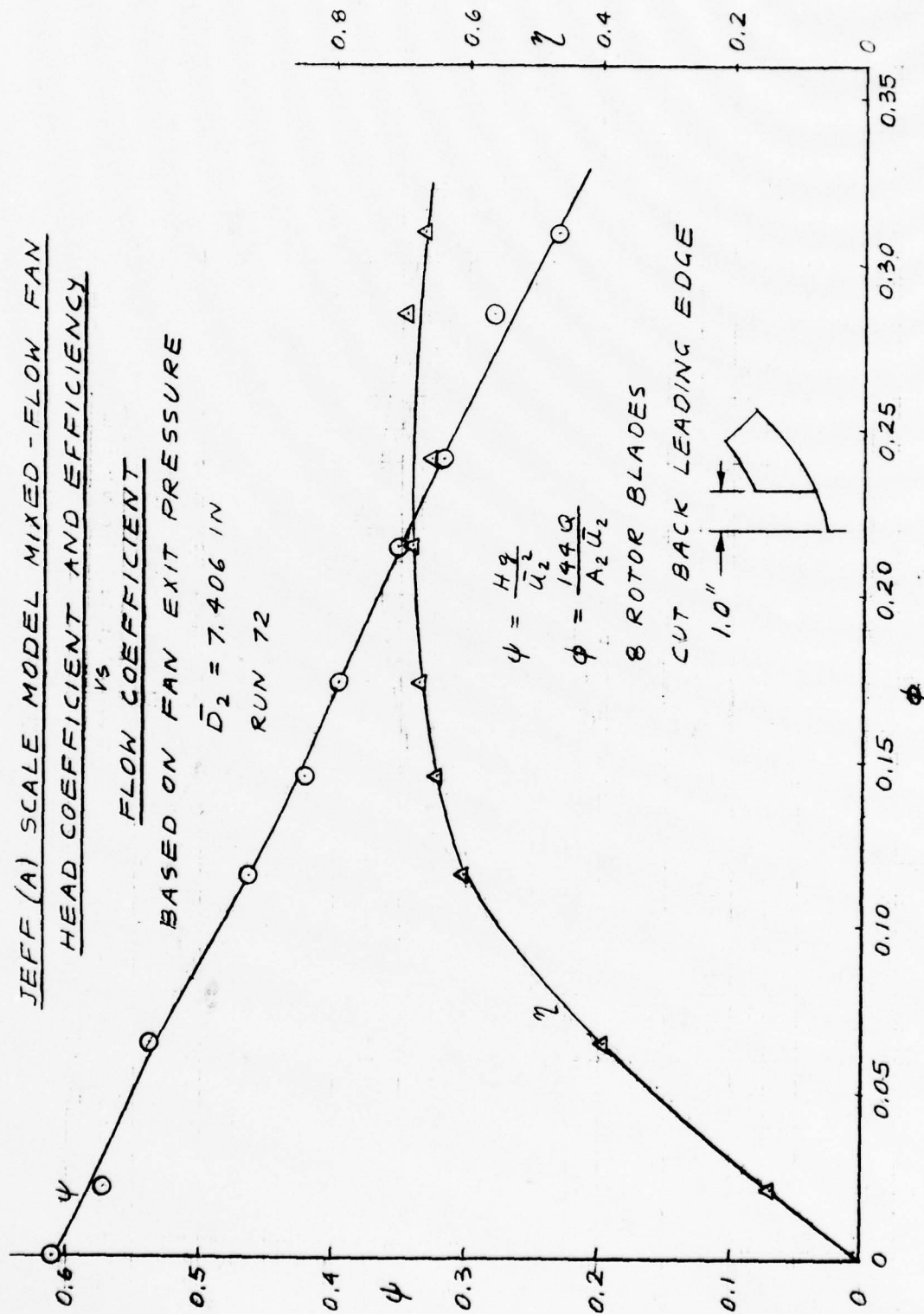


FIGURE 5.1.1-2

JEFF (A) SCALE MODEL MIXED-FLOW FAN
EFFECT OF ROTOR BLADE CUT BACK
ON PERFORMANCE

$\bar{D}_2 = 7.406$ IN
8 ROTOR BLADES

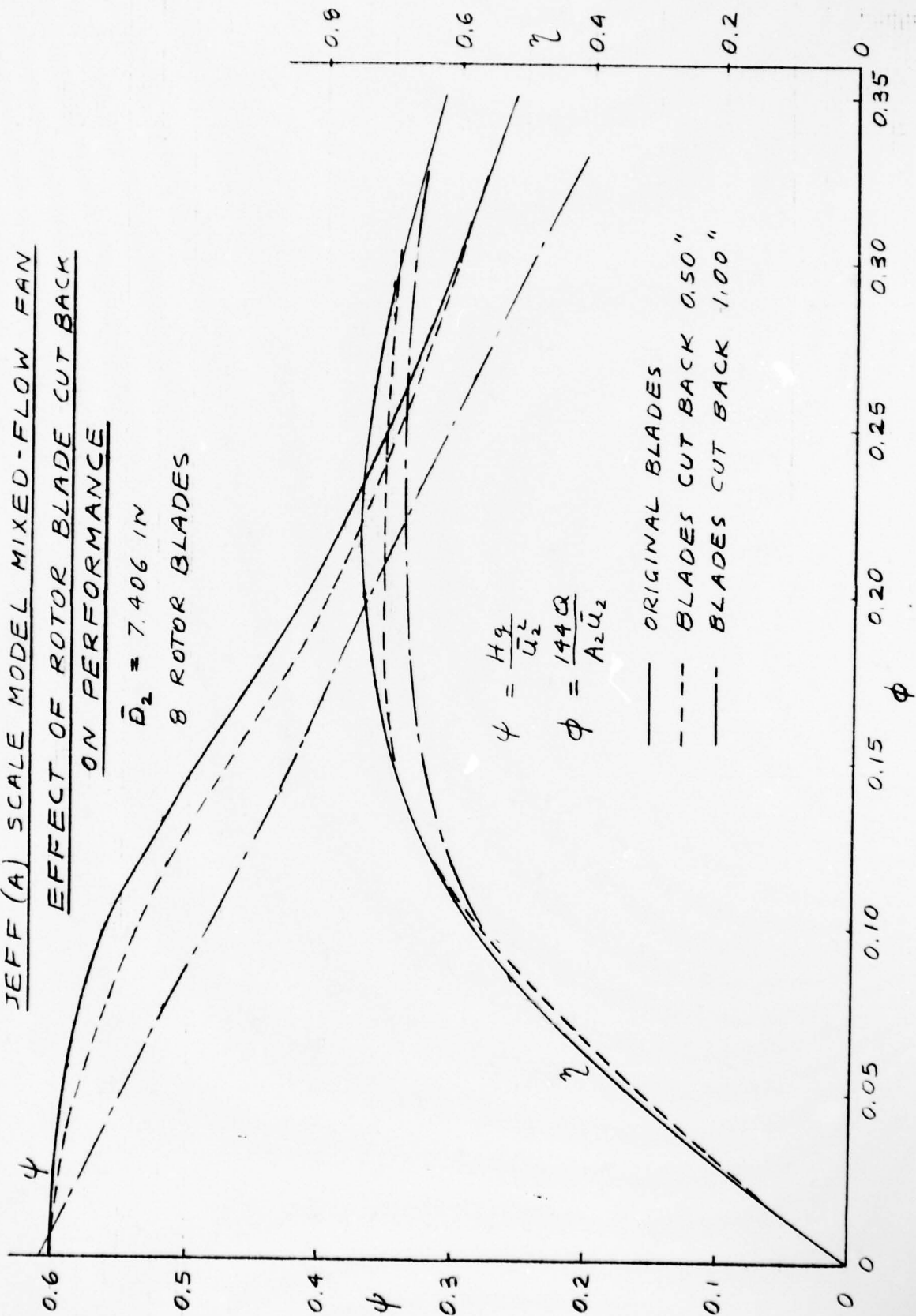


FIGURE 5.1.1-3

5. MODEL FAN PERFORMANCE (cont'd)

- 5.1.2 Effect of Rotor Exit Width on Fan Performance - Exit traverse data obtained using the eight bladed rotor and reported in Reference (3) disclosed the existence of a wake near the outer shroud. It is rationalized that the radial element blading allows the low energy fluid to be centrifuged out forming a wake near the outer shroud. The result is hardly any head rise along the tip streamline.

In order to study the effect of this wake on fan performance, the existing rotor was modified by reducing its exit width and was tested in the existing housing. Figure 5.1.2-1 shows the fan performance and Figure 5.1.2-2 compares it with the performance of the original wide exit rotor. It can be seen that the peak efficiency dropped by about 4 points. Only at flow coefficients $\phi > 0.285$ was efficiency improvement observed. However, the head coefficient was increased throughout the flow range.

In Figure 5.1.2-3, the static pressure distribution along the shroud is presented at three flow coefficients. As expected, the action of the rotor initially reduces the pressure below atmospheric and then increases it above atmospheric pressure. At shut off ($\phi = 0$) surge is taking place throughout the fan system. Air is entering the fan through the center of the rotor and is discharged through the tip clearance. Static pressure is above the atmospheric value over the entire length of the shroud.

Figures 5.1.2-4 and 5.1.2-5 show static and total pressure distributions across the rotor exit at flow coefficients of 0.42 and 0.25, respectively. Comparing the wide and narrow exit rotors, it appears that the head distribution is about the same for both cases. At the design flow coefficient of $\phi = 0.42$, the highest head is generated near the outer wall. At the flow

JEFF (A) SCALE MODEL MIXED-FLOW FAN
HEAD COEFFICIENT AND EFFICIENCY

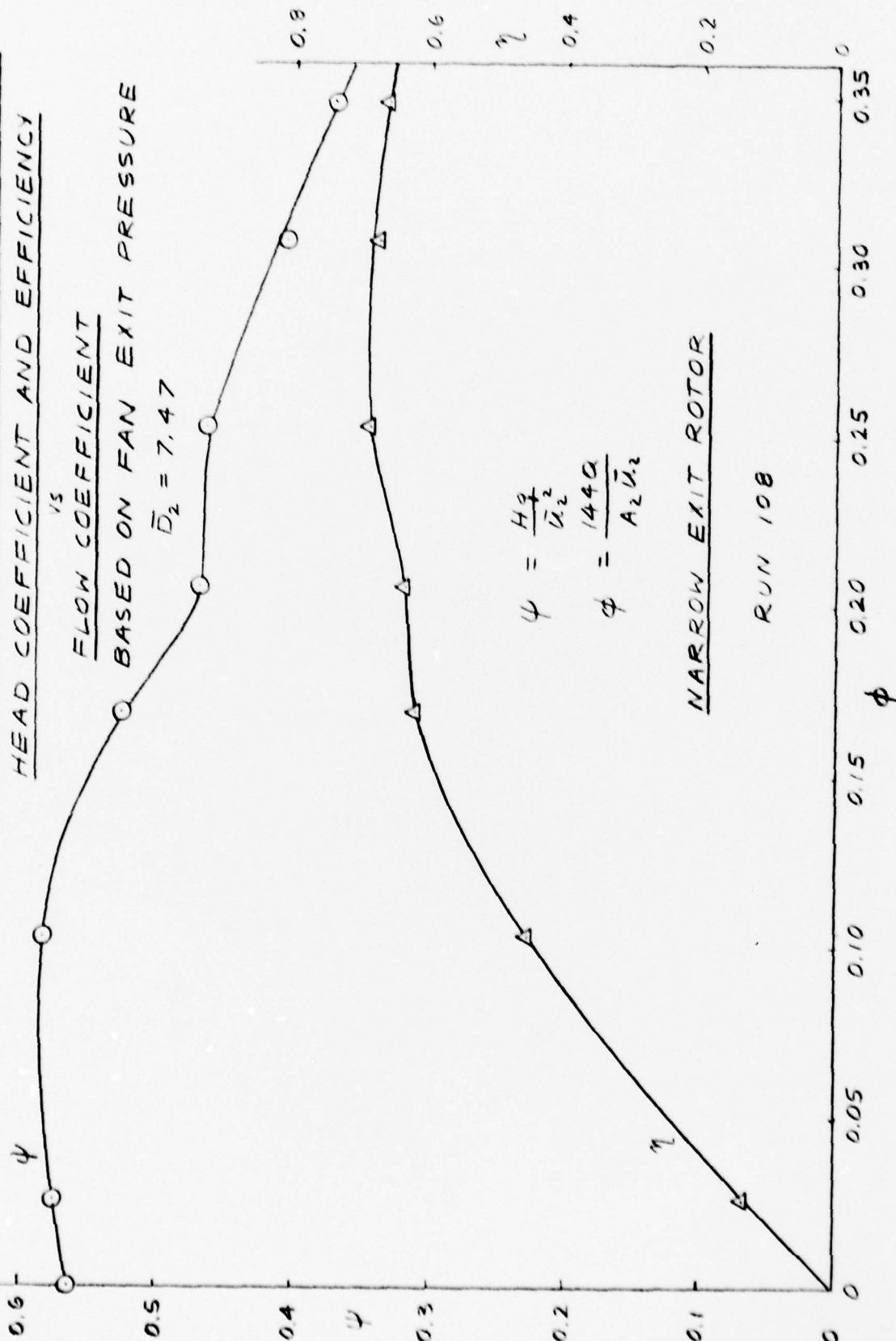


FIGURE 5.1.2-1

JEFF (A) SCALE MODEL MIXED-FLOW FAN
EFFECT OF ROTOR EXIT WIDTH
ON FAN PERFORMANCE

— NARROW ROTOR EXIT WIDTH
 $\bar{D}_2 = 7.47$ IN
--- ORIGINAL ROTOR, $\bar{D}_2 = 7.74$ IN

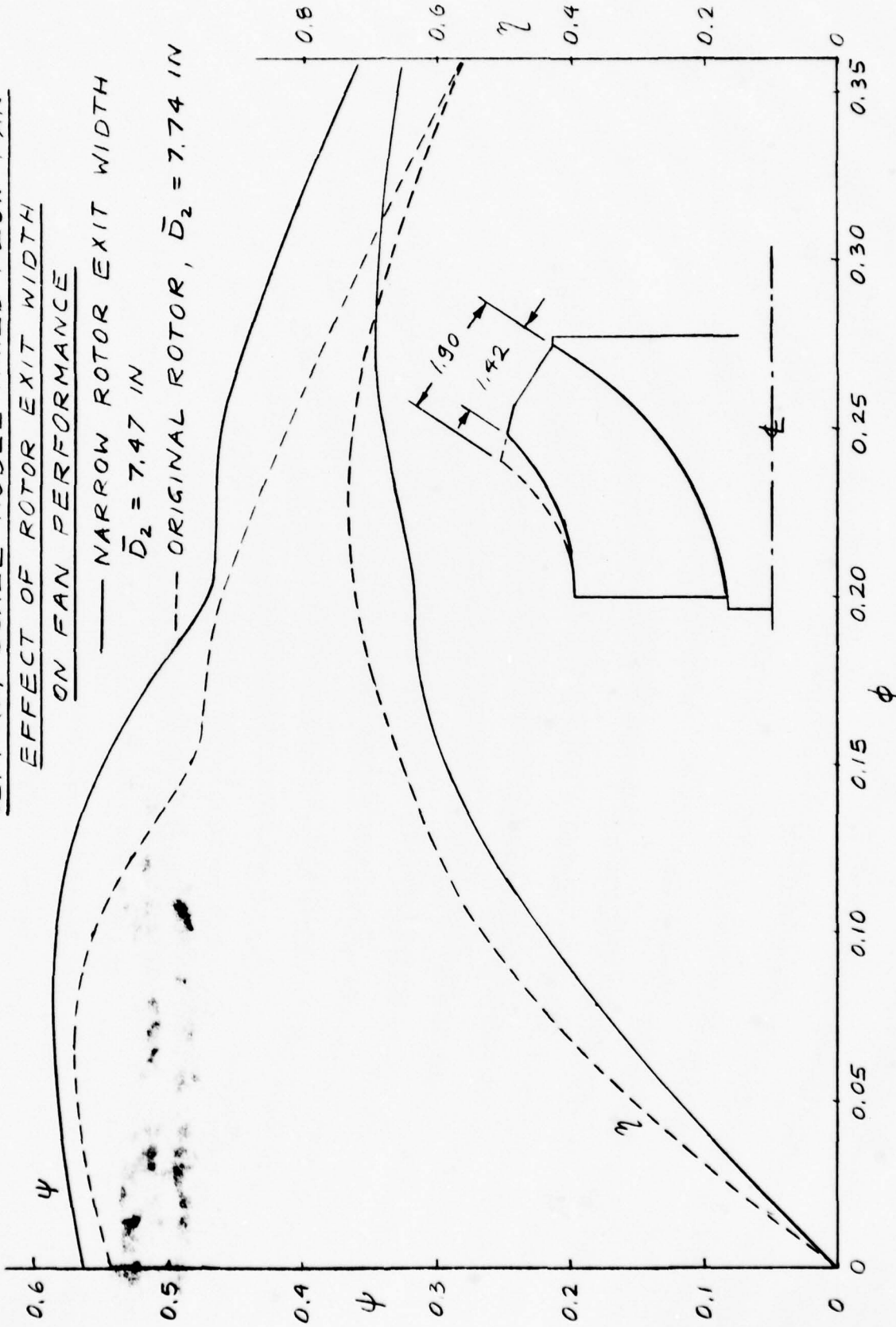


FIGURE 5.1.2-2

JEFF (A) SCALE MODEL MIXED-FLOW FAN

SHROUD STATIC PRESSURE

DISTRIBUTION

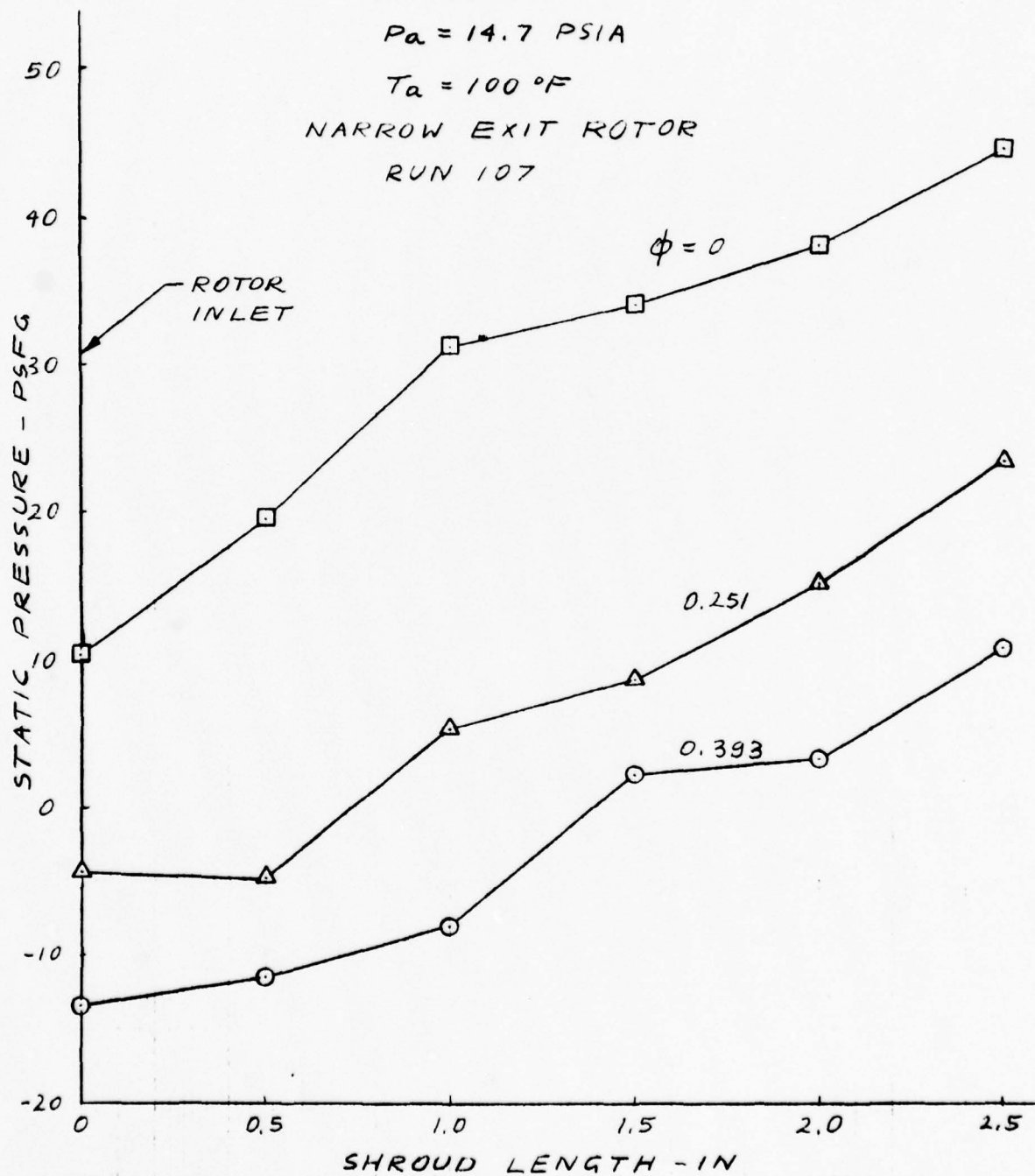
$N = 6000 \text{ RPM}$

$P_a = 14.7 \text{ PSIA}$

$T_a = 100^\circ \text{F}$

NARROW EXIT ROTOR

RUN 107



JEFF (A) SCALE MODEL MIXED-FLOW FAN
PRESSURE DISTRIBUTION AT ROTOR EXIT

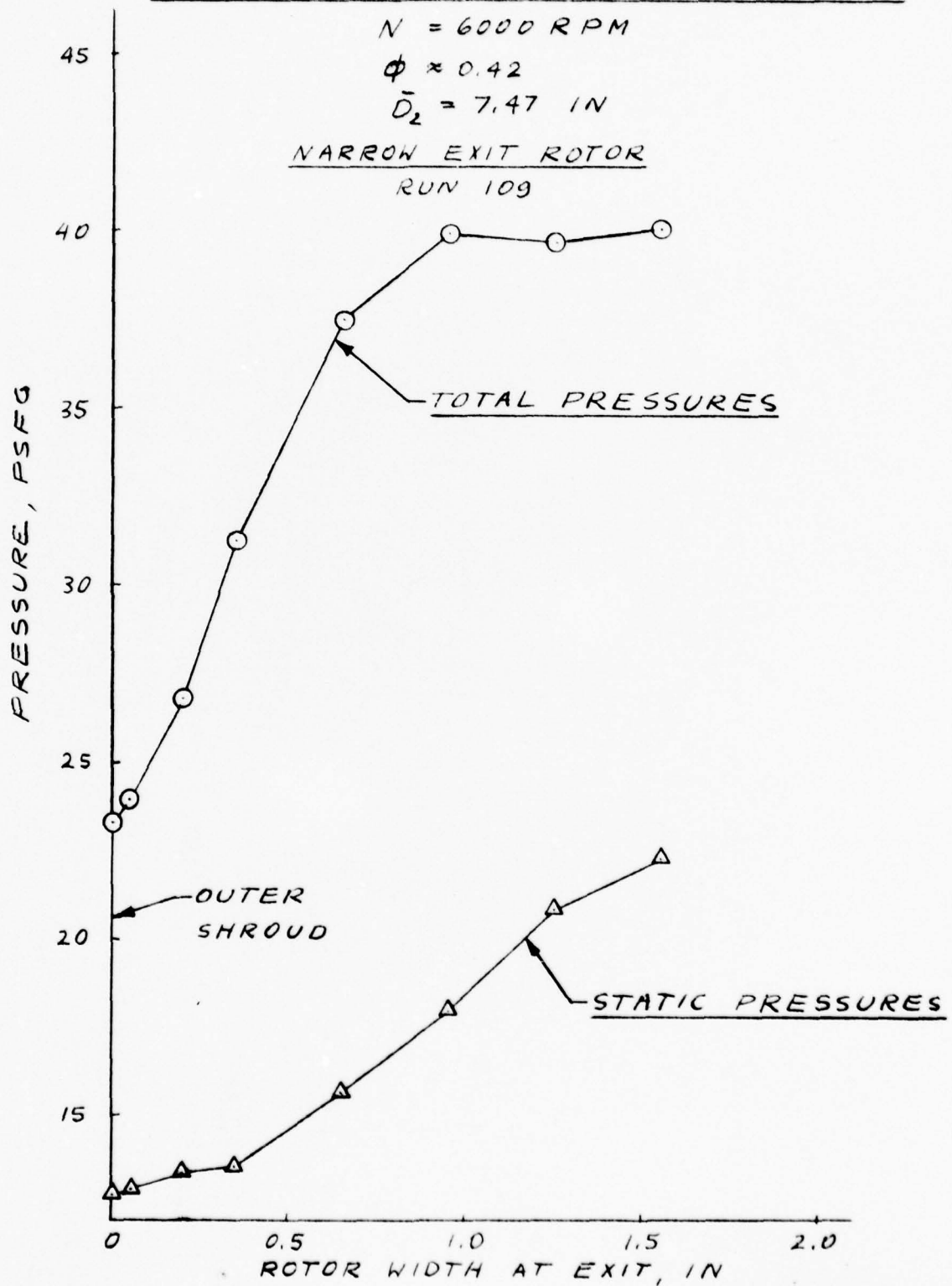
$N = 6000 \text{ RPM}$

$\phi \approx 0.42$

$\bar{D}_2 = 7.47 \text{ IN}$

NARROW EXIT ROTOR

RUN 109



JEFF (A) SCALE MODEL MIXED-FLOW FAN
PRESSURE DISTRIBUTION AT ROTOR EXIT

$N = 6000 \text{ RPM}$

$\phi \approx 0.25$

$\bar{D}_2 = 7.47 \text{ IN}$

NARROW EXIT ROTOR

RUN 109

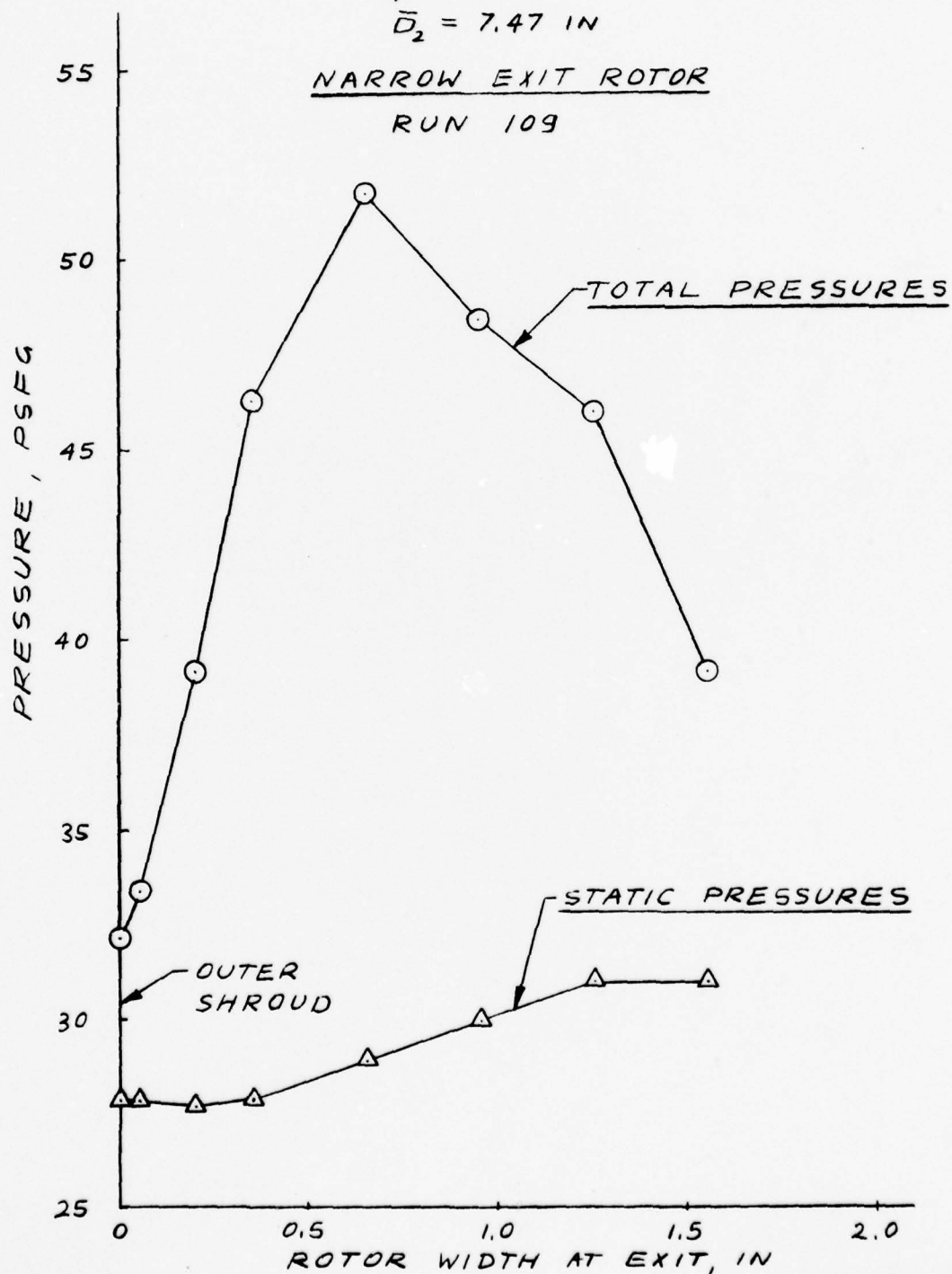


FIGURE 5.1.2-5

5. MODEL FAN PERFORMANCE (cont'd)

coefficient of $\phi = 0.25$, the highest head is generated near the mean exit radius.

Maldistribution of head at the rotor exit is attributed to the radial element blading. Three dimensional (twisted) blades are required to produce more uniform flow conditions.

5.2 Effect of IGV Position on Fan Performance

Inlet guide vanes can be used for ride control. Deflecting guide vanes in the direction of rotation throttles flow while deflection in the opposite direction may increase flow. However, the sensitivity of the fan to negative pre-whirl depends on rotor inlet to exit diameter ratio, specific speed and blade leading edge aerodynamic loading. With large diameter ratios, an impressive increase in flow has been demonstrated (Reference 4, Page 312).

5.2.1 Hub-To-Tip Pre-whirl Distribution

5.2.1.1 Rotor induced prerotation

The effect of the rotor on the flow extends into the fan inlet. This effect depends on the rotor inlet angles, flow capacity and peripheral velocity.

To determine inlet velocity diagrams, flow traverses were conducted prior to installation of the inlet guide vanes. Figure 5.2.1.1-1 shows a plot of blade angle β_1 , pre-whirl angle α_1 and incidence angle i versus radius to tip radius ratio. The flow survey was made at 6000 rpm and flow coefficients of 0.182, 0.299 and 0.331. It can be seen that the pre-whirl angle α_1 is positive every where except near the shroud where a wide variation of angles was measured, indicating possible flow reversal. At a flow coefficient of 0.299, which is close to the design flow coefficient, the rotor induced an average prerotation of about 9.5° resulting in an incidence angle of about 12.5° . As ϕ is reduced, both α_1 and i are increased (Figure 5.1.1.1-2).

JEFF (A) SCALE MODEL MIXED-FLOW FAN
 ROTOR INLET FLOW ANGLES

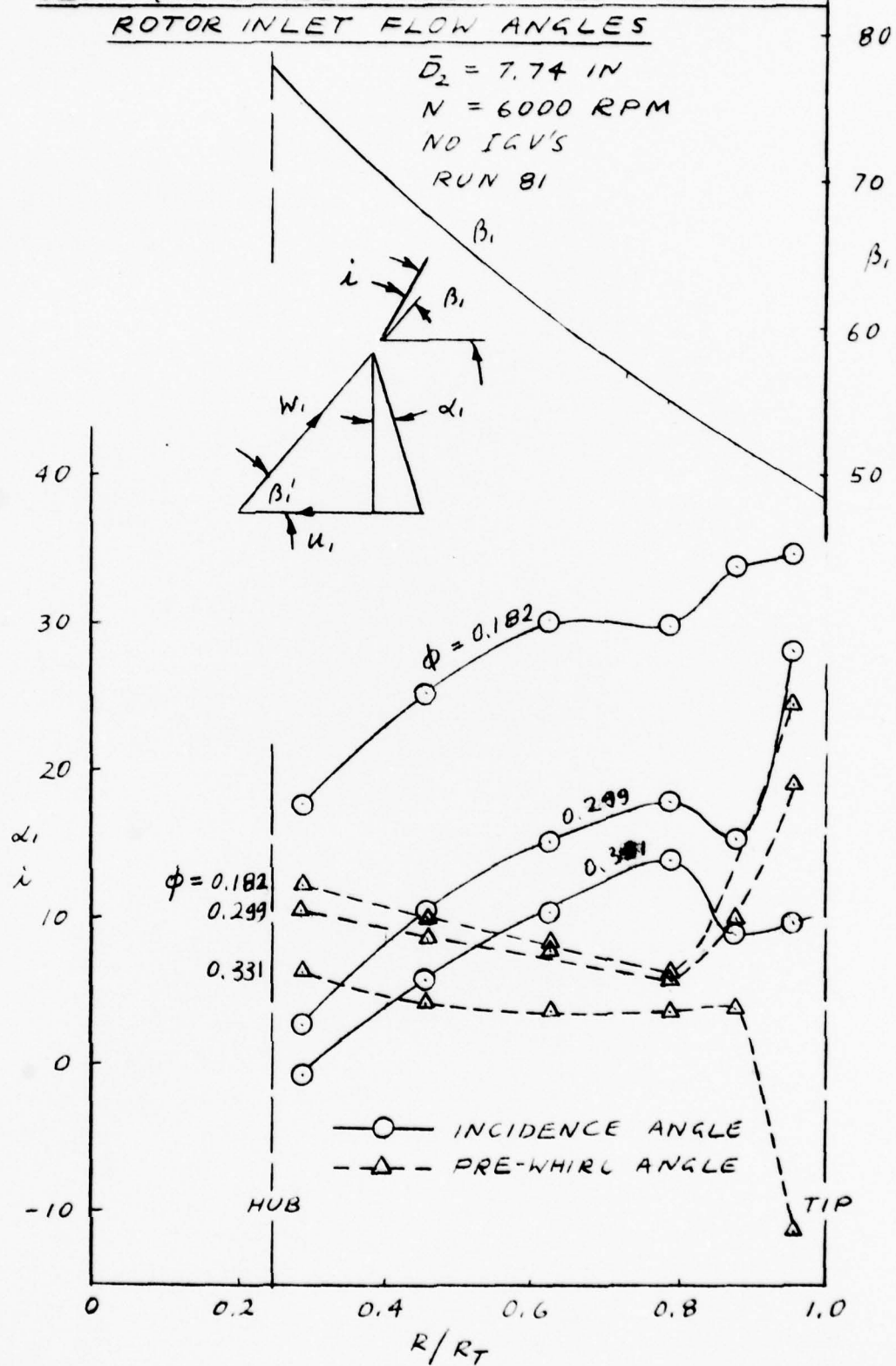


FIGURE 5.2.1.1-1

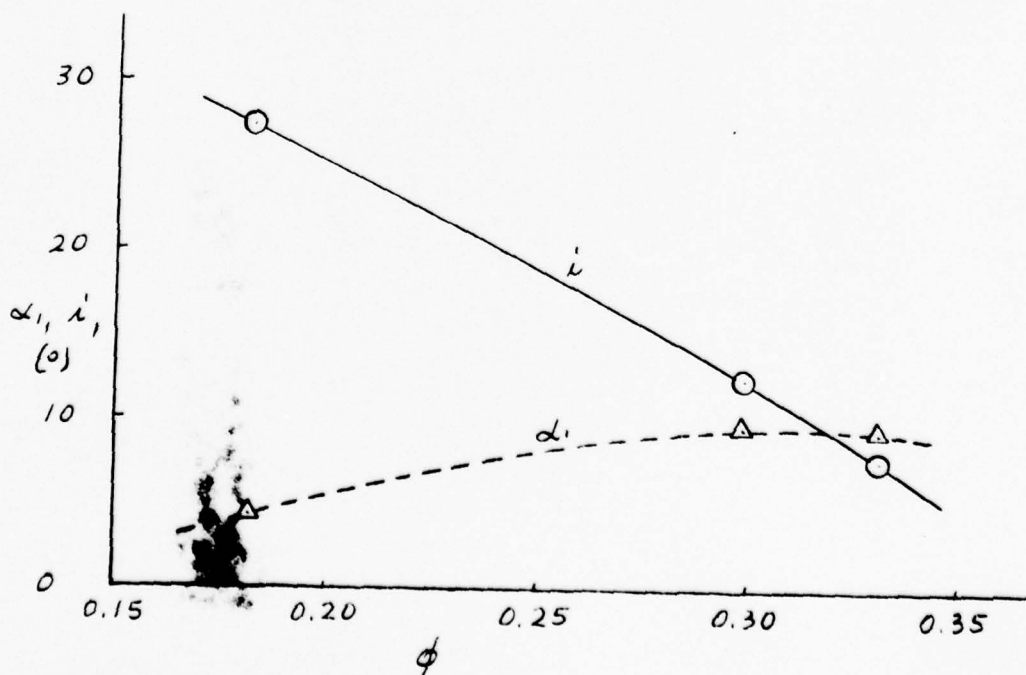
JEFF (A) SCALE MODEL MIXED-FLOW FAN
PRE-WHIRL AND INCIDENCE ANGLES

VS
FLOW COEFFICIENT

$$\bar{D}_2 = 7.74 \text{ IN}$$

$$N = 6000 \text{ RPM}$$

RUN 81
(AVERAGE ANGLES)



12/12/78

FIGURE 5.2.1.1-2

5. MODEL FAN PERFORMANCE (cont'd)

5.2.1.2 Pre-whirl Distribution - IGV Position $\alpha_1=0^\circ$

In Figure 5.2.1.2-1, the pre-whirl angle is plotted versus IGV pitch in degrees (-12° to $+12^\circ$) with radius as a parameter. The highest prerotation angles are recorded at the suction side of the blades (-4° on the plot). The lowest prerotation angles occur on the pressure surface ($+4^\circ$). It was not possible to conduct a flow traverse in the blade wake (0° on the plot) and it was necessary to assume $\alpha_1=0^\circ$ at that point. For this reason, an α_1 distribution in the range of -4° to $+4^\circ$ is indicated by means of dotted lines.

By averaging the prerotation angles along each radius, the α_1 distribution with radius ratio can be plotted as seen in Figure 5.2.1.2-2. With this rotor's inlet angles, IGV's smooth out the pre-whirl and incidence angle distributions with radius. The average prerotation is reduced and the average incidence angle is increased.

5.2.1.3 Pre-whirl Distribution - IGV Position $\alpha_1=+20^\circ$

In order to reduce the average incidence angle to zero, the flow traverse was conducted with an IGV setting of $+20^\circ$. Figure 5.2.1.3-1 shows the tangential and radial pre-whirl distributions. A comparison of Figures 5.2.1.2-1 and 5.2.1.3-1 indicates a higher level of pre-whirl and also a more uniform tangential pre-whirl distribution for IGV setting of $+20^\circ$. Even more revealing is the plot of tangential averaged α_1 versus radius ratio, as seen in Figure 5.2.1.3-2. Setting the IGV at $+20^\circ$ produces about $+24^\circ$ pre-whirl and close to 0° average incidence angle. A subsequent test of the fan model with an IGV setting of $+20^\circ$ demonstrated the highest fan efficiency.

PREWHIRL ANGLE DISTRIBUTION

THICK IGV POSITION 0°

$$\phi = 0.296$$

$N = 6000 \text{ RPM}$

$$\bar{D}_2 = 7.74 \text{ IN}$$

RUN 85

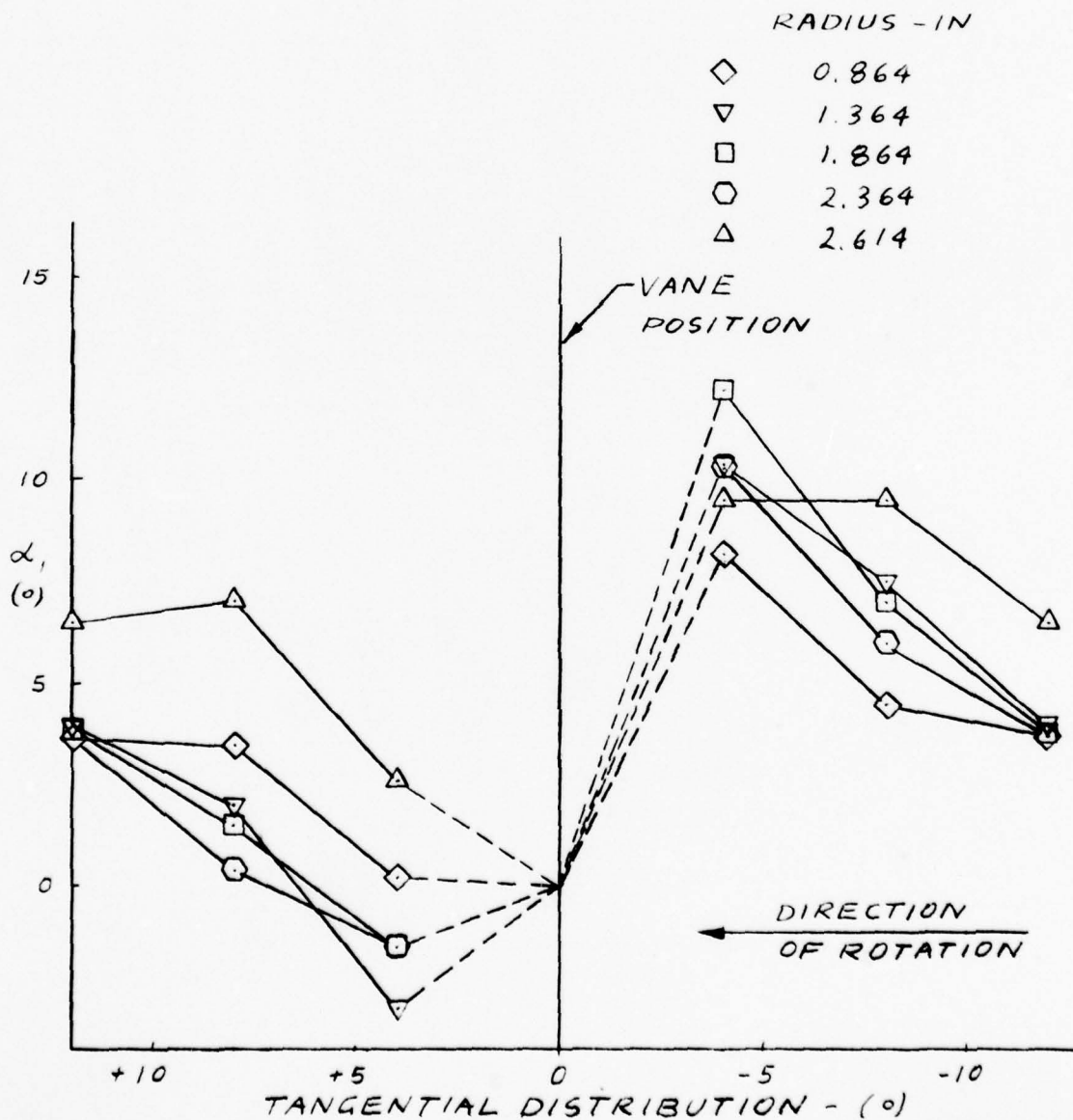


FIGURE 5.2.1.2-1

JEFF (A) SCALE MODEL MIXED-FLOW FAN
ROTOR INLET FLOW ANGLES

$$\bar{D}_2 = 7.74 \text{ IN}$$

$$N = 6000 \text{ RPM}$$

$$\phi \approx 0.296$$

THICK IGV'S IN NEUTRAL POSITION
 RUN 85

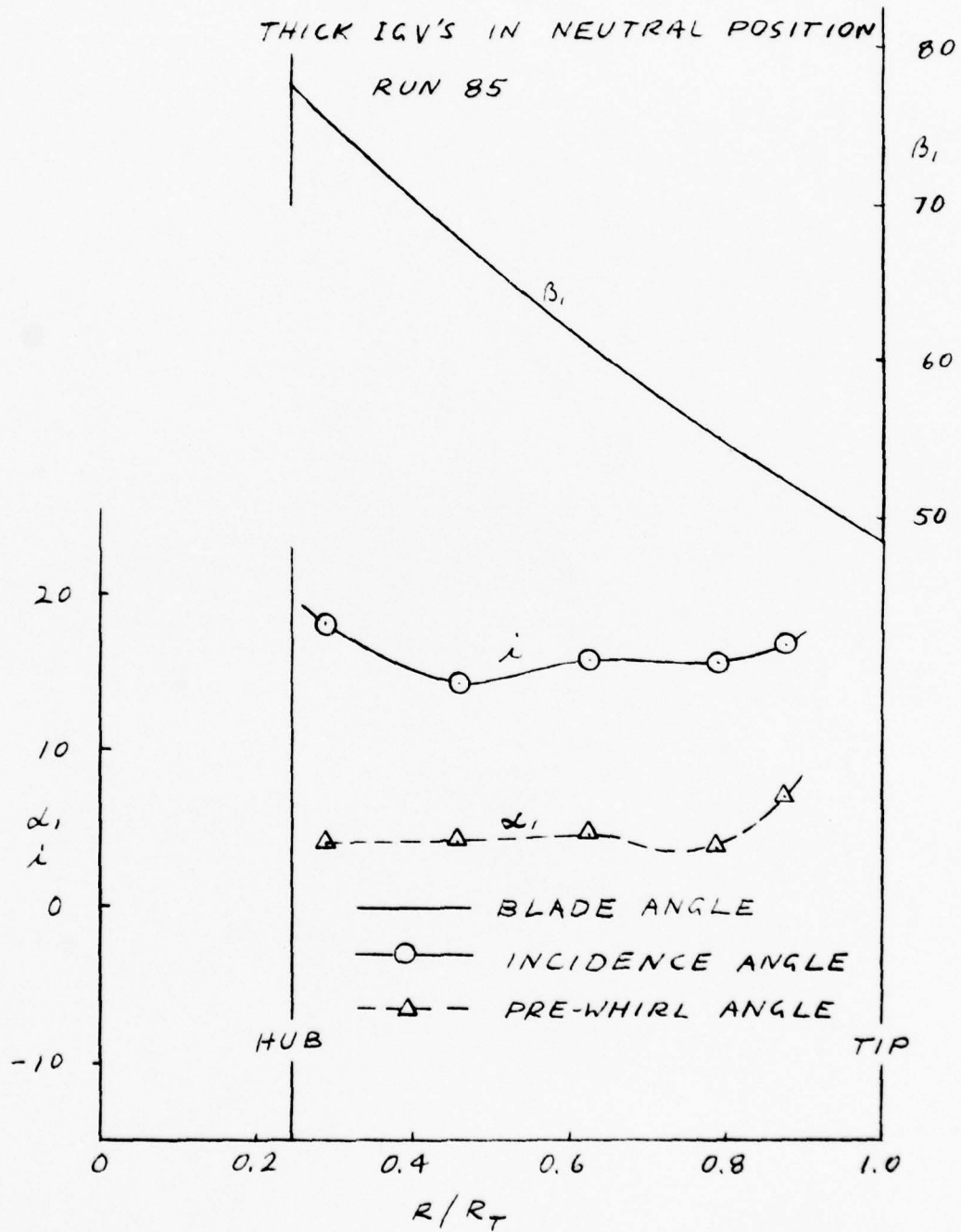


FIGURE 5.2.1.2-2

PRE-WHIRL ANGLE DISTRIBUTION

THICK IGV POSITION +20°

$$\phi \approx 0.287$$

$N = 6000 \text{ RPM}$

$\bar{D}_2 = 7.74 \text{ IN}$

RUN 86

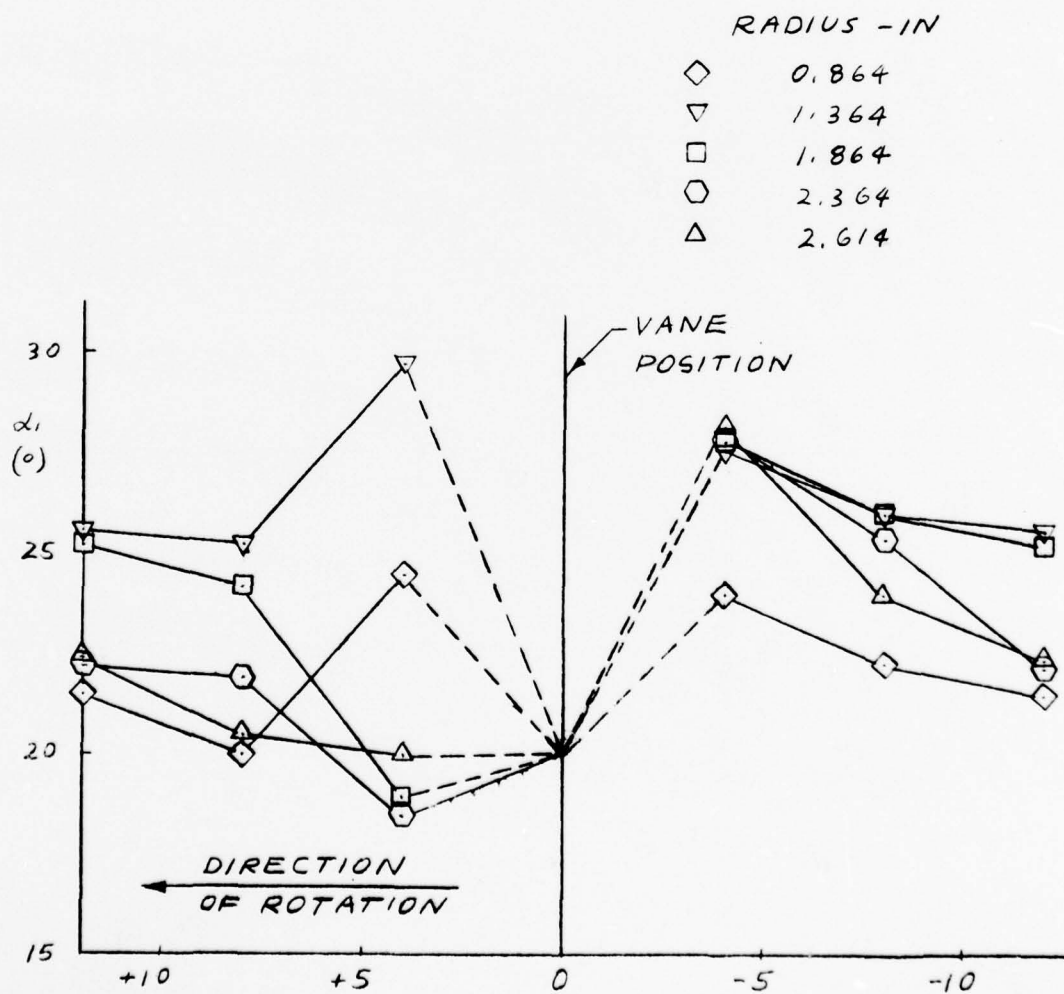


FIGURE 5.2, 1.3-1

JEFF (A) SCALE MODEL MIXED-FLOW FAN
ROTOR INLET FLOW ANGLES

$$\bar{D}_2 = 7.74 \text{ IN}$$

$$N = 6000 \text{ RPM}$$

$$\phi \approx 0.287$$

$$\text{IGV POSITION} = +20^\circ$$

RUN 86

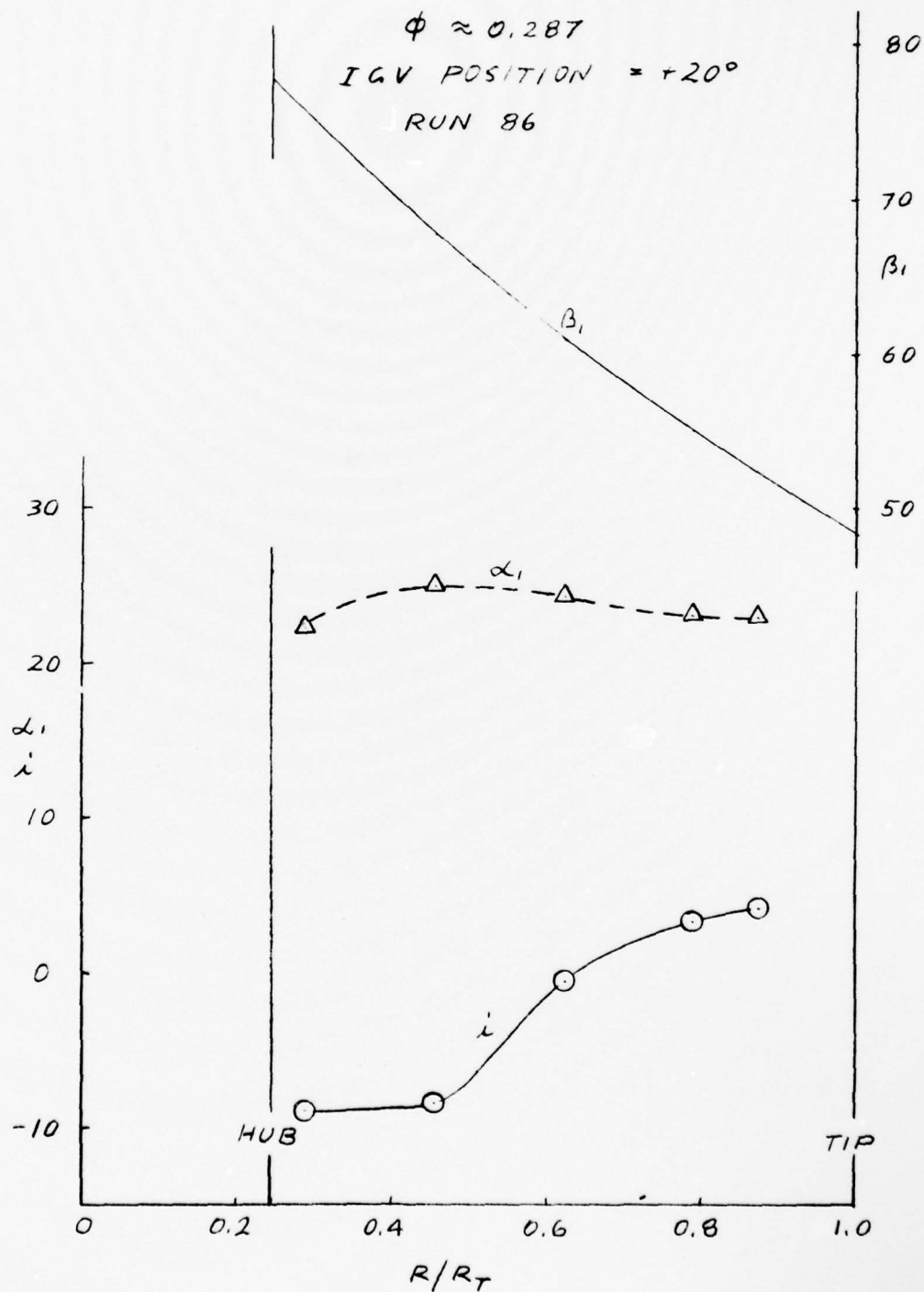


FIGURE 5.2.1.3-2

5.2.1.4 Pre-whirl Distribution, Thin IGV's, $\alpha_1=0^0$

The wide tangential variation in pre-whirl angle can be reduced by reducing the inlet vanes thickness as can be seen in Figure 5.2.1.4-1. Vanes having a constant thickness of 0.04 IN produced a substantially lower blockage (higher blockage factor). Averaging the prerotation angles along each radius gives the plot of α_1 and i in Figure 5.2.1.4-2.

5.2.1.5 Summary of Rotor Inlet Traverse Data

The results of the rotor inlet traverse data are summarized in Table 6. Examination of this summary leads to the following conclusions:

- (a) A rotor designed for large incidence angles will induce positive prerotation.
- (b) This prerotation can be reduced by placing inlet guide vanes at zero position.
- (c) Thick vanes produce a wider tangential variation in the pre-whirl distribution than thin ones.
- (d) For this particular rotor, an IGV setting of $+20^0$ produces an average prerotation of $+24^0$ and an average incidence of -2^0 .

5.2.2 Effect of IGV Setting on Fan Performance - Flat Vanes

Thick Vanes

Figures 5.2.2-1 to 5.2.2-5 show fan performance at IGV settings of 0^0 to $+40^0$. It can be seen that IGV's cause a loss in efficiency even at zero setting angle compared to a fan without inlet guide vanes (Figure 5.2.2-6). The loss in efficiency is due primarily to incidence at the rotor inlet. The best efficiency was obtained with an IGV

PREWHIRL ANGLE DISTRIBUTION

THIN IGV POSITION 0°

$N = 6000 \text{ RPM}$

$\phi = 0.299$

$\bar{D}_2 = 7.74 \text{ IN}$

RUN 96

RADIUS - IN

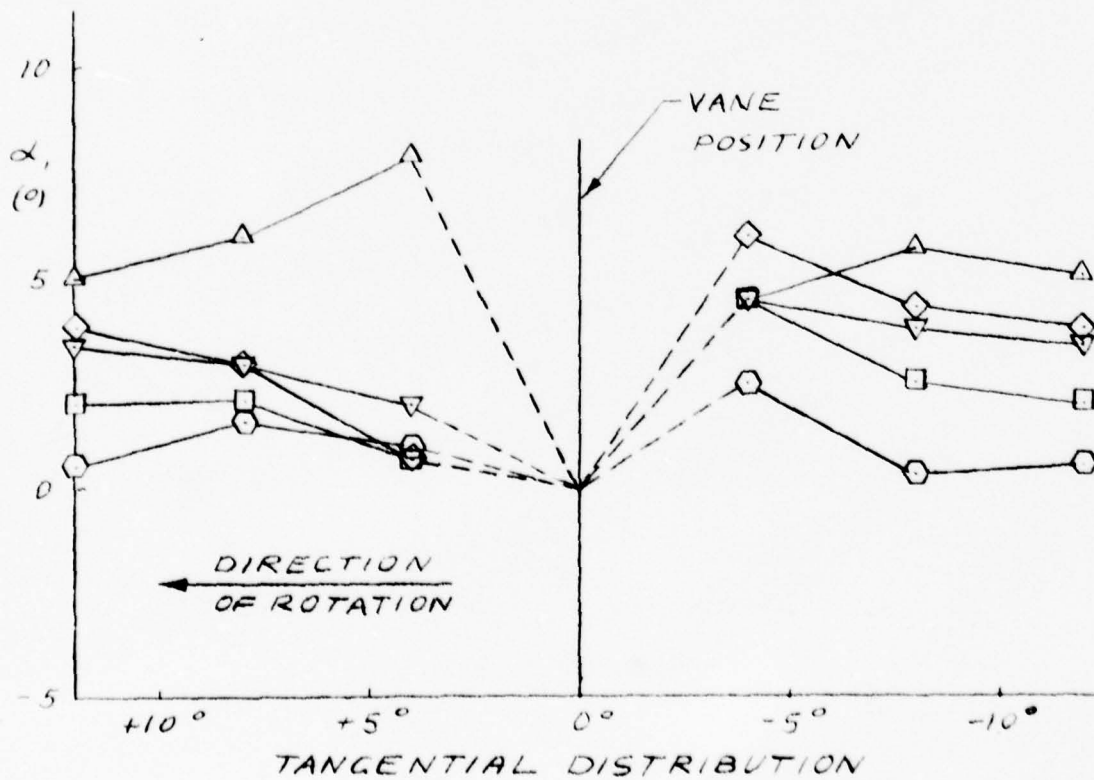
0.864

1.364

1.864

2.364

2.614



12/7/78

FIGURE 5.2.1.4-1

JEFF (A) SCALE MODEL MIXED-FLOW FAN
ROTOR INLET FLOW ANGLES

$$\bar{D}_2 = 7.74 \text{ IN}$$

$$N = 6000 \text{ RPM}$$

$$\phi = 0.299$$

THIN ICV POSITION = 0°

RUN 96

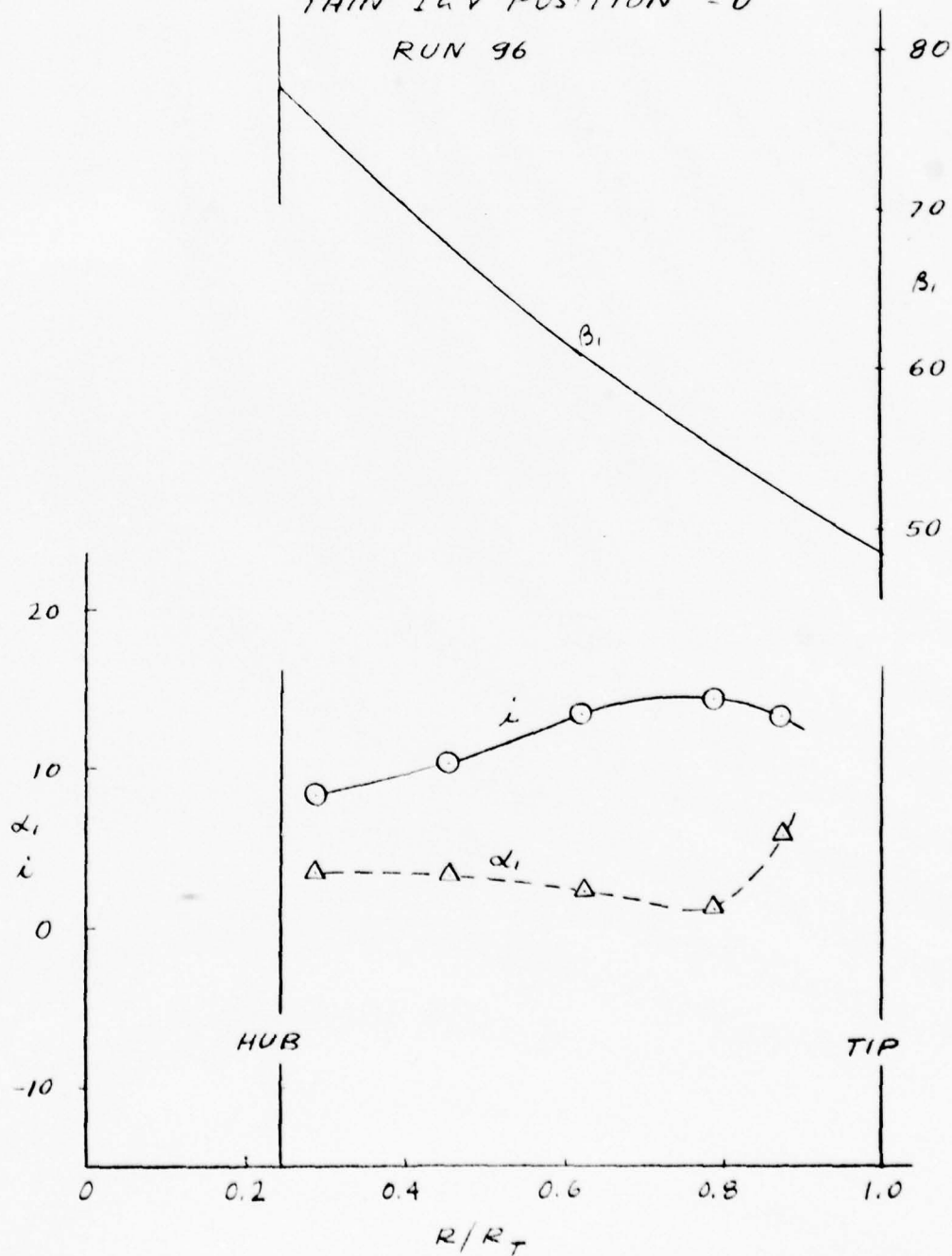


FIGURE 5,2,1,4-2

TABLE 6

SUMMARY OF MODEL ROTOR INLET TRAVERSE DATA

N = 6000 RPM

IGV SETTING		NO IGV'S	THIN IGV'S	THICK IGV'S	
				0°	+20°
FLOW COEFFICIENT	ϕ	0.299	0.299	0.296	0.287
PRE-WHIRL ANGLE, (°)		+ 9.5	+ 3.2	+ 4.7	+23.6
INCIDENCE ANGLE, (°)	i	+12.5	+15.0	+16.2	- 2.0

JEFF (A) SCALE MODEL MIXED-FLOW FAN
HEAD COEFFICIENT AND EFFICIENCY

vs

FLOW COEFFICIENT

BASED ON FAN EXIT PRESSURE

$\bar{D}_2 \approx 7.74$ IN

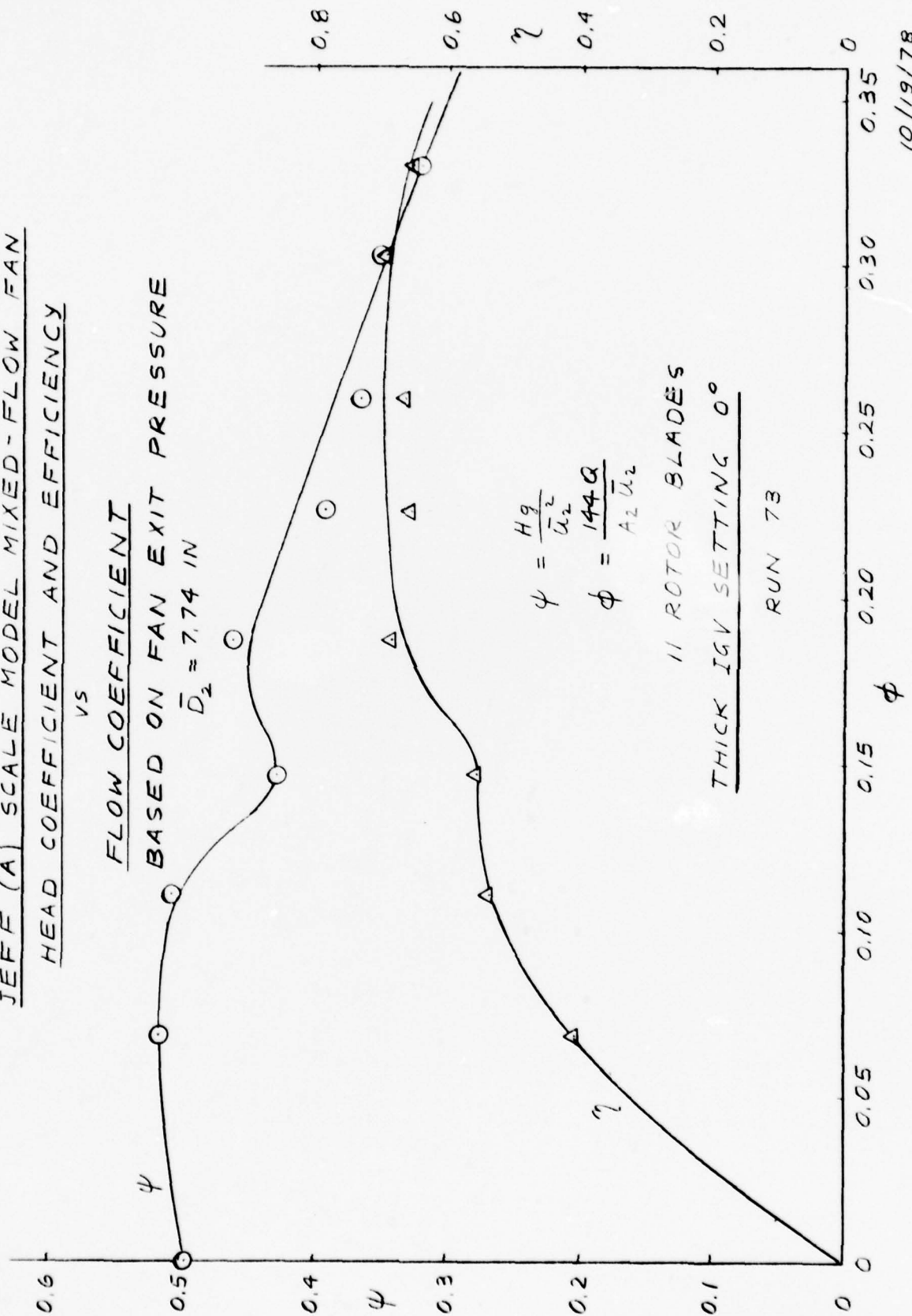


FIGURE 5.2.2-1

JEFF (A) SCALE MODEL MIXED-FLOW FAN
HEAD COEFFICIENT AND EFFICIENCY

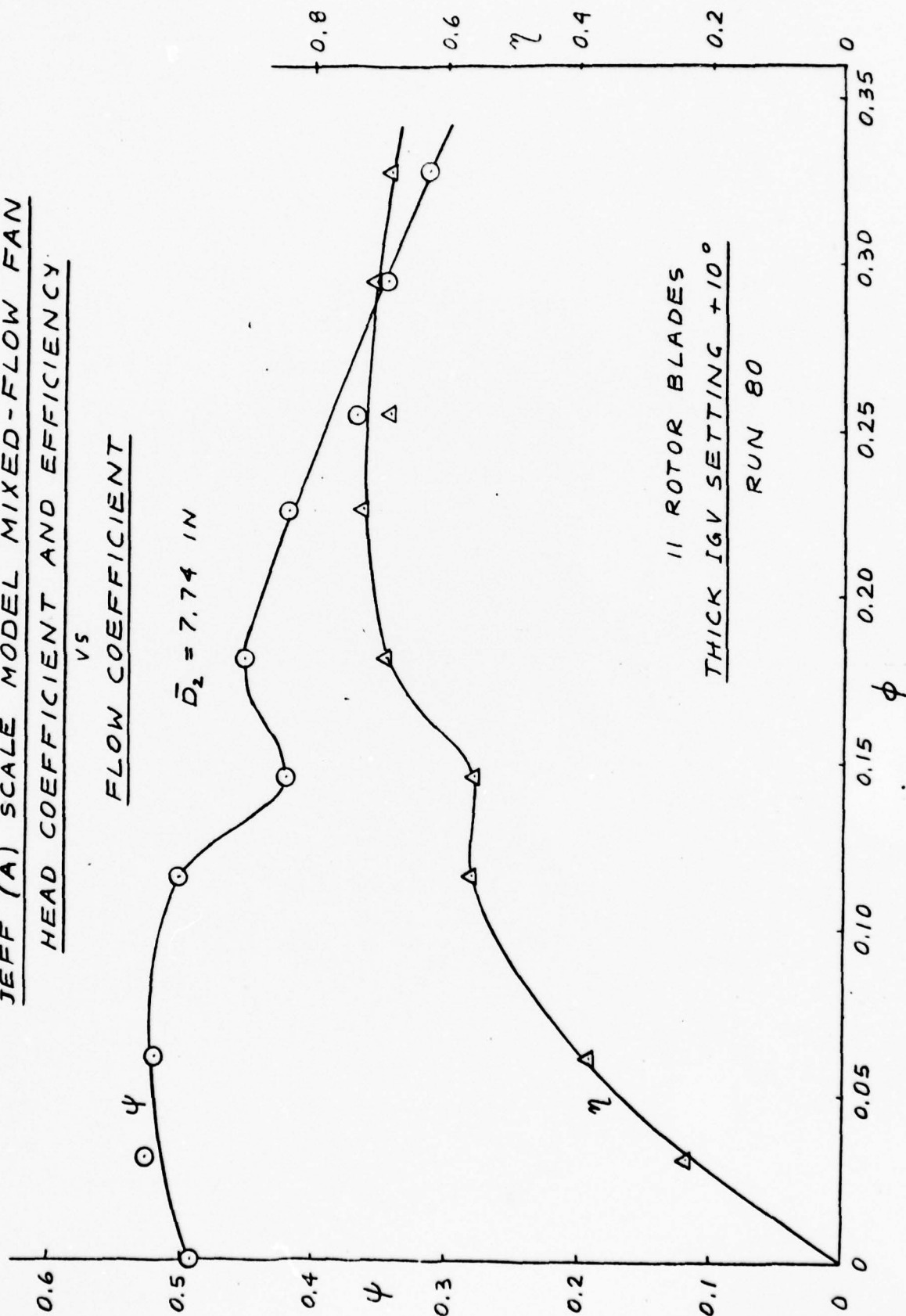


FIGURE 5.2.2-2

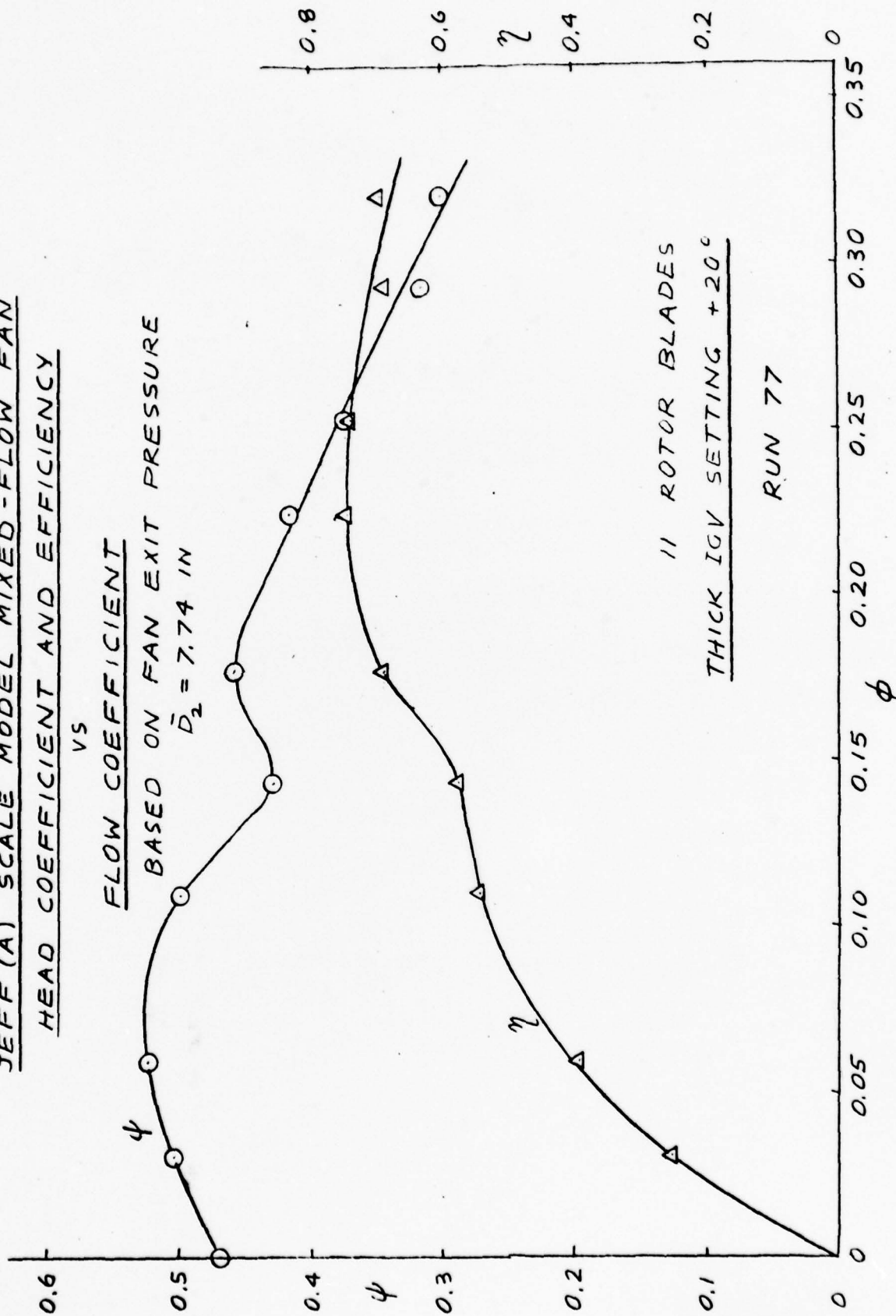
JEFF (A) SCALE MODEL MIXED-FLOW FAN
HEAD COEFFICIENT AND EFFICIENCY

VS

FLOW COEFFICIENT

BASED ON FAN EXIT PRESSURE

$\bar{D}_2 = 7.74$ IN



11 ROTOR BLADES

THICK IGV SETTING +20°

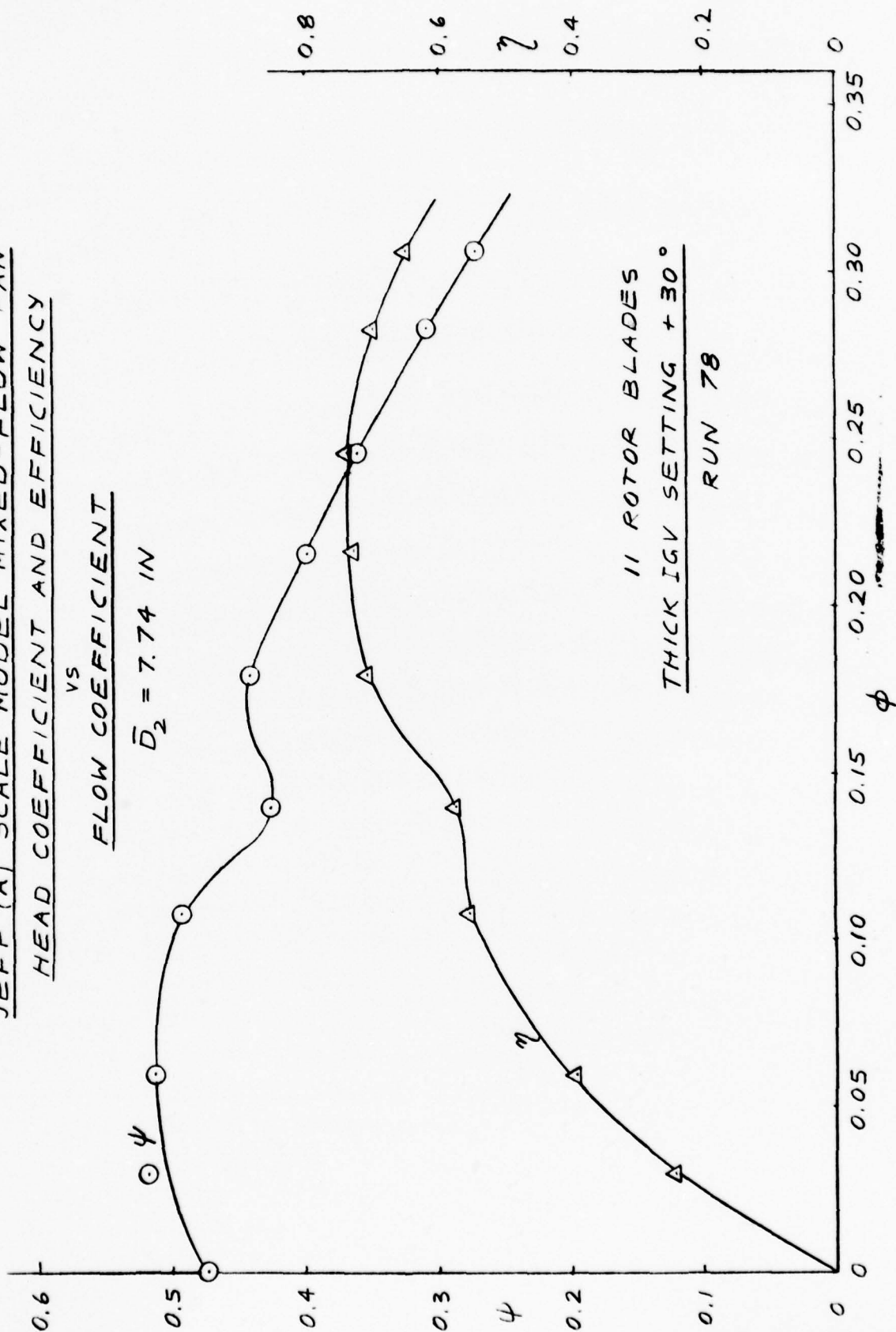
RUN 77

FIGURE 5.2.2-3

JEFF (A) SCALE MODEL MIXED-FLOW FAN
HEAD COEFFICIENT AND EFFICIENCY

vs
FLOW COEFFICIENT

$\bar{D}_2 = 7.74$ IN



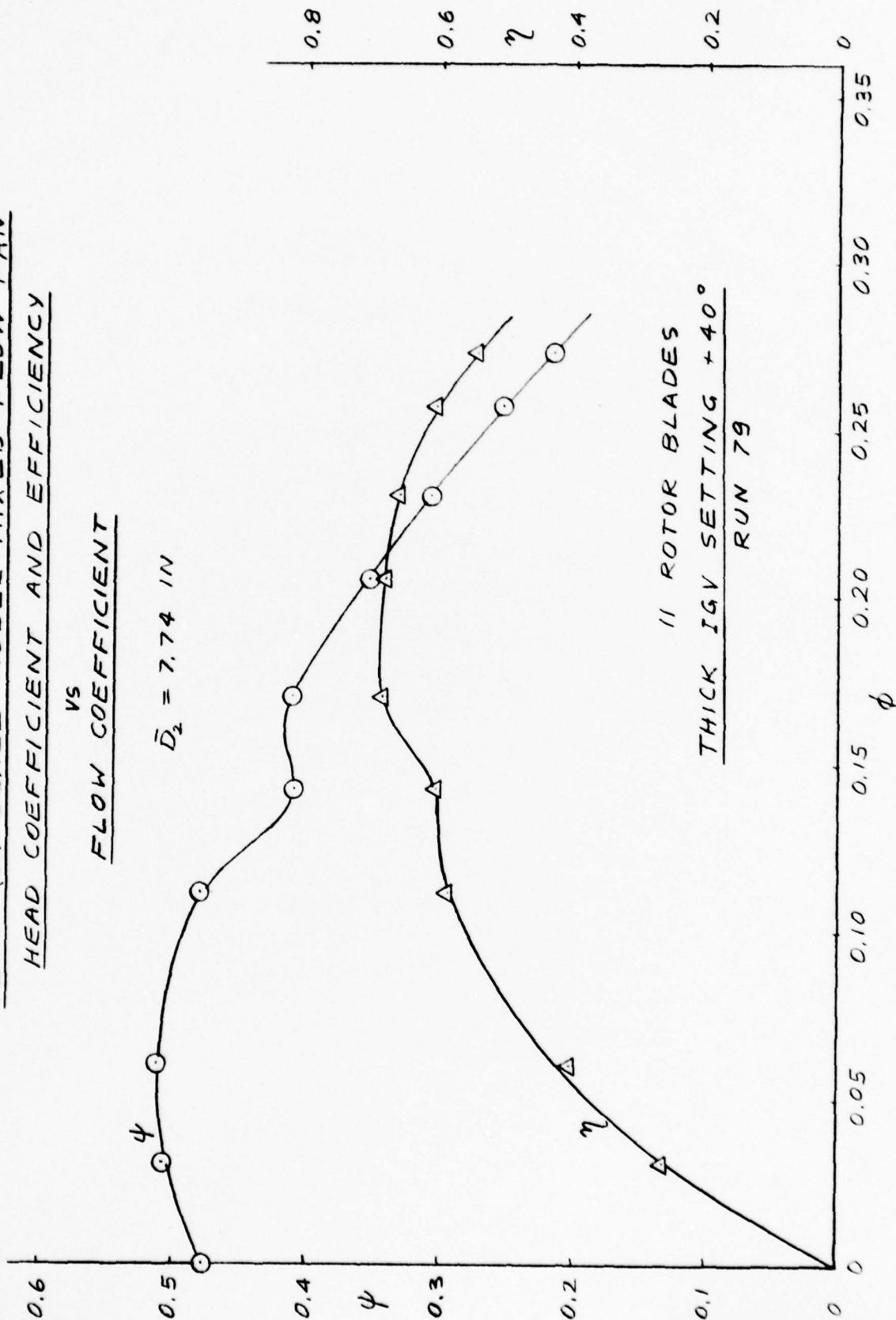
11 ROTOR BLADES
THICK IGV SETTING +30°
 RUN 78

FIGURE 5.2.2-4

JEFF (A) SCALE MODEL MIXED-FLOW FAN
HEAD COEFFICIENT AND EFFICIENCY

VS
FLOW COEFFICIENT

$\bar{D}_2 = 7.74$ IN



11 ROTOR BLADES
 THICK IG V SETTING +40°
 RUN 79

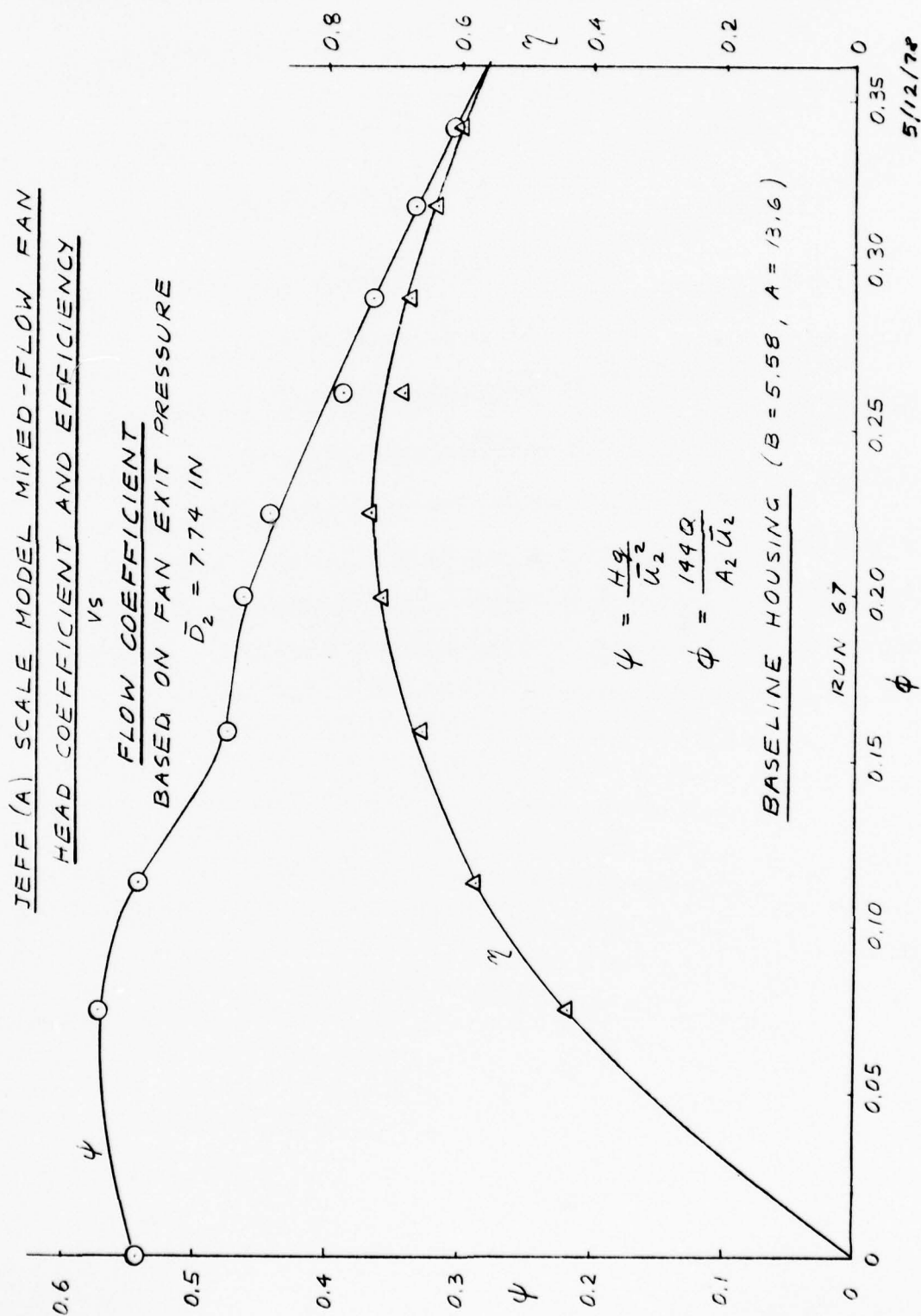


FIGURE 5.2.2 -6

5. MODEL FAN PERFORMANCE (CONT'D)

setting of $+20^\circ$ which coincides with a minimum of incidence as determined by traverse data (Figure 5.2.1.3-2).

In Figure 5.2.2-7, test results for four IGV settings are combined to illustrate the throttling capability of the guide vanes. It can be seen that the peak efficiency at IGV settings of 0° and $+40^\circ$ is about the same, and at a setting of $+20^\circ$ is about 5 points higher.

Inlet guide vanes, regardless of their setting intensifies stall at a flow coefficient of 0.15. It is expected that if the rotor inlet angles are reduced (thereby reducing aerodynamic loading), the stall would be eliminated.

Figures 5.2.2-8 to 5.2.2-11 show fan performance at negative IGV settings of -10° to -40° . It can be seen that the fan performance is poor and flow throttling is taking place. It is evident from traverse tests that the negative IGV setting increases rotor incidence angles which in turn, causes rotor resistance to flow to increase. A rotor designed for zero incidence angles is expected to improve fan performance at negative IGV positions.

In Figure 5.2.2-12, the results for all negative IGV settings are plotted together to show the change in head coefficient and efficiency with flow coefficient.

Thin Vanes

The IGV's used in the above tests had thick airfoil profiles which produced a substantial blockage ($B=0.81$). In order to assess the effect of IGV blockage on fan performance, 0.04" thick vanes were constructed and tested in 0° , -20° , and $+20^\circ$ positions. Figures 5.2.2-13 to 5.2.2-15 show the fan performance with the thin IGV's. At vane positions

JEFF (A) SCALE MODEL MIXED-FLOW FAN
EFFECT OF POSITIVE IGV SETTING ON
FAN PERFORMANCE

FLAT VANES

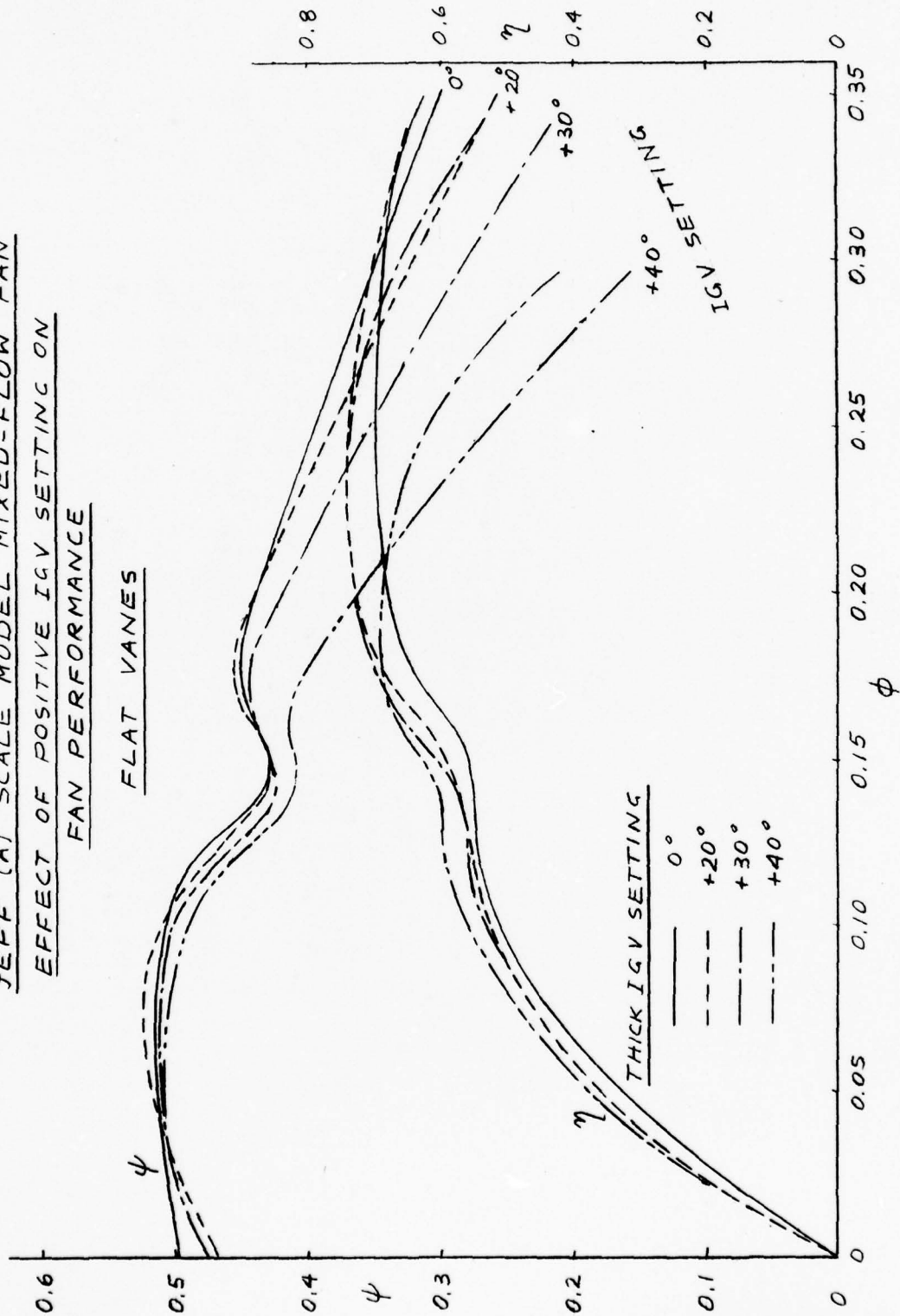


FIGURE 5.2.2-7

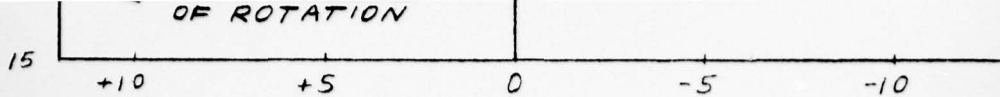


FIGURE 5.2.1.3-1

JEFF (A) SCALE MODEL MIXED-FLOW FAN
HEAD COEFFICIENT AND EFFICIENCY

VS

FLOW COEFFICIENT
BASED ON FAN EXIT PRESSURE

$\bar{D}_2 = 7.74$ IN

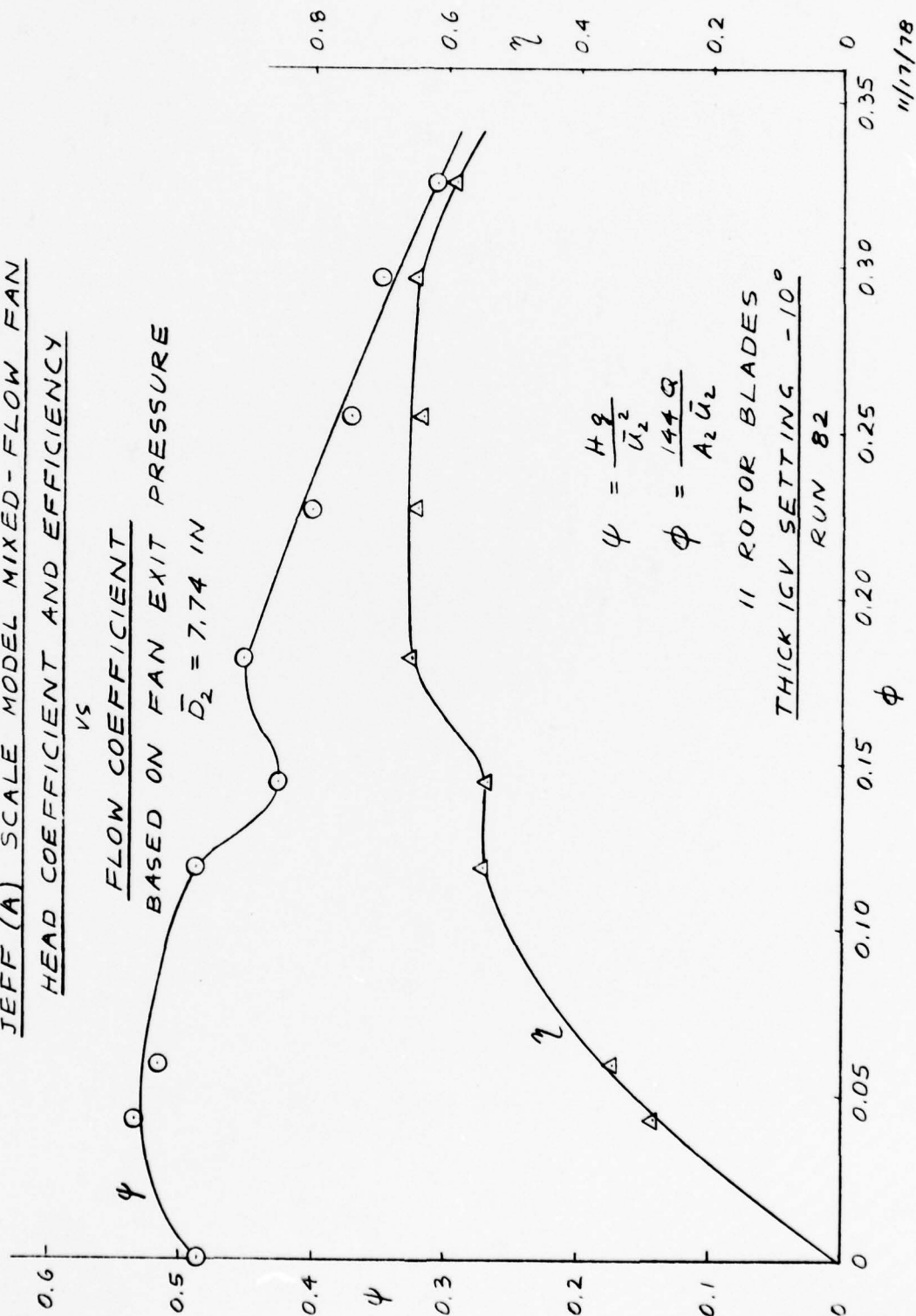


FIGURE 5.2.2-8

JEFF (A) SCALE MODEL MIXED-FLOW FAN
HEAD COEFFICIENT AND EFFICIENCY

vs
FLOW COEFFICIENT

$\bar{D}_2 = 7.74$ IN

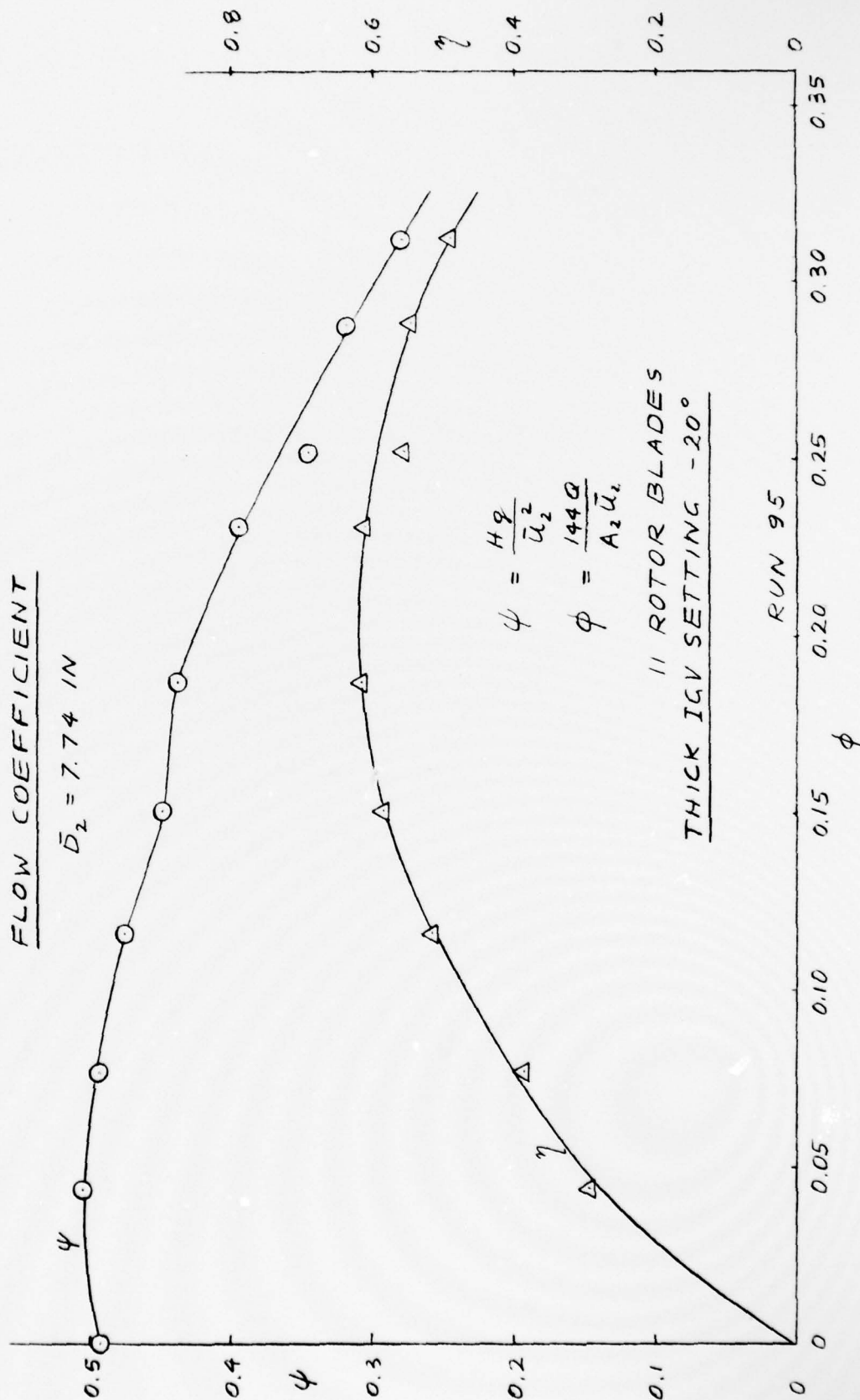


FIGURE 5.2.2-9

JEFF (A) SCALE MODEL MIXED-FLOW FAN
HEAD COEFFICIENT AND EFFICIENCY

1/5

FLOW COEFFICIENT

BASED ON FAN EXIT PRESSURE

$\bar{D}_2 = 7.74$ IN

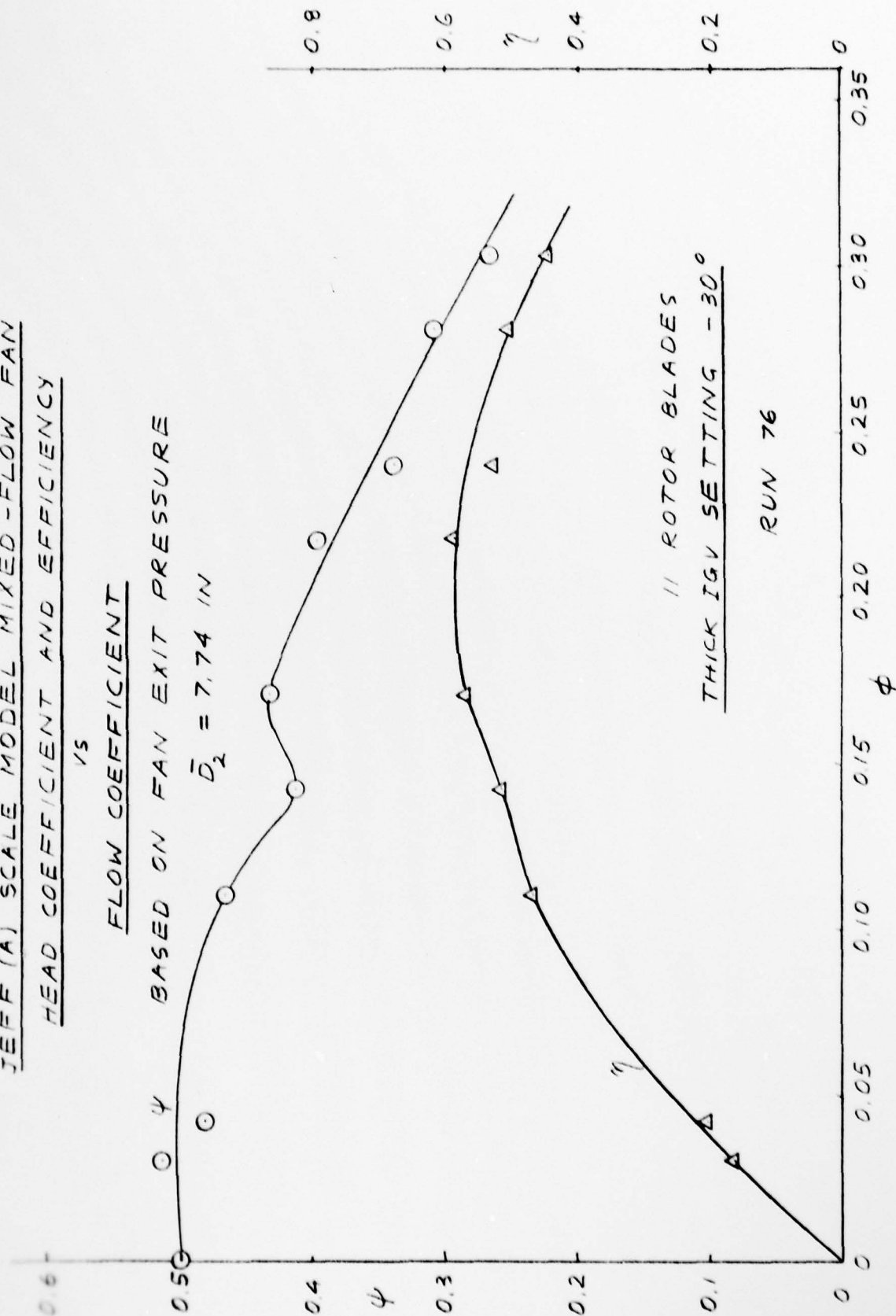


FIGURE 5.2.2-10

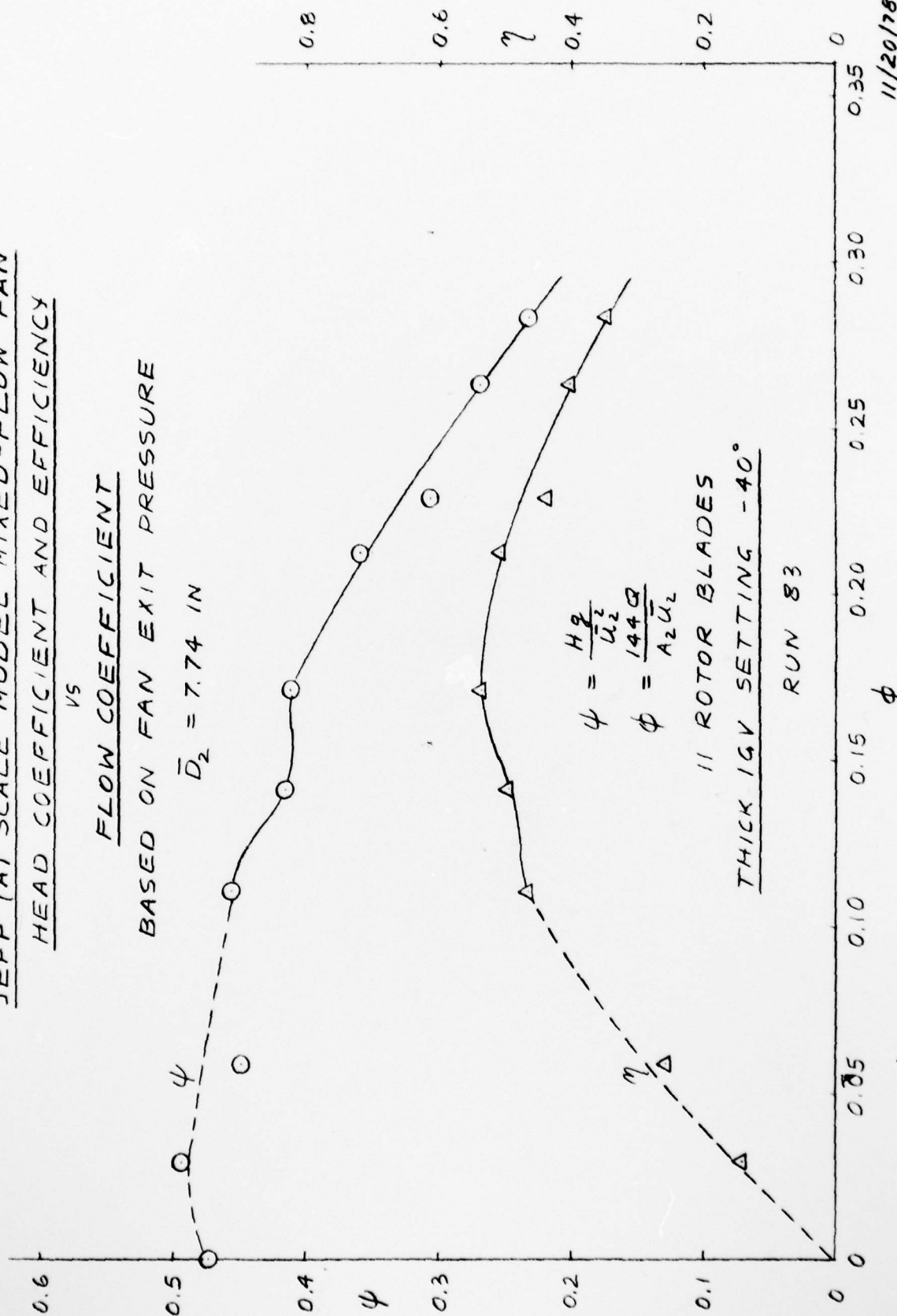
JEFF (A) SCALE MODEL MIXED-FLOW FAN
HEAD COEFFICIENT AND EFFICIENCY

VS

FLOW COEFFICIENT

BASED ON FAN EXIT PRESSURE

$\bar{D}_2 = 7.74$ IN



$$\psi = \frac{H_2}{U_2^2}$$

$$\phi = \frac{144 Q}{A_2 U_2}$$

11 ROTOR BLADES
 THICK IGV SETTING -40°

RUN 83

11/20/78

FIGURE 5.2.2 - 11

JEFF (A) SCALE MODEL MIXED-FLOW FAN
EFFECT OF NEGATIVE IGV SETTING ON
FAN PERFORMANCE

FLAT VANES

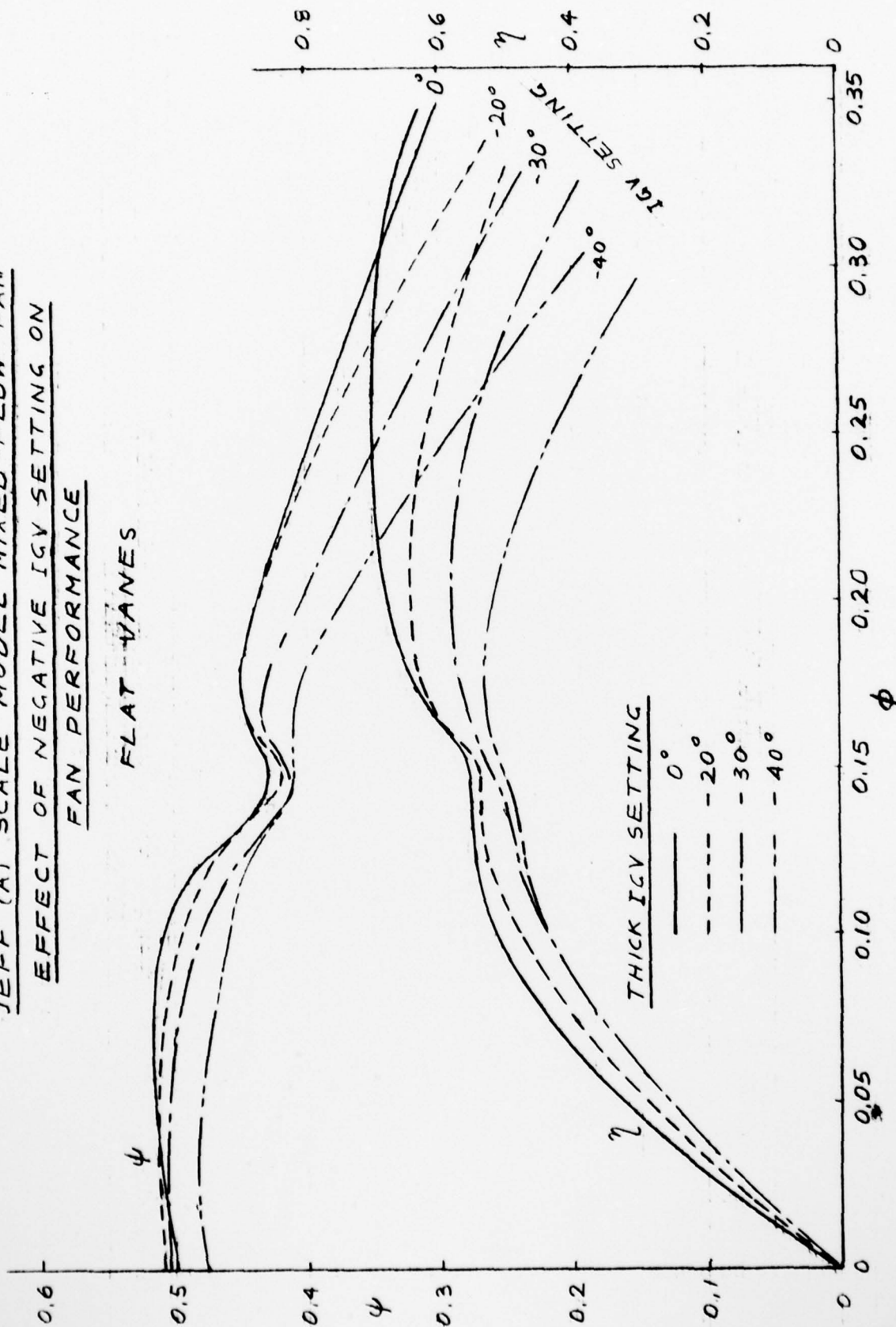


FIGURE 5.2.2-12

JEFF (A) SCALE MODEL MIXED-FLOW FAN
HEAD COEFFICIENT AND EFFICIENCY

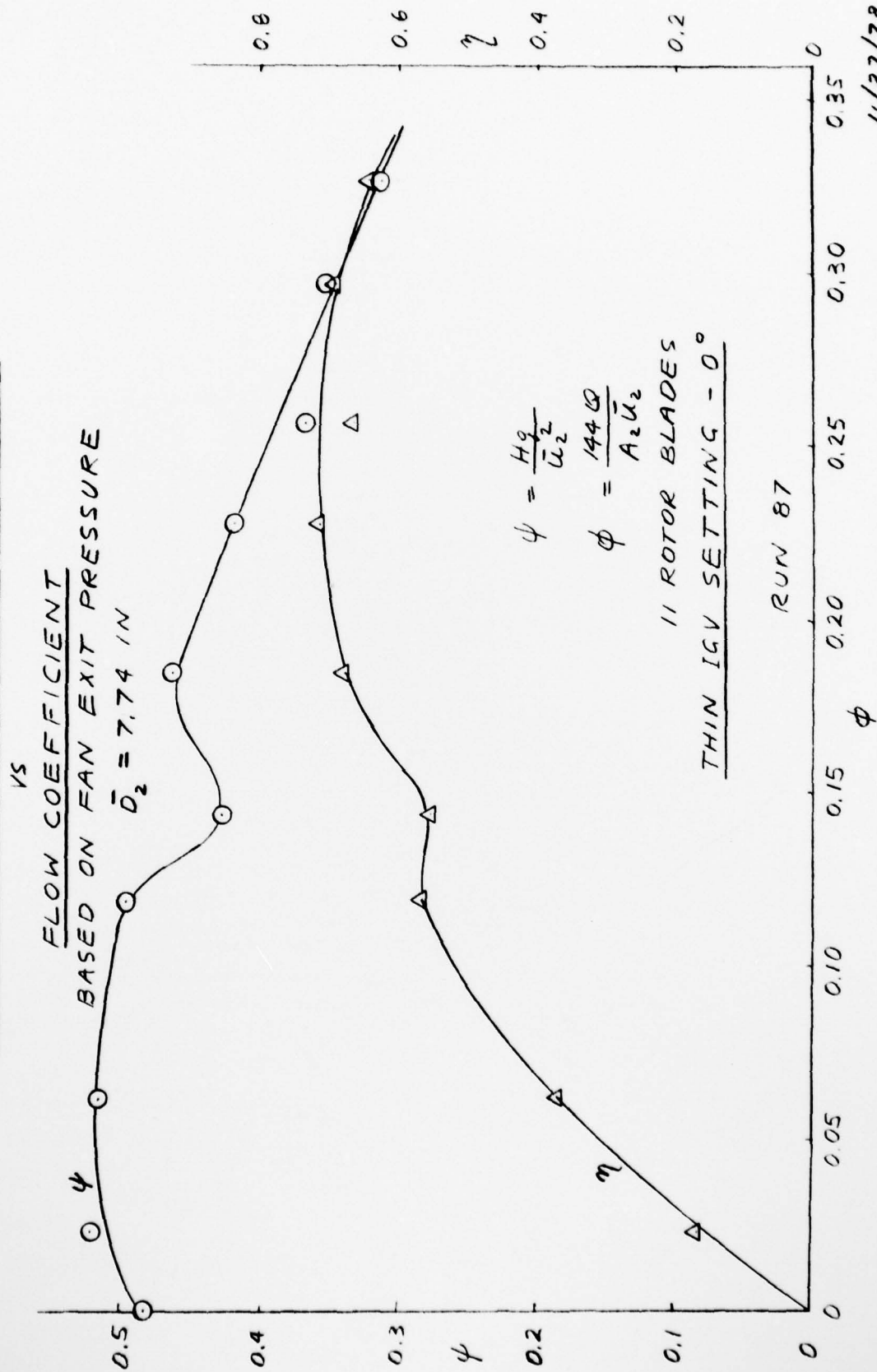


FIGURE 5.2.2-13

JEFF (A) SCALE MODEL MIXED-FLOW FAN
HEAD COEFFICIENT AND EFFICIENCY

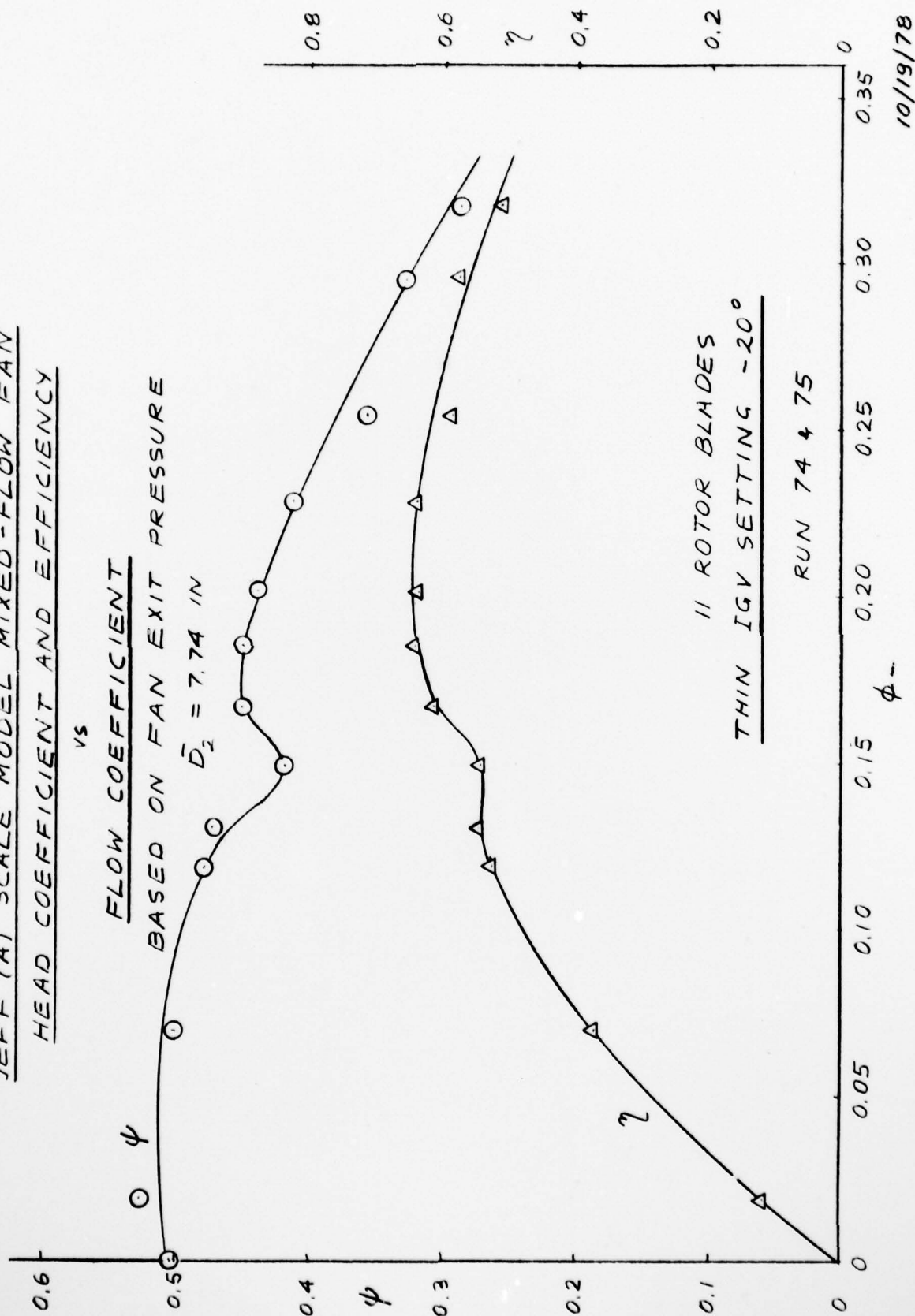
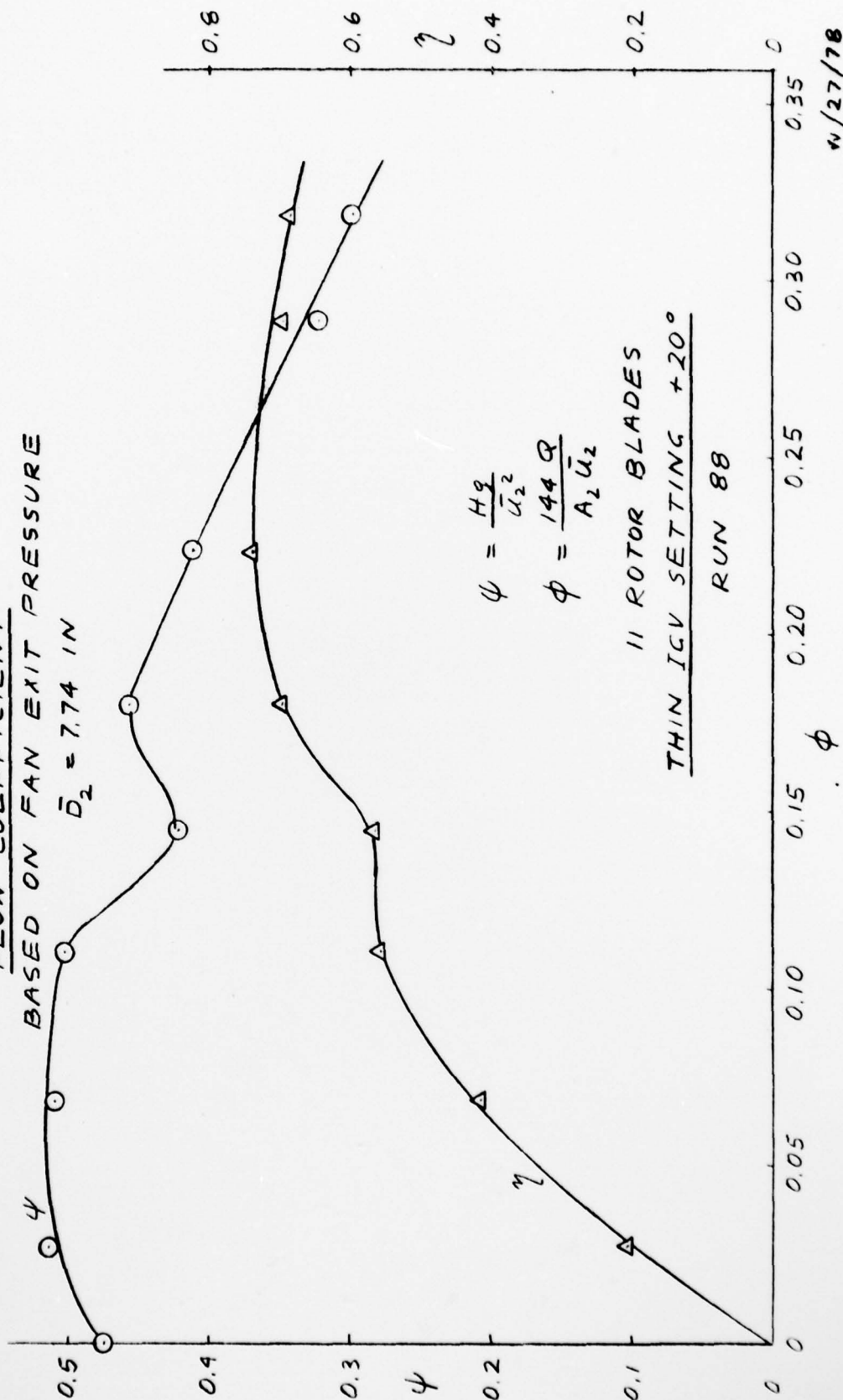


FIGURE 5.2.2-14

JEFF (A) SCALE MODEL MIXED-FLOW FAN
HEAD COEFFICIENT AND EFFICIENCY
 vs

FLOW COEFFICIENT
BASED ON FAN EXIT PRESSURE

$\bar{D}_2 = 7.74 \text{ IN}$



$$\psi = \frac{H_2}{\bar{U}_2^2}$$

$$\phi = \frac{144 Q}{A_2 \bar{U}_2}$$

11 ROTOR BLADES
 THIN ICV SETTING +20°
 RUN 88

4/27/78

FIGURE 5.2.2-15

5. MODEL FAN PERFORMANCE (cont'd)

of 0^0 and $+20^0$, fan performance is substantially the same for thick and thin vanes. But at an IGV setting of -20^0 , thick IGV's give both higher peak (2 points higher) efficiency and head coefficient. Figure 5.2.2-16 combines all three previous plots.

5.2.3 Effect of IGV Setting on Fan Performance - Twisted Vanes

The third set of vanes had a 15^0 twist between the tip and hub. It was constructed from 0.04" thick aluminum stock. Figures 5.2.3-1 to 5.2.3-6 show fan performance for twisted IGV's at positive tip deflections ranging from 0^0 to $+50^0$, and Figure 5.2.3-7 combines all these plots into one. An examination of these results indicates that twisted vanes perform in a similar manner to flat vanes.

5.2.4 Summary of Fan Performance With IGV's

In Figure 5.2.4-1, a comparison is made between a fan without IGV's and a fan equipped with flat IGV's set at 0^0 . It is evident that the fan without IGV's gives superior performance at flow coefficients smaller than 0.25. At higher flow coefficients, small improvements in performance due to inlet guide vanes are realized. As previously stated, the performance with twisted IGV's is similar to that of flat IGV's at zero deflection.

In Figure 5.2.4-2, fan performance without IGV's is compared with flat vanes set at $+20^0$ and twisted vanes set at $+30^0$ tip ($+15^0$ hub) position. The effect of IGV's is to reduce the head coefficient throughout the flow range while increasing efficiency at $\phi > 0.2$.

In Table 7, fan performance at the maximum efficiency point is tabulated using actual test points without smoothing the data.

JEFF (A) SCALE MODEL MIXED-FLOW FAN

EFFECT OF IGV SETTING ON

FAN PERFORMANCE

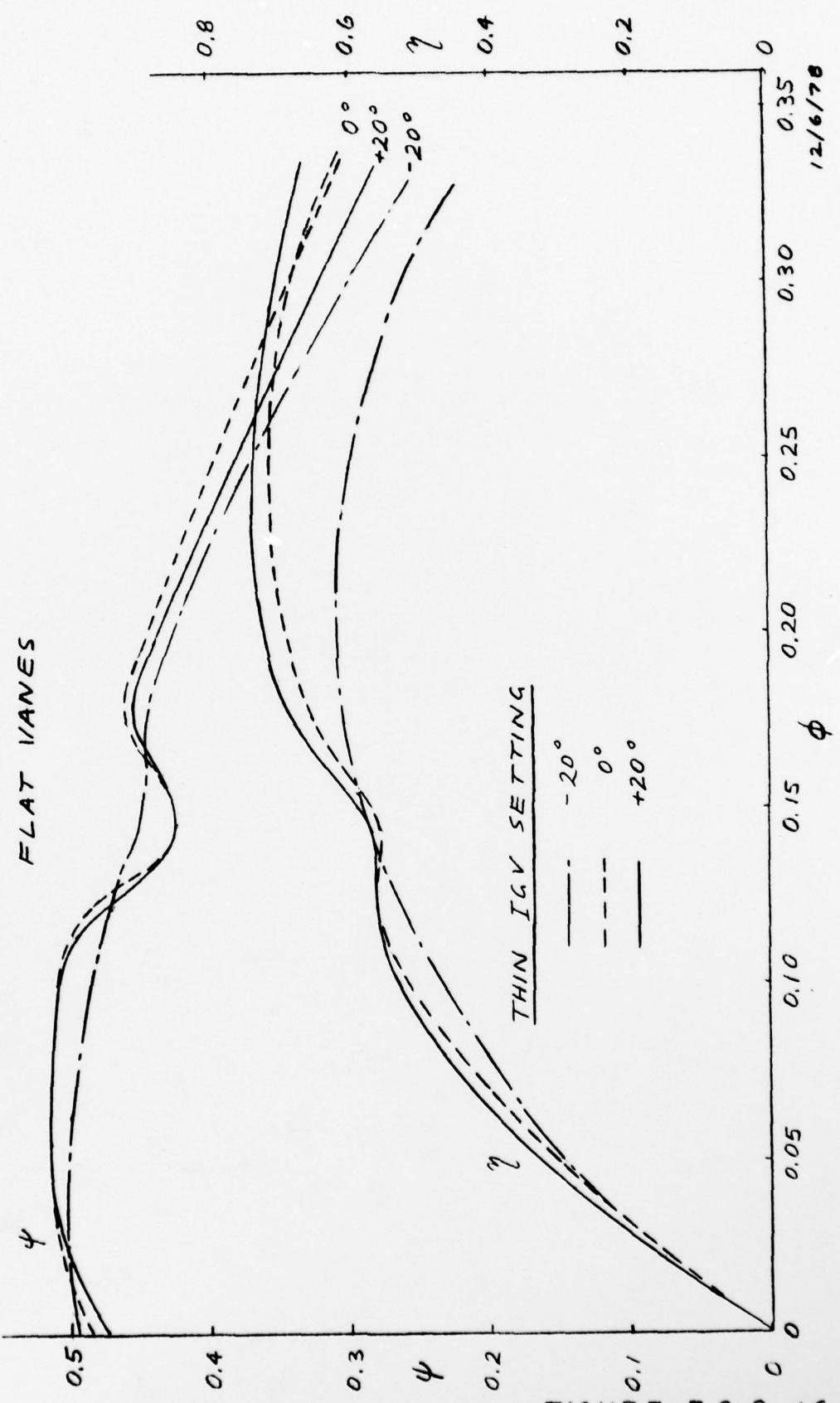


FIGURE 5.2.2-16

JEFF (A) SCALE MODEL MIXED-FLOW FAN
HEAD COEFFICIENT AND EFFICIENCY

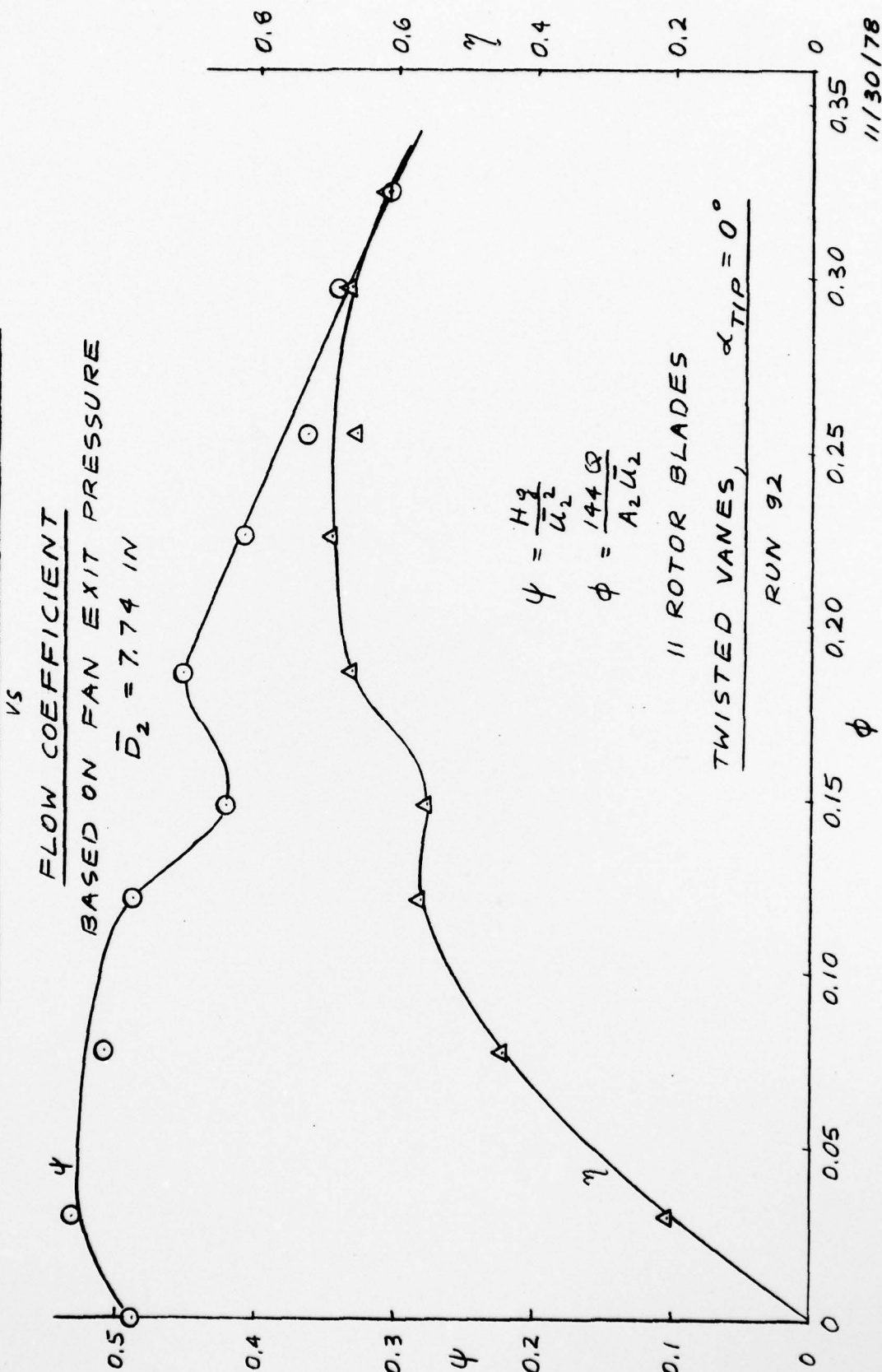


FIGURE 5.2.3-1

JEFF (A) SCALE MODEL MIXED-FLOW FAN
HEAD COEFFICIENT AND EFFICIENCY

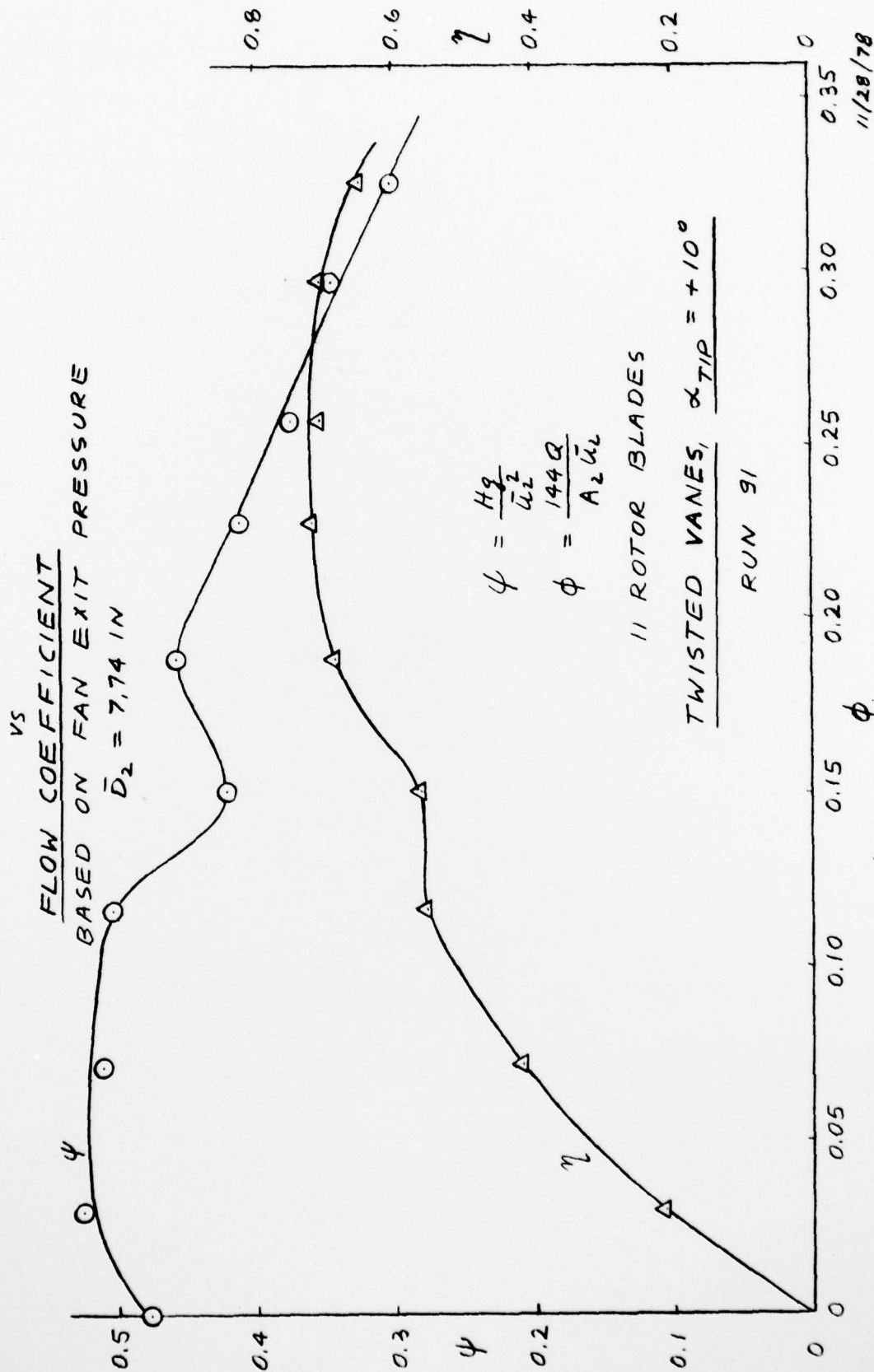


FIGURE 5.2.3-2

JEFF (A) SCALE MODEL MIXED-FLOW FAN
HEAD COEFFICIENT AND EFFICIENCY

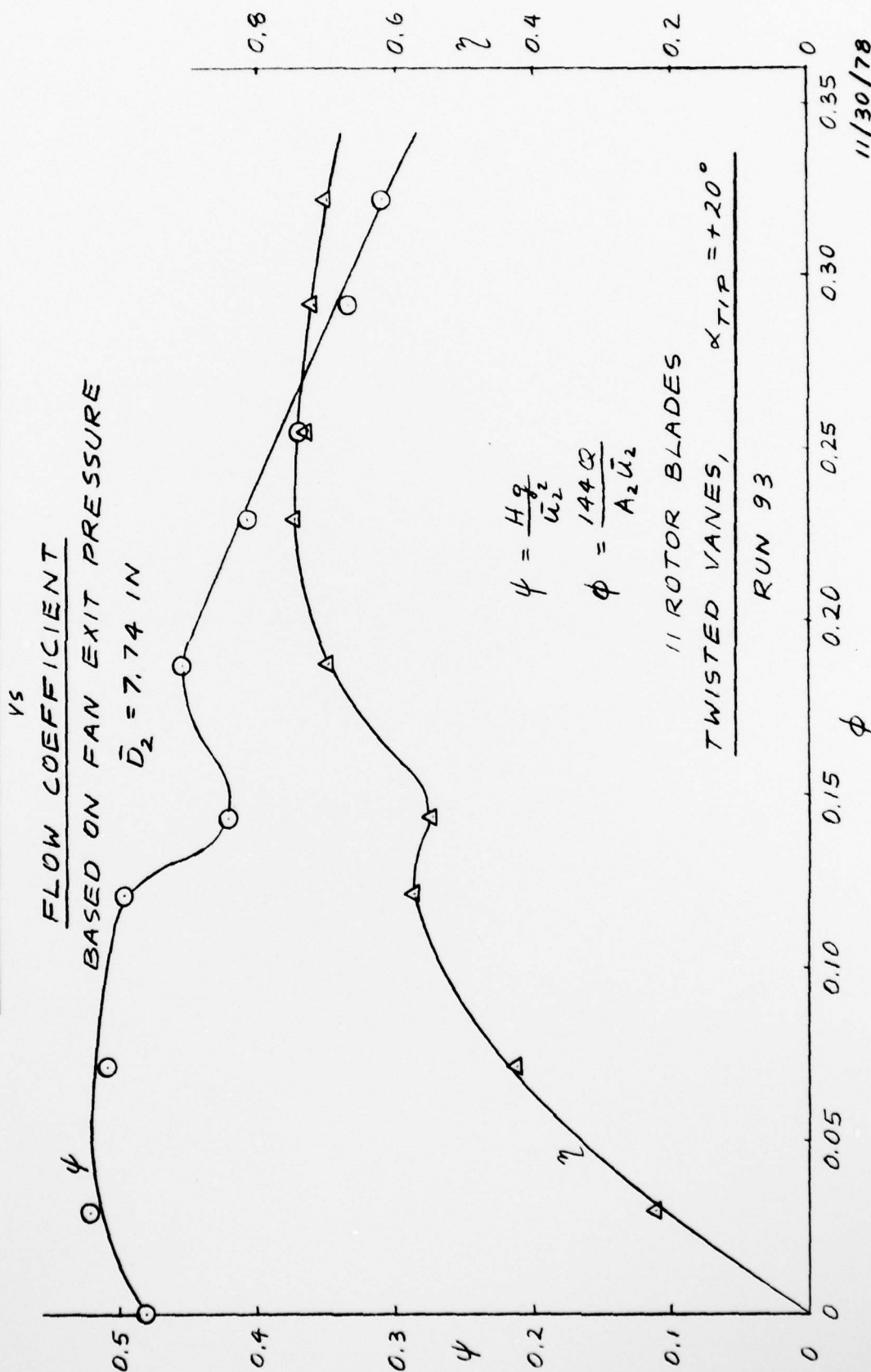
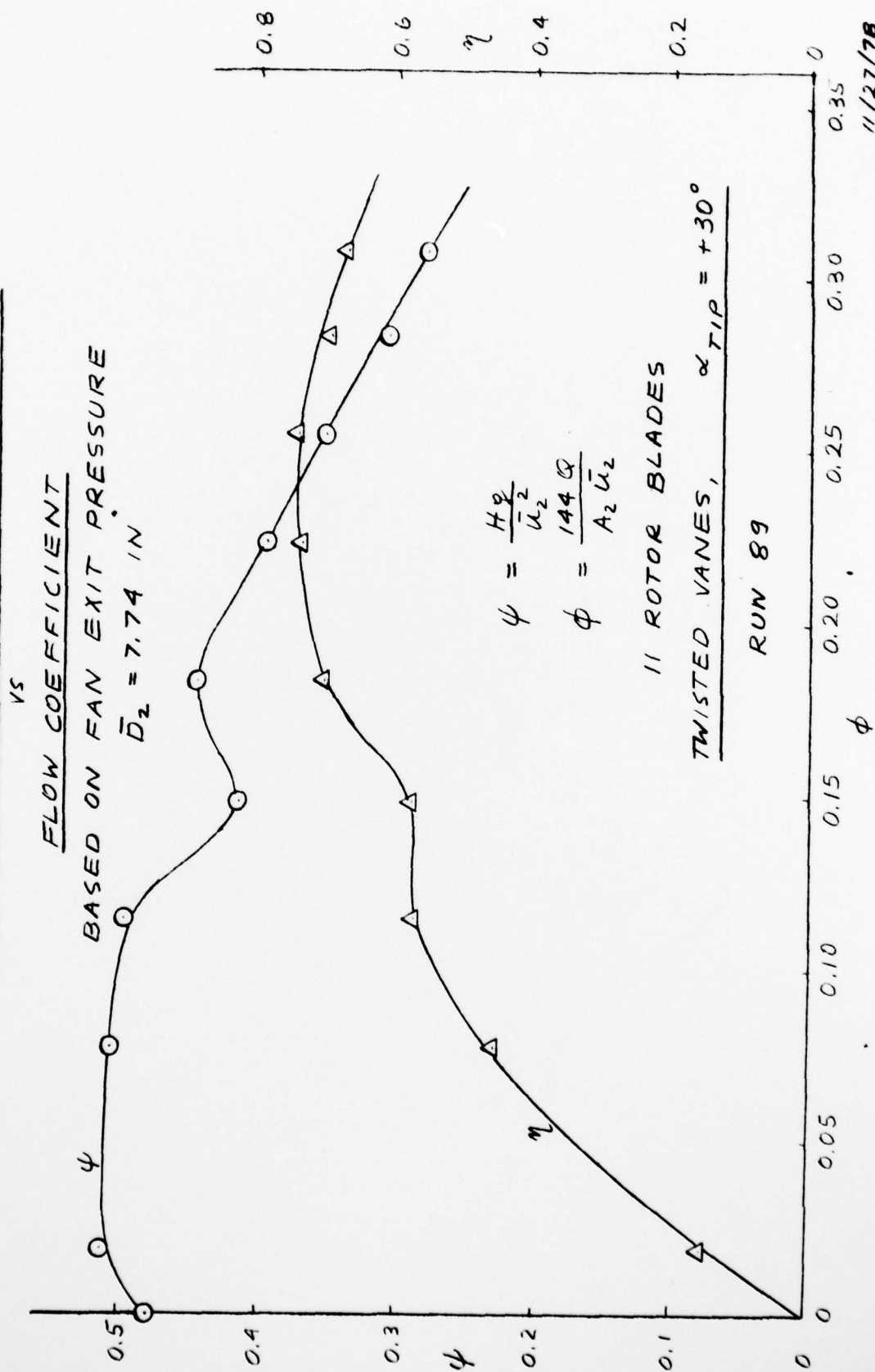


FIGURE 5.2.3

JEFF (A) SCALE MODEL MIXED-FLOW FAN
HEAD COEFFICIENT AND EFFICIENCY



11/27/78

FIGURE 5.2.3-4

JEFF (A) SCALE MODEL MIXED-FLOW FAN
HEAD COEFFICIENT AND EFFICIENCY

VS

FLOW COEFFICIENT

BASED ON FAN EXIT PRESSURE

$\bar{D}_2 = 7.74$ IN

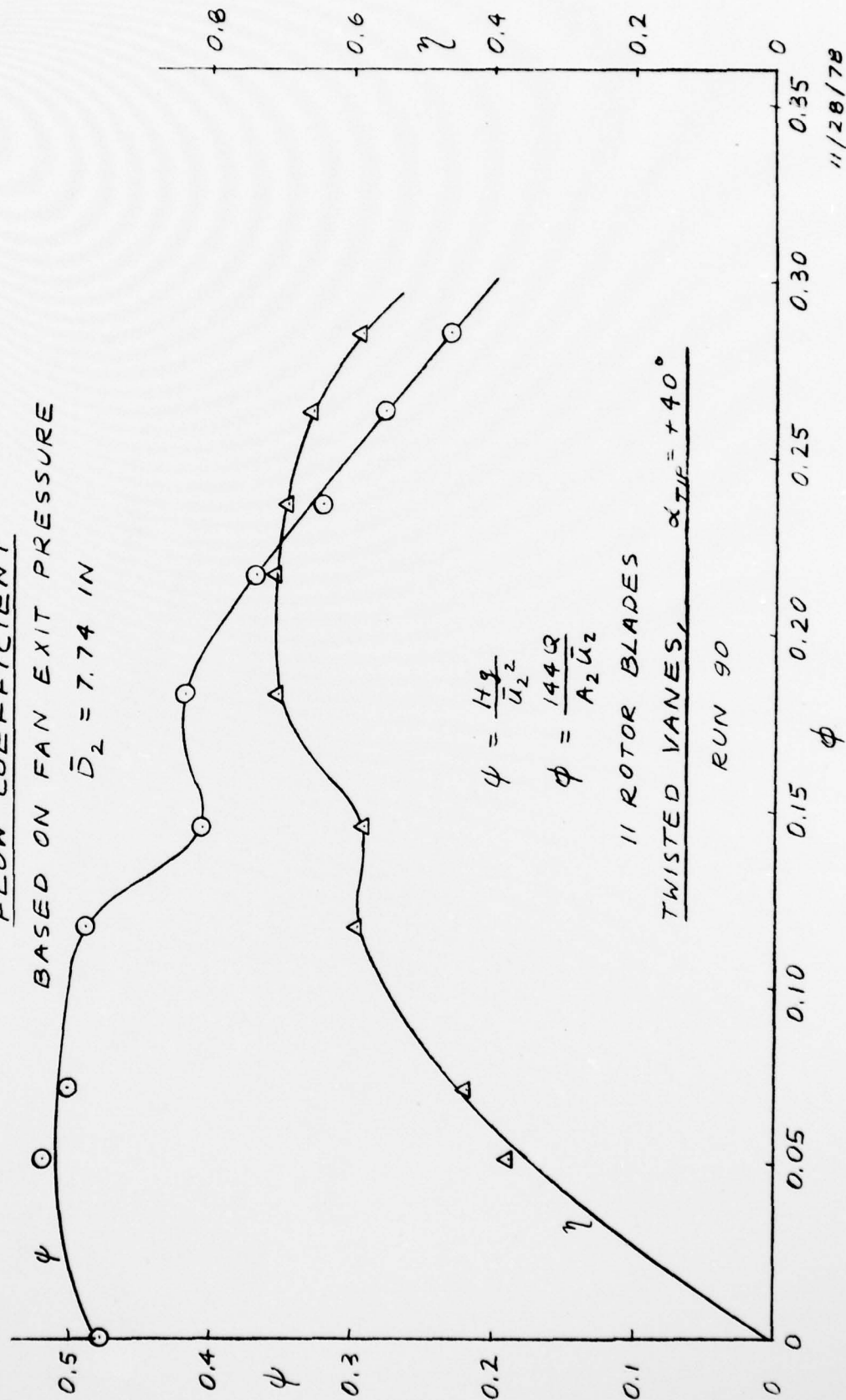


FIGURE 5.2.3-5

JEFF (A) SCALE MODEL MIXED-FLOW FAN
HEAD COEFFICIENT AND EFFICIENCY

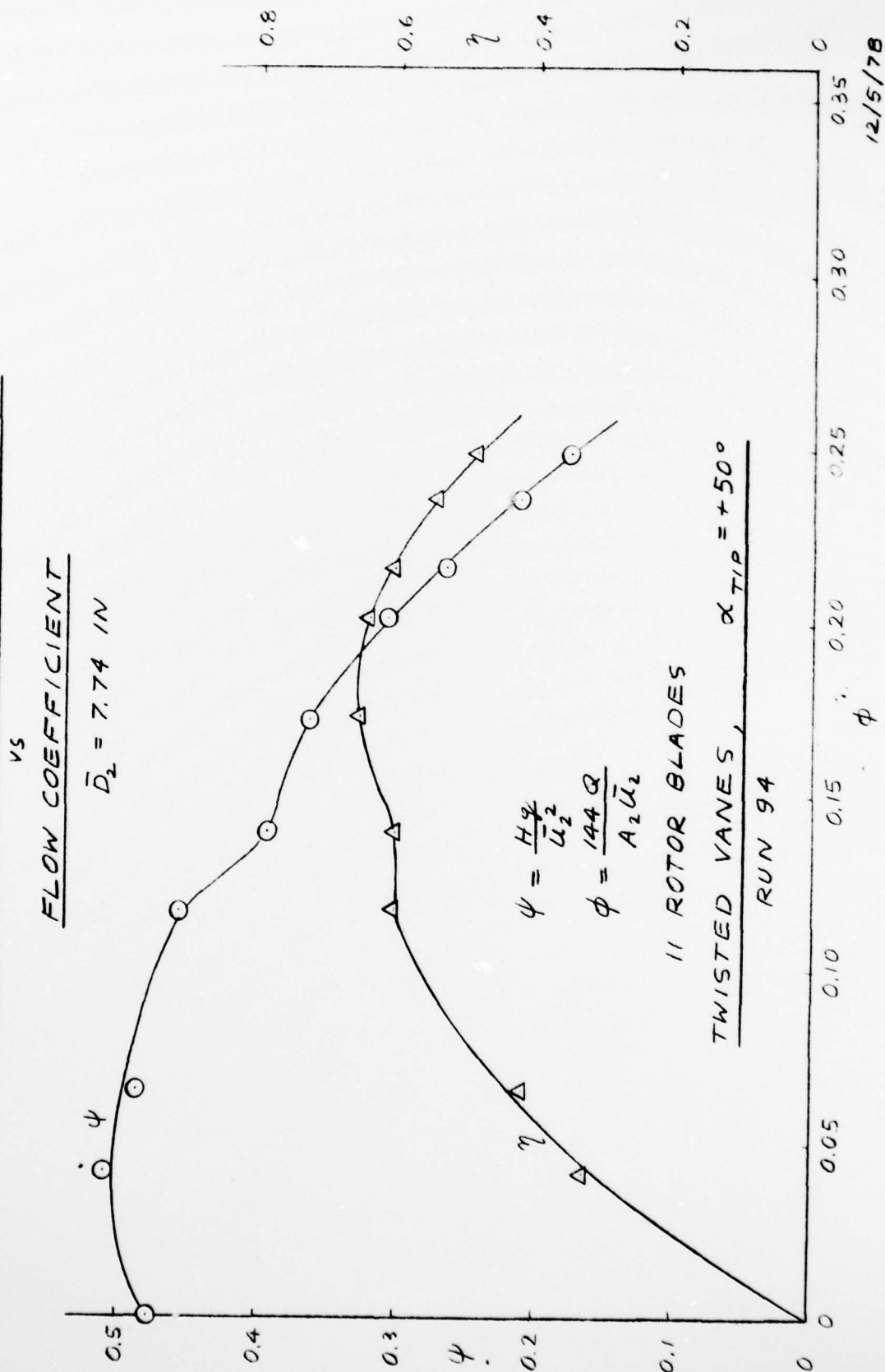


FIGURE 5.2.3-6

AD-A074 571

AEROJET LIQUID ROCKET CO SACRAMENTO CA

F/G 13/10

JEFF(A) MIXED-FLOW MODEL FAN PERFORMANCE OPTIMIZATION.(U)

JUN 79 S A LORENC

N00014-78-C-0441

UNCLASSIFIED

ALRC-FD9630-001

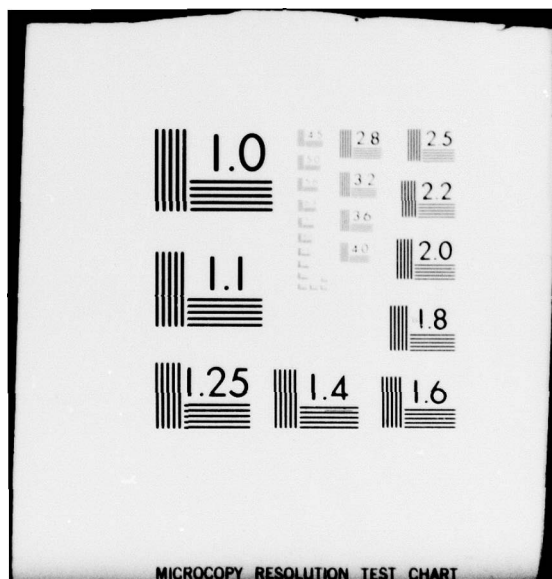
NL

2 OF 2

AD
A074571



END
DATE
FILMED
11-79
DDC



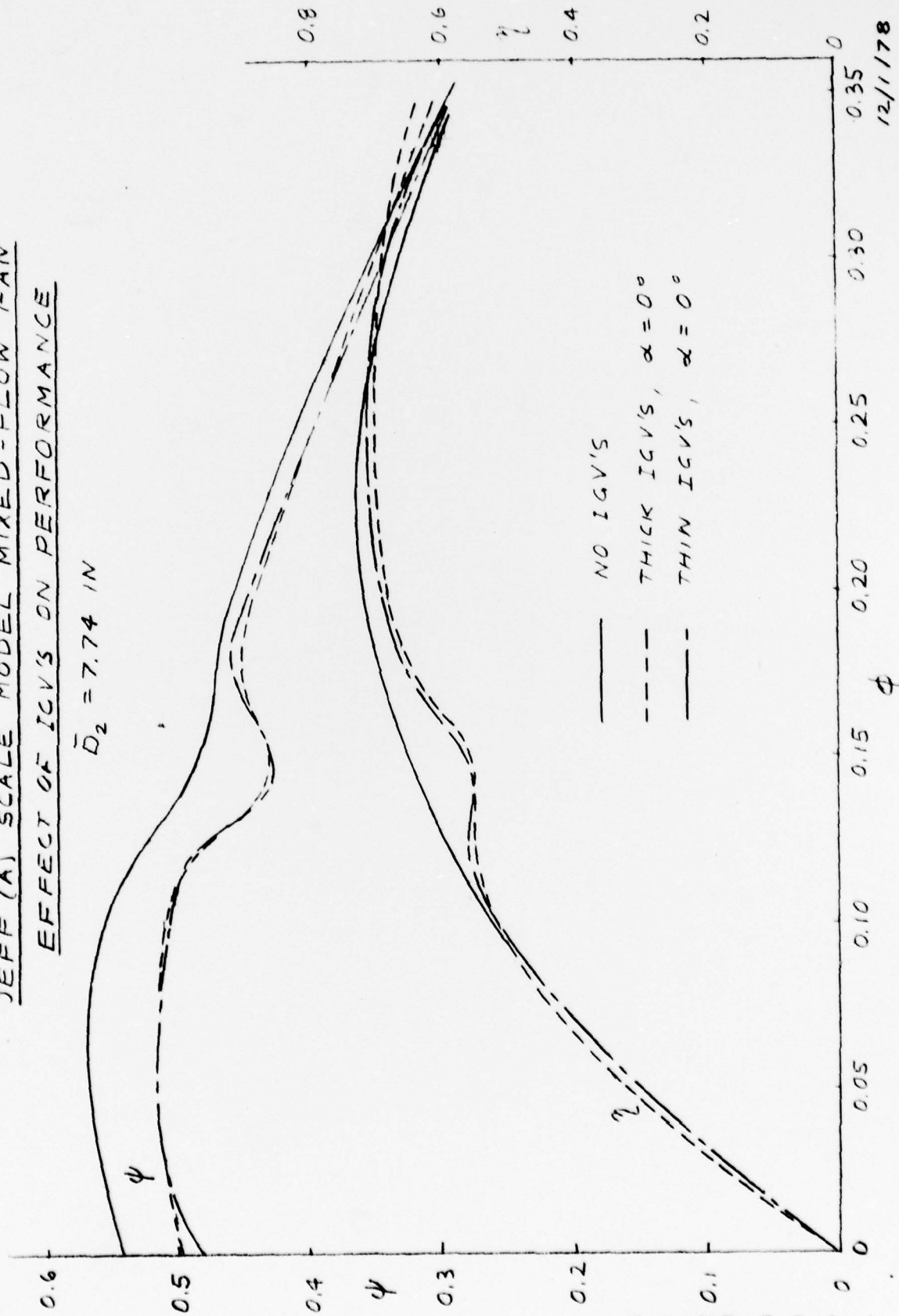
JEFF (A) SCALE MODEL MIXED-FLOW FAN
EFFECT OF IGV SETTING
ON FAN PERFORMANCE



FIGURE 5.2.3-7

JEFF (A) SCALE MODEL MIXED-FLOW FAN
EFFECT OF IGV'S ON PERFORMANCE

$\bar{D}_2 = 7.74$ IN

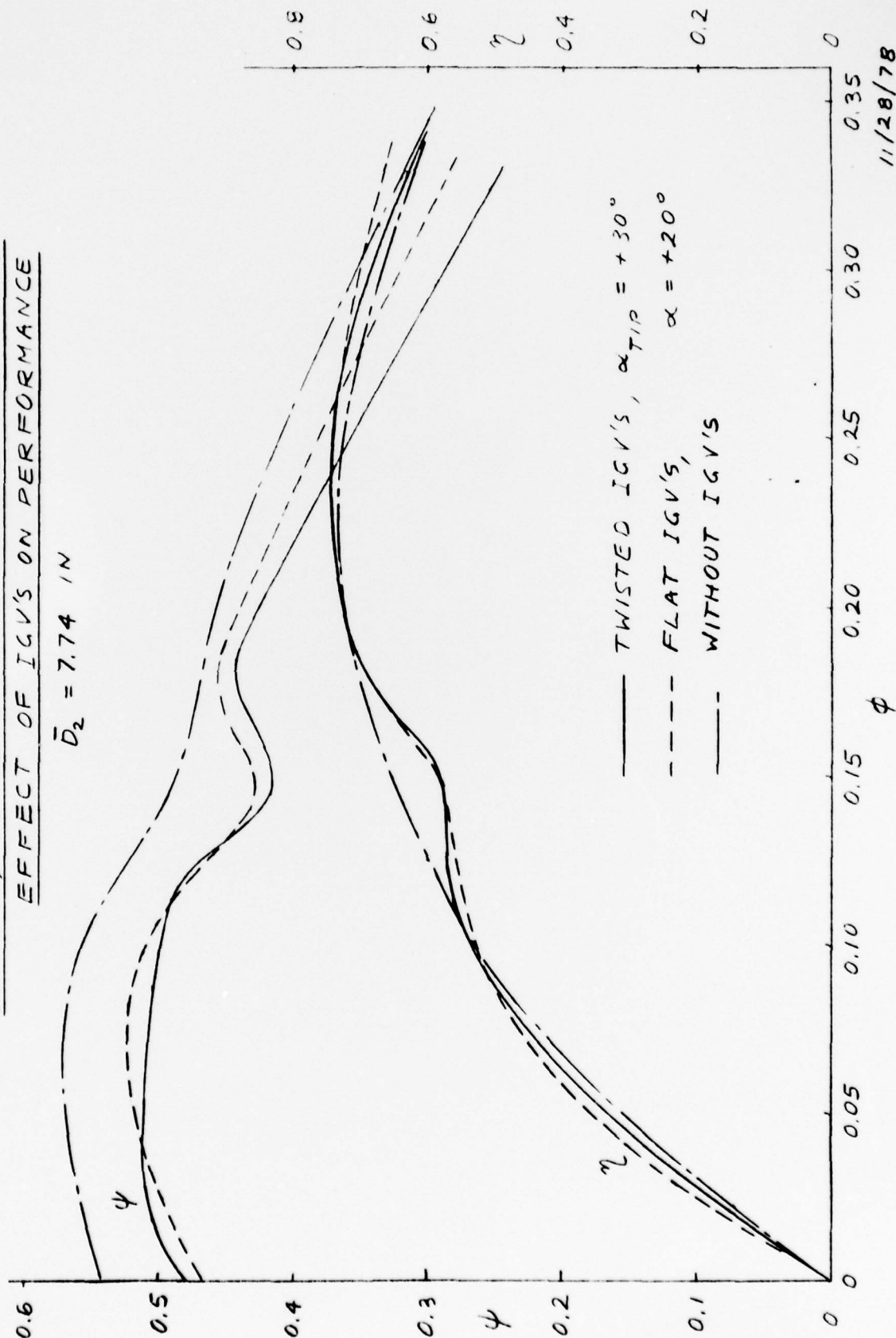


12/1/78

FIGURE 5.2.4-1

JEFF (A) SCALE MODEL MIXED-FLOW FAN
EFFECT OF IGV'S ON PERFORMANCE

$\bar{D}_2 = 7.74$ IN



11/28/78

FIGURE 5.2.4-2

TABLE 7
PERFORMANCE COMPARISON
OF FLAT AND TWISTED IGV'S AT MAXIMUM EFFICIENCY POINT

		VANE DEFLECTION ANGLE										
		-40	-30	-20	-10	0°	+10	+20	+30	+40	+50	
WITHOUT IGV'S	ϕ	0.225 0.443 0.735										
	ψ											
	η _{MAX}											
FLAT (THICK) IGV'S	ϕ	0.172	0.218	0.187	0.182	0.225	0.226	0.225	0.230	0.180		
	ψ	0.411	0.397	0.439	0.454	0.415	0.419	0.415	0.382	0.397		
	η _{MAX}	0.535	0.587	0.619	0.651	0.69	0.728	0.744	0.737	0.690		
FLAT (THIN) IGV'S	ϕ	0.186 0.449 0.641										
	ψ											
	η _{MAX}											
TWISTED IGV'S	ϕ	0.226 0.409 0.691										
	ψ											
	η _{MAX}											

5. MODEL FAN PERFORMANCE (CONT'D)

It is interesting to notice that peak efficiency is considerably higher when IGV's are deflected in a positive direction (direction of rotation) than in the opposite direction. Also, by increasing the deflection from $+10^\circ$ to $+30^\circ$ the head coefficient is reduced by no more than 11%, but the efficiency changes by about 3%.

5. MODEL FAN PERFORMANCE (cont'd)

5.3 Effect of Housing Size on Fan Performance

In order to evaluate the effect of housing size on fan performance, a large plenum housing was constructed, and styrofoam inserts were used to change the housing volume. The housing exit area and exit diffuser area were also changed in such a manner that the diffuser area ratio and length remained constant. The interior surfaces of the styrofoam inserts were coated with Spackle for smoothness.

An adapter was used to connect the rectangular diffuser exit to the existing 8" diameter facility exhaust duct. The instrumented adapter is also fitted with styrofoam inserts for each volute configuration to assure a smooth transition from a rectangular to a circular shape.

The housing volume was first varied by varying the axial width and then by changing the volute diameter.

5.3.1 Housing Axial Width Increase

Figures 5.3.1-1 to 5.3.1-3 show fan performance for housing axial widths $B=5.58$, 6.67 , and 7.76 IN while keeping volute diameter constant ($A=13.60$ IN). A width of 5.58 IN and a volute diameter of 13.60 IN represent the dimensions of the baseline wooden housing.

Comparison of Figure 5.3.1-1 and 5.3.1-4 shows that the styrofoam volute gave considerably lower performance than the original baseline housing (Figure 5.3.1-4). Although the volutes in these two cases are similar, the exit diffusers are not. The performance of all new housings are based on the total pressure at the diffuser exit. This pressure is measured by means of 12 probes located as shown in Figures 4.1-5 to 4.1-9 instead of 8 probes for the baseline housing.

JEFF (A) SCALE MODEL MIXED-FLOW FAN
HEAD COEFFICIENT AND EFFICIENCY

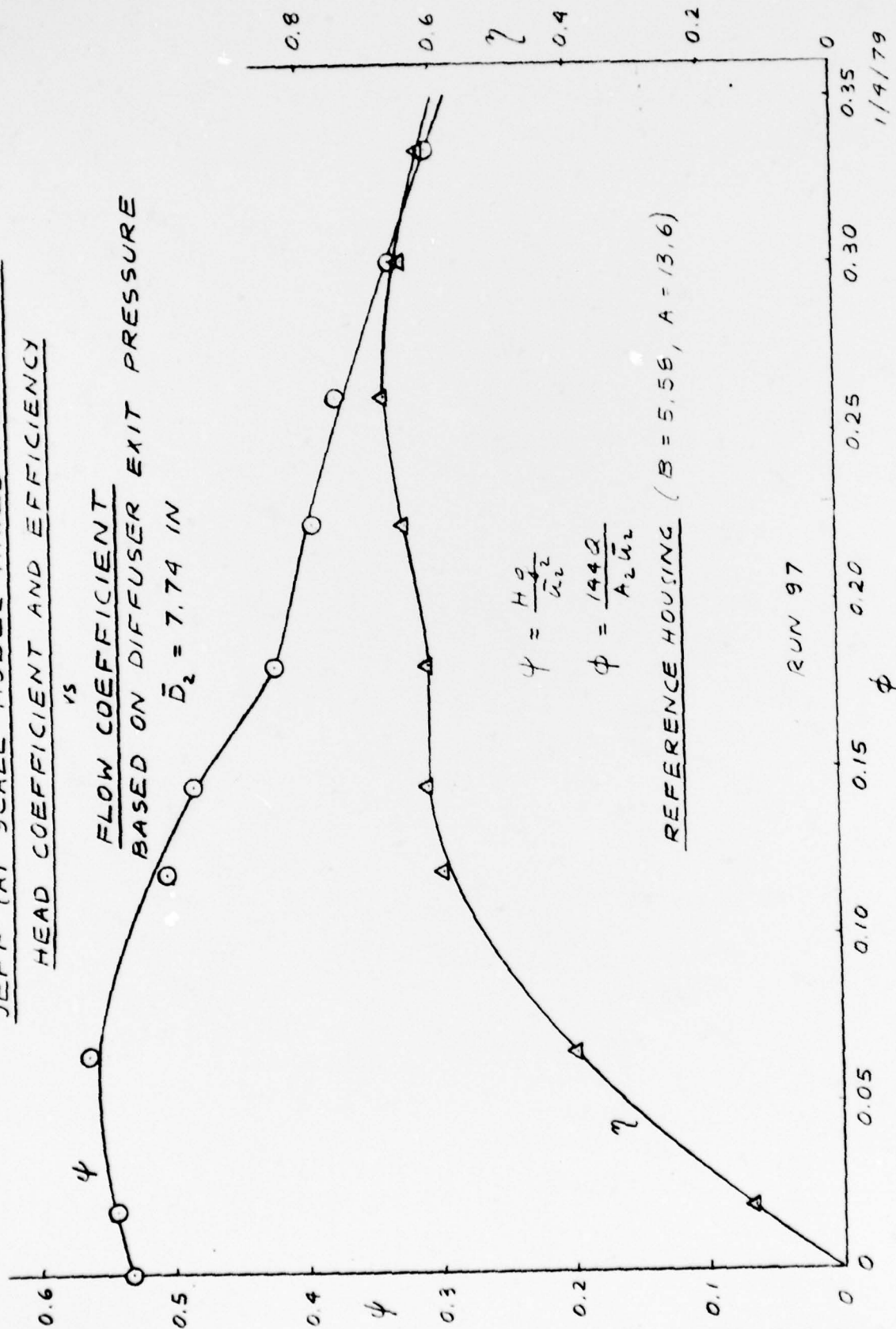


FIGURE 5.3.1 - 1

JEFF (A) SCALE MODEL MIXED-FLOW FAN
HEAD COEFFICIENT AND EFFICIENCY

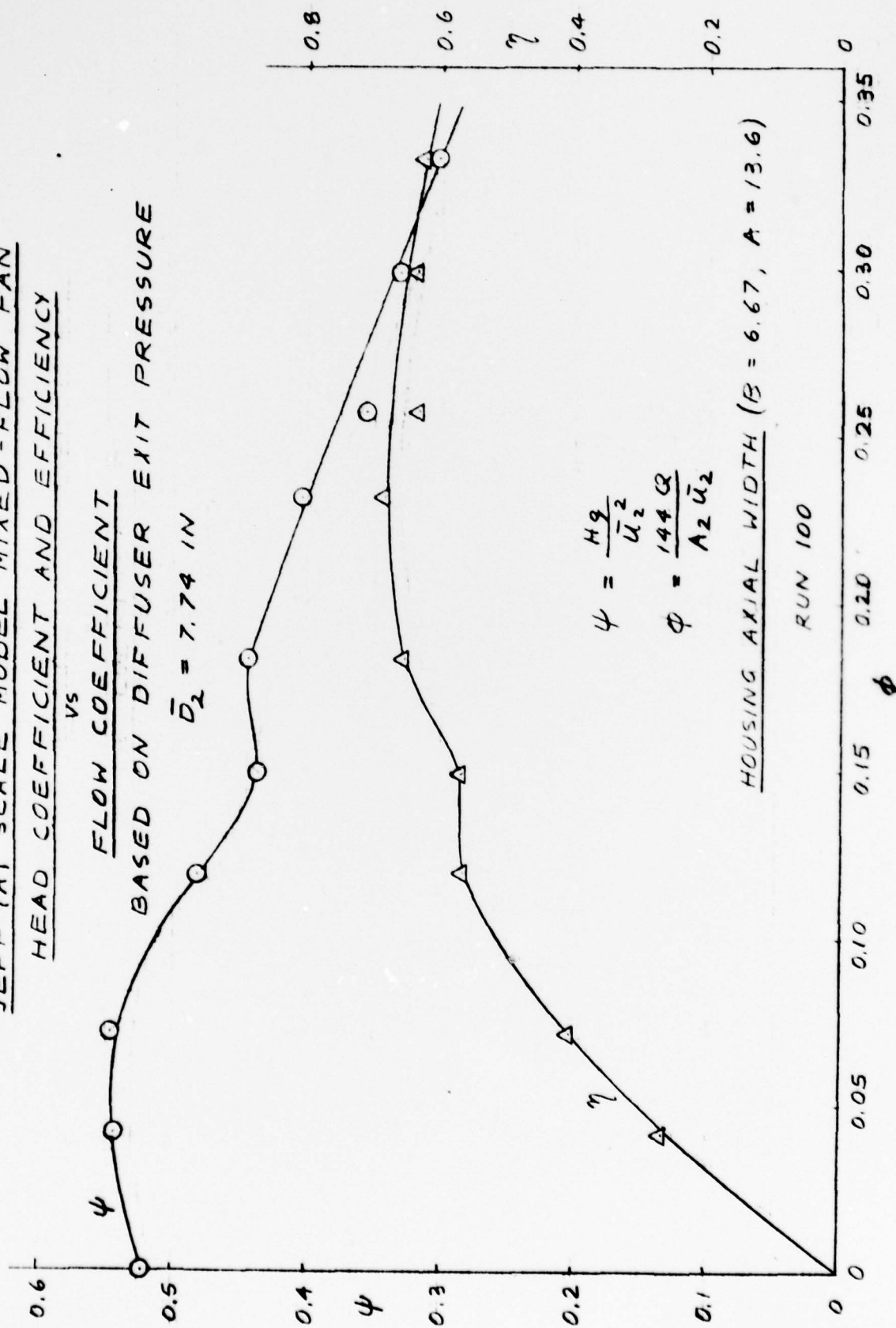


FIGURE 5.3.1-2

JEFF (A) SCALE MODEL MIXED-FLOW FAN
HEAD COEFFICIENT & EFFICIENCY

FLOW COEFFICIENT
 BASED ON DIFFUSER EXIT PRESSURE

$\bar{D}_2 = 7.74 \text{ IN}$

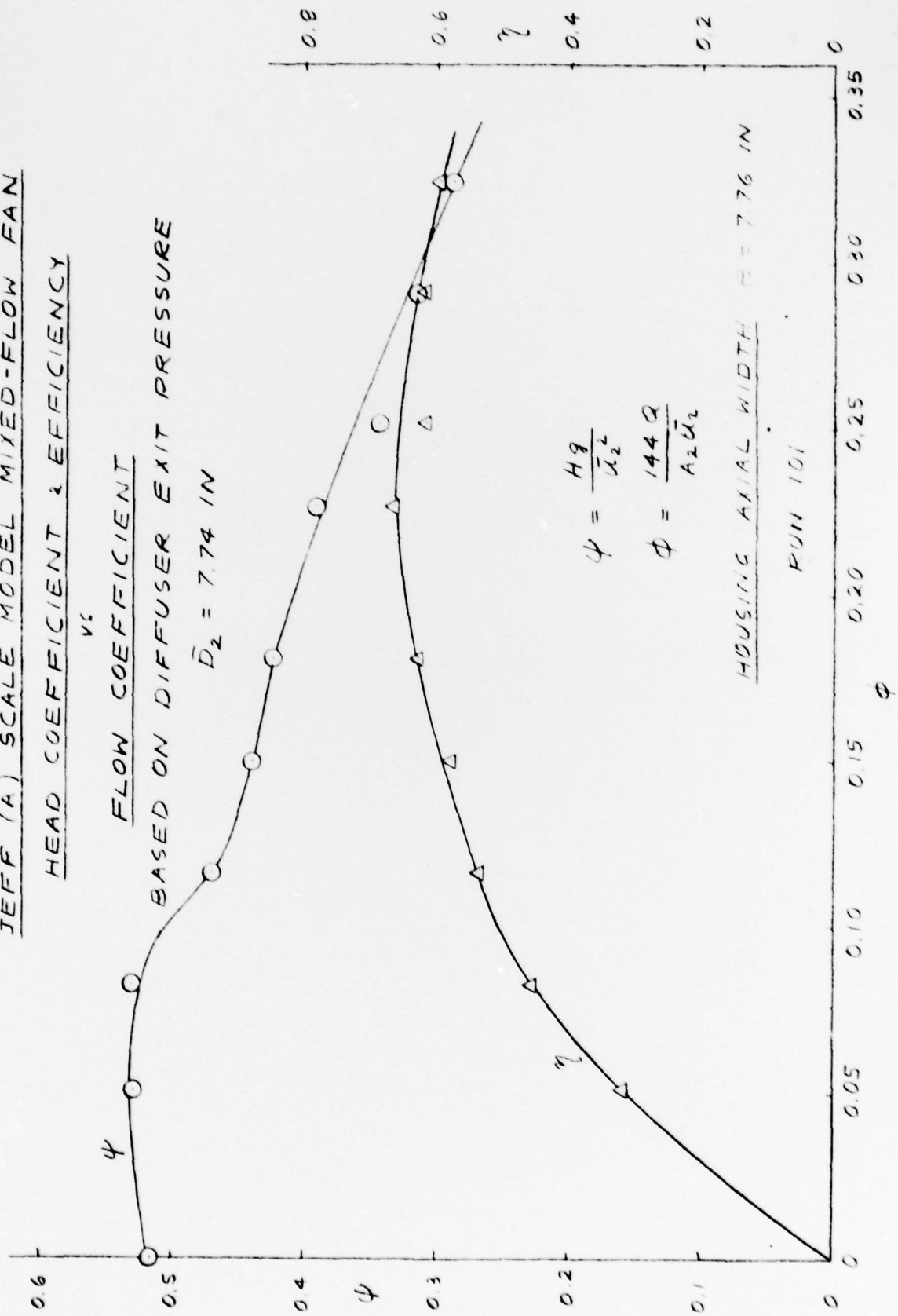
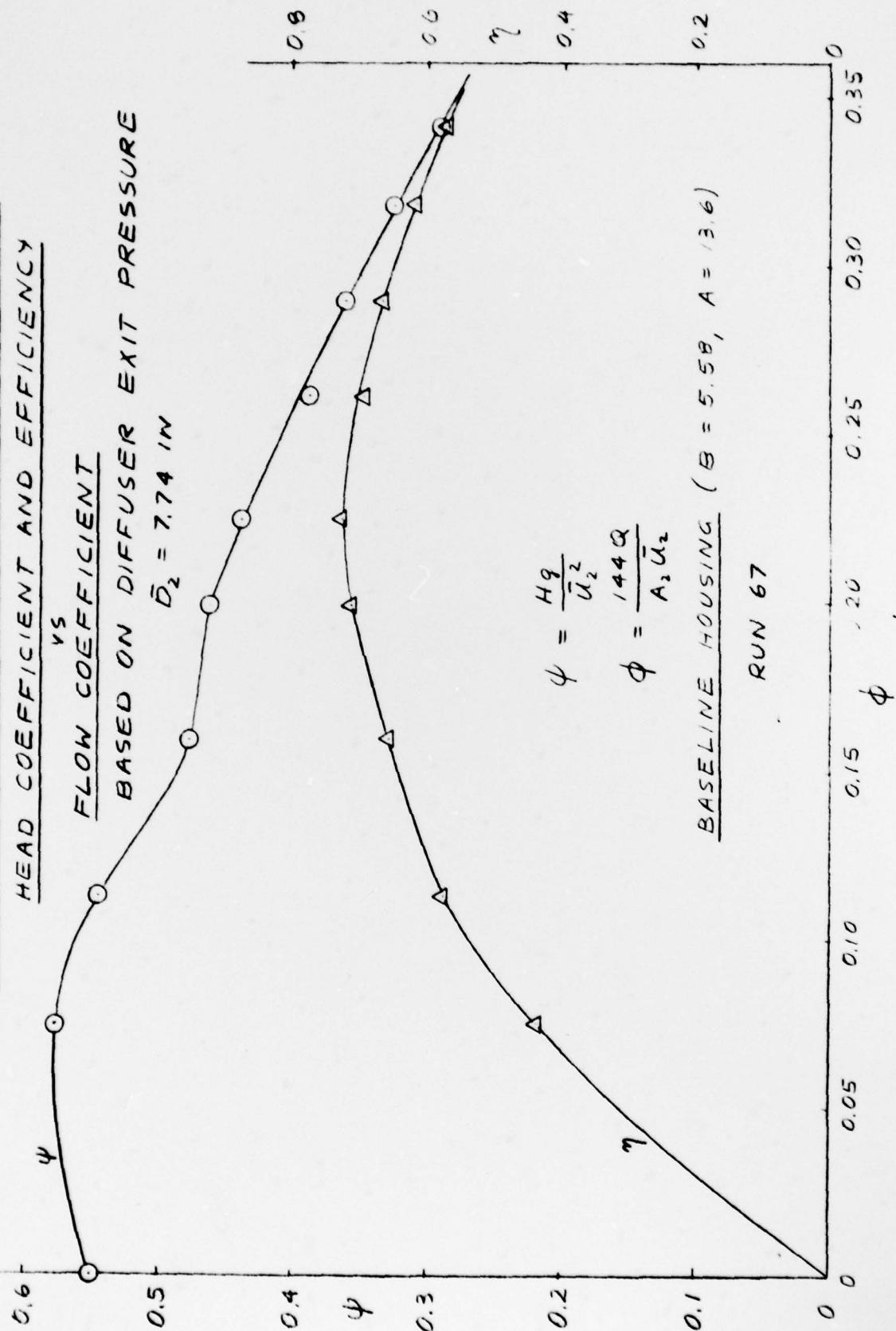


FIGURE 5.3.1-3

JEFF (A) SCALE MODEL MIXED-FLOW FAN
HEAD COEFFICIENT AND EFFICIENCY

vs
FLOW COEFFICIENT
 BASED ON DIFFUSER EXIT PRESSURE
 $\bar{D}_2 = 7.74$ IN



$$\psi = \frac{Hg}{\bar{U}_2^2}$$

$$\phi = \frac{144Q}{A_2 \bar{U}_2}$$

BASELINE HOUSING ($B = 5.58$, $A = 13.6$)

RUN 67

FIGURE 5.3.1-4

5. MODEL FAN PERFORMANCE (cont'd)

5.3.1 Housing Axial Width Increase (Cont'd)

For the sake of consistency, all the housing variations will be compared with the so called reference housing for which performance is shown in Figure 5.3.1-1. The summary plot in Figure 5.3.1-5 shows that the axial volute width increase is largely ineffective. The flow leaving the rotor follows the back wall and does not fill in the volume above the inlet bell. In fact, when the width is increased to 7.76 ($K=9.91$), fan performance is actually decreased.

5.3.2 Housing Diameter Increase

When the housing diameter is increased while keeping the axial width constant at 5.58 in., the fan performance is as shown in Figures 5.3.2-1 and 5.3.2-2. The summary plot in Figure 5.3.2-3 shows a small performance improvement when the diameter A is increased from 13.6 to 15.1.

Table 8 compares all housings tested to the new reference housing at the maximum efficiency point. The best efficiency gain of 4.2% is achieved when the volute diameter is increased from 13.6" to 15.1". The conclusion from these tests is that although the roll over volutes are smaller, they are not the most efficient. The most efficient volute is the one that is wrapped around the rotor exit.

5.3.3 Plenum Housing

Figure 5.3.3-1 shows fan performance when the styrofoam is removed and the plenum housing (Figure 3.2-2) is used. Compared with the reference housing (Figure 5.3.1-1), both head coefficient and efficiency are substantially reduced over the entire flow range.

JEFF (A) SCALE MODEL MIXED-FLOW FAN
EFFECT OF HOUSING WIDTH
ON FAN PERFORMANCE

$\bar{D}_2 = 7.74$ IN

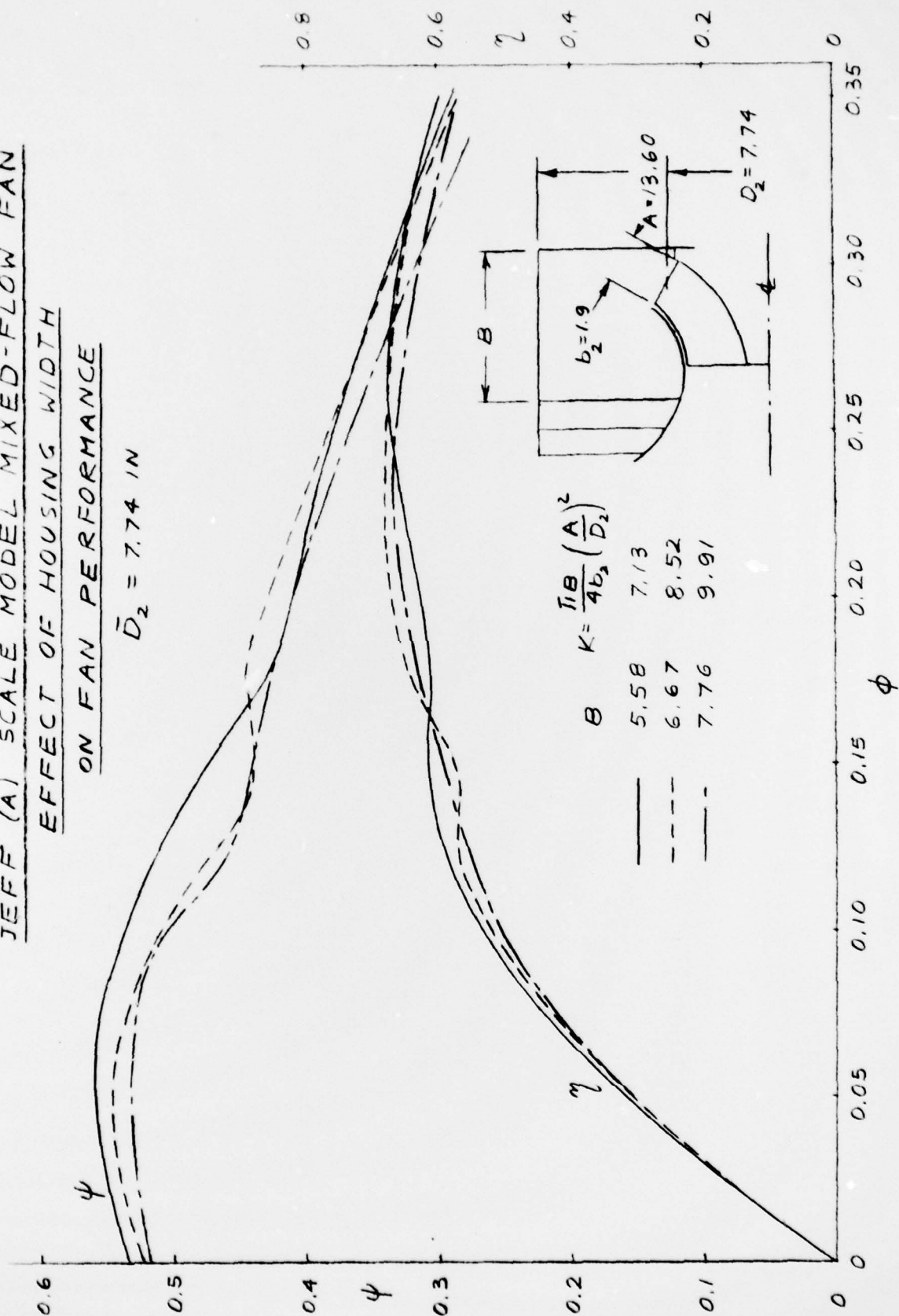


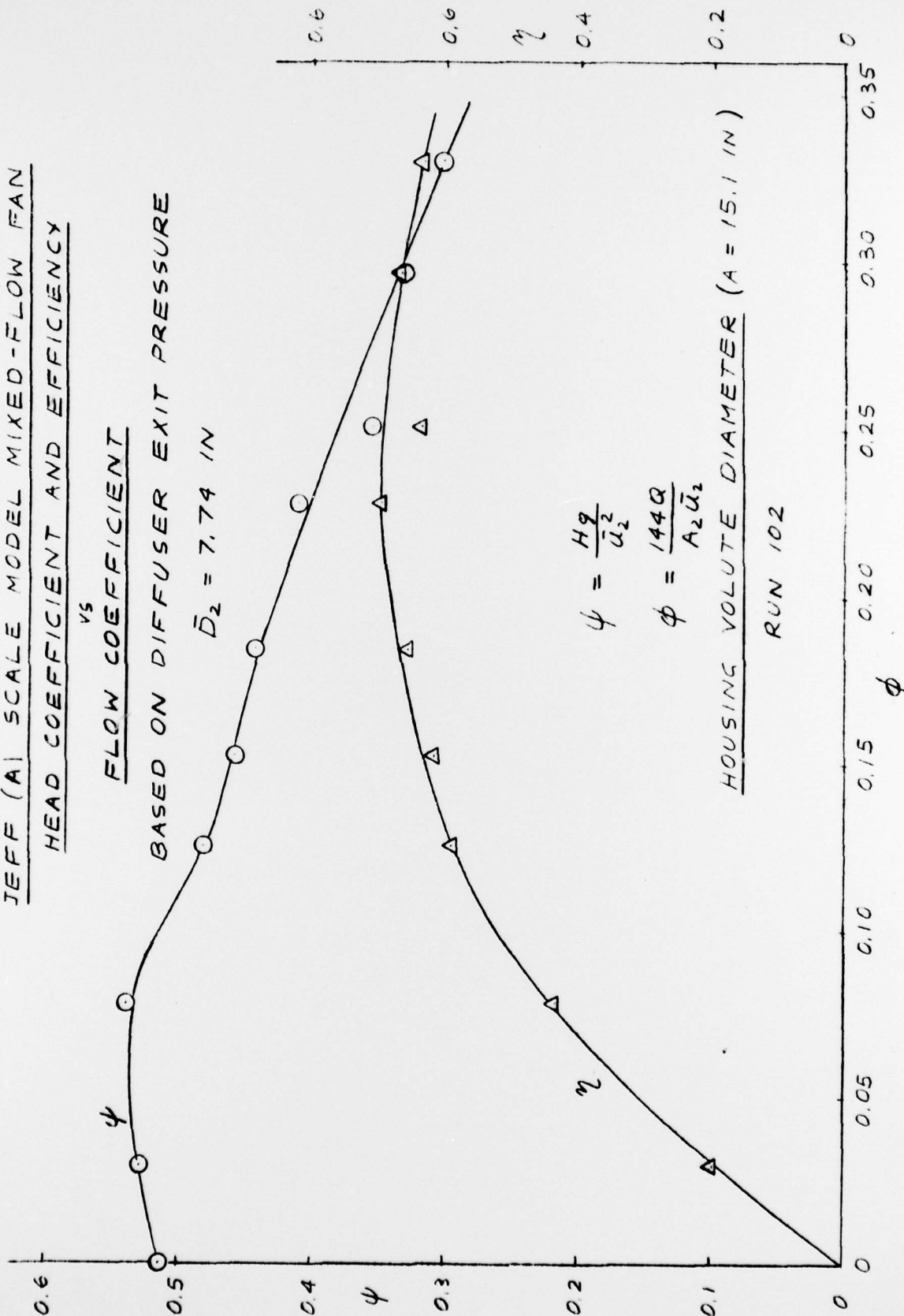
FIGURE 5.3.1-5

JEFF (A) SCALE MODEL MIXED-FLOW FAN
HEAD COEFFICIENT AND EFFICIENCY

vs
FLOW COEFFICIENT

BASED ON DIFFUSER EXIT PRESSURE

$\bar{D}_2 = 7.74$ IN



$$\psi = \frac{H_2}{\bar{u}_2^2}$$

$$\phi = \frac{144Q}{A_2 \bar{u}_2}$$

HOUSING VOLUTE DIAMETER ($A = 15.1$ IN)

RUN 102

FIGURE 5.3.2-1

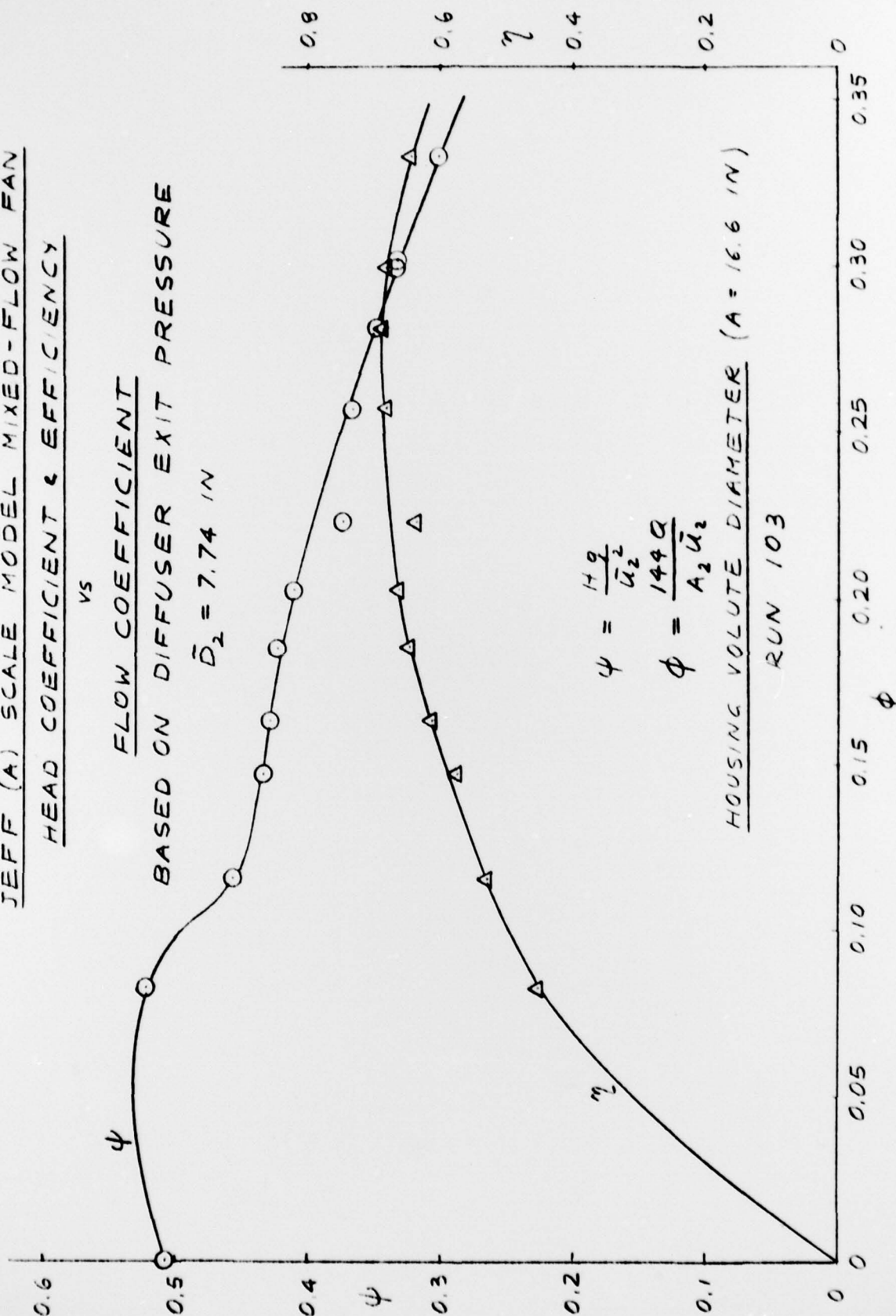
JEFF (A) SCALE MODEL MIXED-FLOW FAN
HEAD COEFFICIENT & EFFICIENCY

VS

FLOW COEFFICIENT

BASED ON DIFFUSER EXIT PRESSURE

$\bar{D}_2 = 7.74$ IN



$$\psi = \frac{H_2}{\bar{u}_2^2}$$

$$\phi = \frac{144Q}{A_2 \bar{u}_2}$$

HOUSING VOLUTE DIAMETER ($A = 16.6$ IN)

RUN 103

FIGURE 5.3.2-2

JEFF (A) SCALE MODEL MIXED-FLOW FAN
EFFECT OF HOUSING DIAMETER
ON FAN PERFORMANCE

$\bar{D}_2 = 7.74$ IN

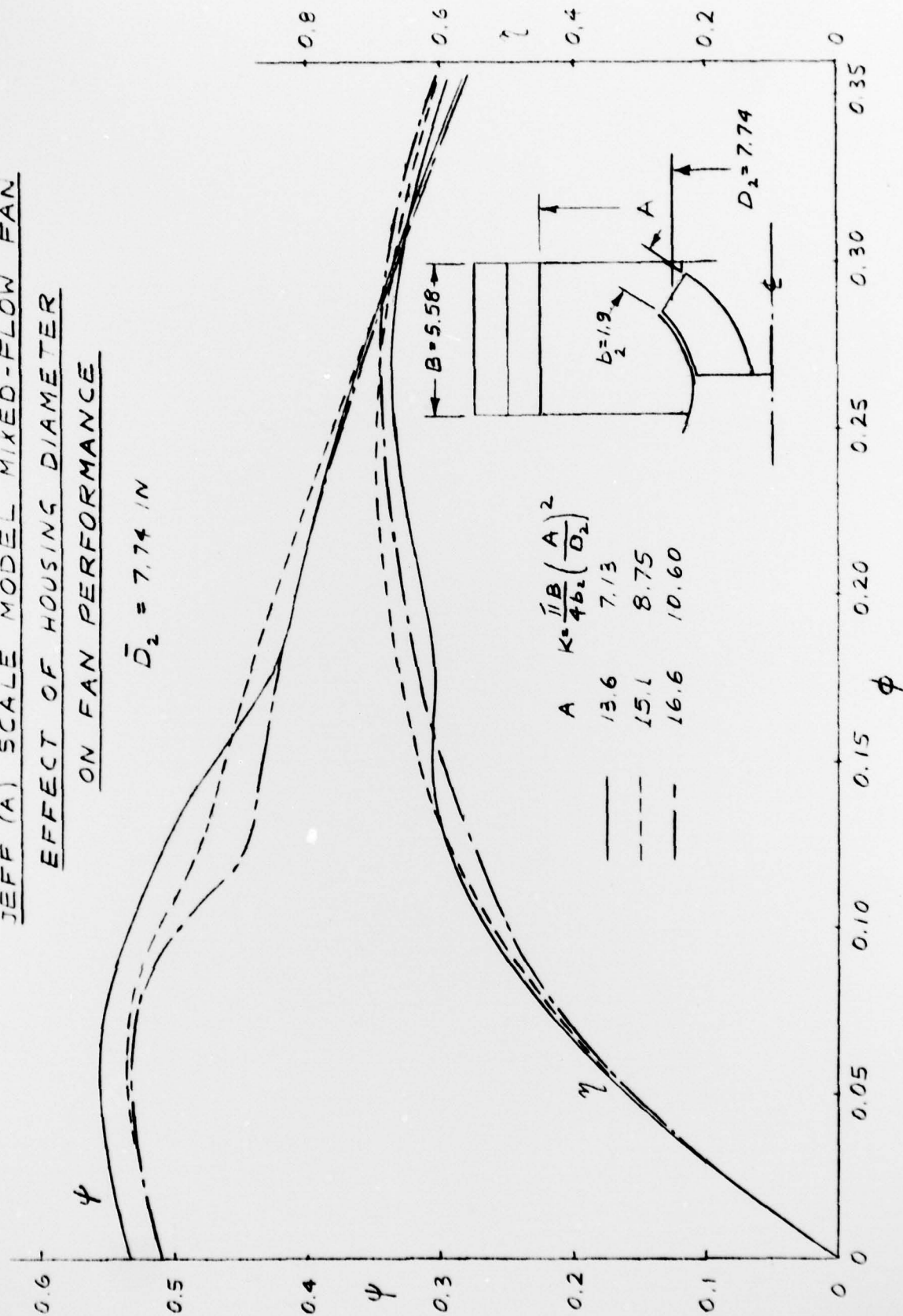
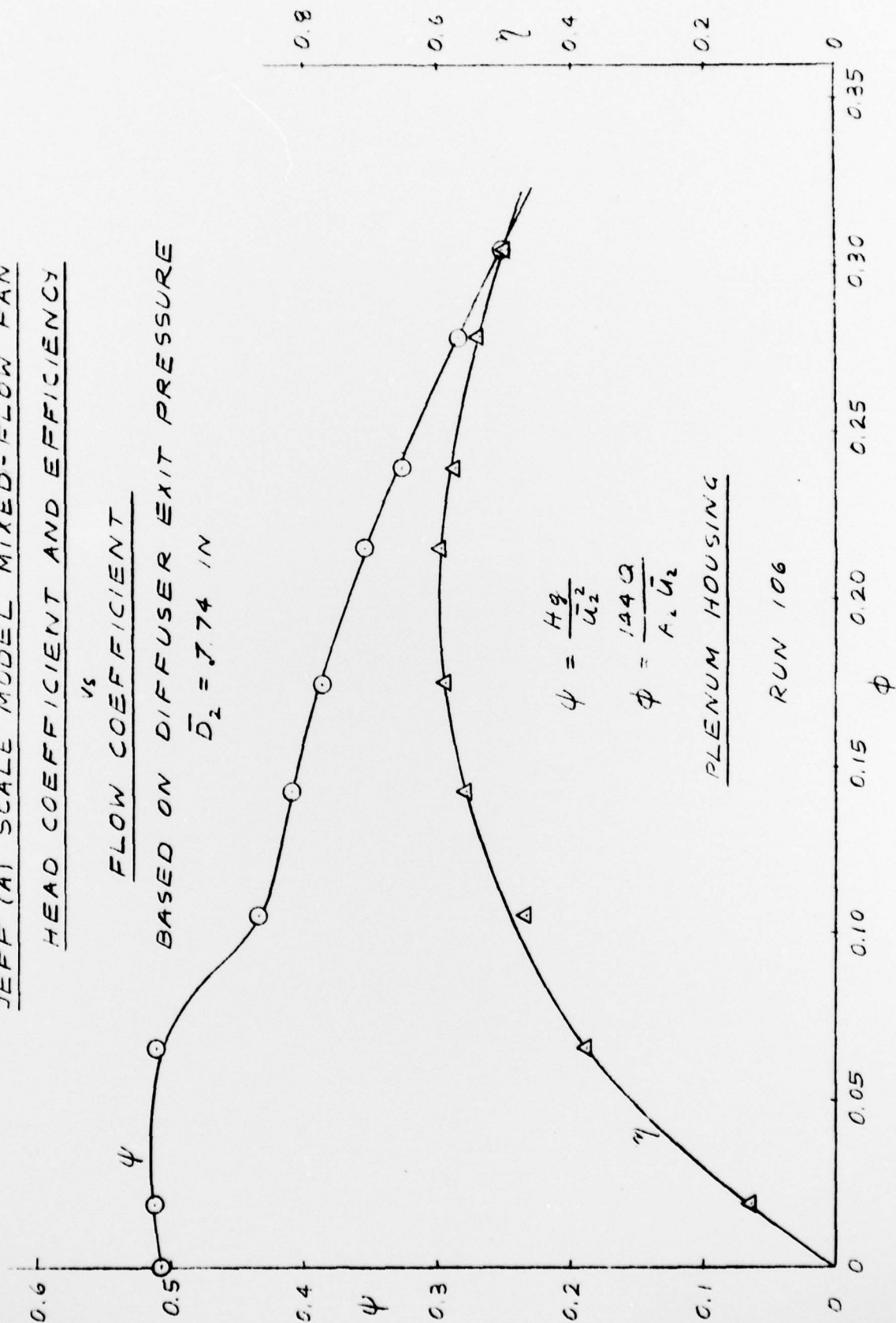


FIGURE 5.3.2-3

TABLE 8
EFFECT OF HOUSING SIZE ON FAN PERFORMANCE

	Baseline Housing	New Housing	Axial Increase		Radial Increase	
D_2 , IN	7.74	7.74	7.74	7.74	7.74	7.74
b_2 , IN	1.9	1.9	1.9	1.9	1.9	1.90
B, IN	5.58	5.58	6.67	7.76	5.58	5.58
A, IN	13.6	13.6	13.6	13.6	15.10	16.60
$K = \frac{\pi B}{4b_2} \left(\frac{A}{D_2} \right)^2$	7.13	7.13	8.52	9.91	8.75	10.60
$\psi_{\text{Shut Off}}$	0.549	0.531	0.522	0.516	0.515	0.507
$\phi_{\text{Max. Eff.}}$	0.225	0.259	0.232	0.227	0.228	0.282
$\psi_{\text{Max. Eff.}}$	0.439	0.371	0.405	0.392	0.411	0.349
η_{Max}	0.728	0.672	0.686	0.664	0.70	0.688
$\Delta \eta_1$ %		0	2.1	-1.2	4.2	2.4

JEFF (A) SCALE MODEL MIXED-FLOW FAN
 HEAD COEFFICIENT AND EFFICIENCY
 vs
 FLOW COEFFICIENT
 BASED ON DIFFUSER EXIT PRESSURE
 $\bar{D}_2 = 7.74$ IN



$$\psi = \frac{Hg}{\bar{u}_2^2}$$

$$\phi = \frac{144 Q}{A_2 \bar{u}_2}$$

PLENUM HOUSING

RUN 106

FIGURE 5.3.3-1

5. MODEL FAN PERFORMANCE (cont'd)

5.4 Predicted Performance of the Optimum Fan

Figure 5.4-1 shows the estimated performance of the optimum JEFF(A) Fan. The accomplishment of this performance will require refinements which are beyond the scope of the present investigation. The following aerodynamic improvements are necessary:

Rotor:

- a) Optimization of the blade leading edge angles.

Housing:

- a) Design of a volute housing symmetrically wrapped around the rotor exit.
- b) Matching of the volute to the rotor.
- c) Design of three dimensional exit diffuser.

JEFF (A) MIXED-FLOW FAN
PREDICTED OPTIMUM FAN PERFORMANCE

$P_a = 14.7 \text{ PSIA}$

$T_a = 100^\circ\text{F}$

$N = 2100 \text{ RPM}$

$\bar{D}_2 = 48.0 \text{ IN}$

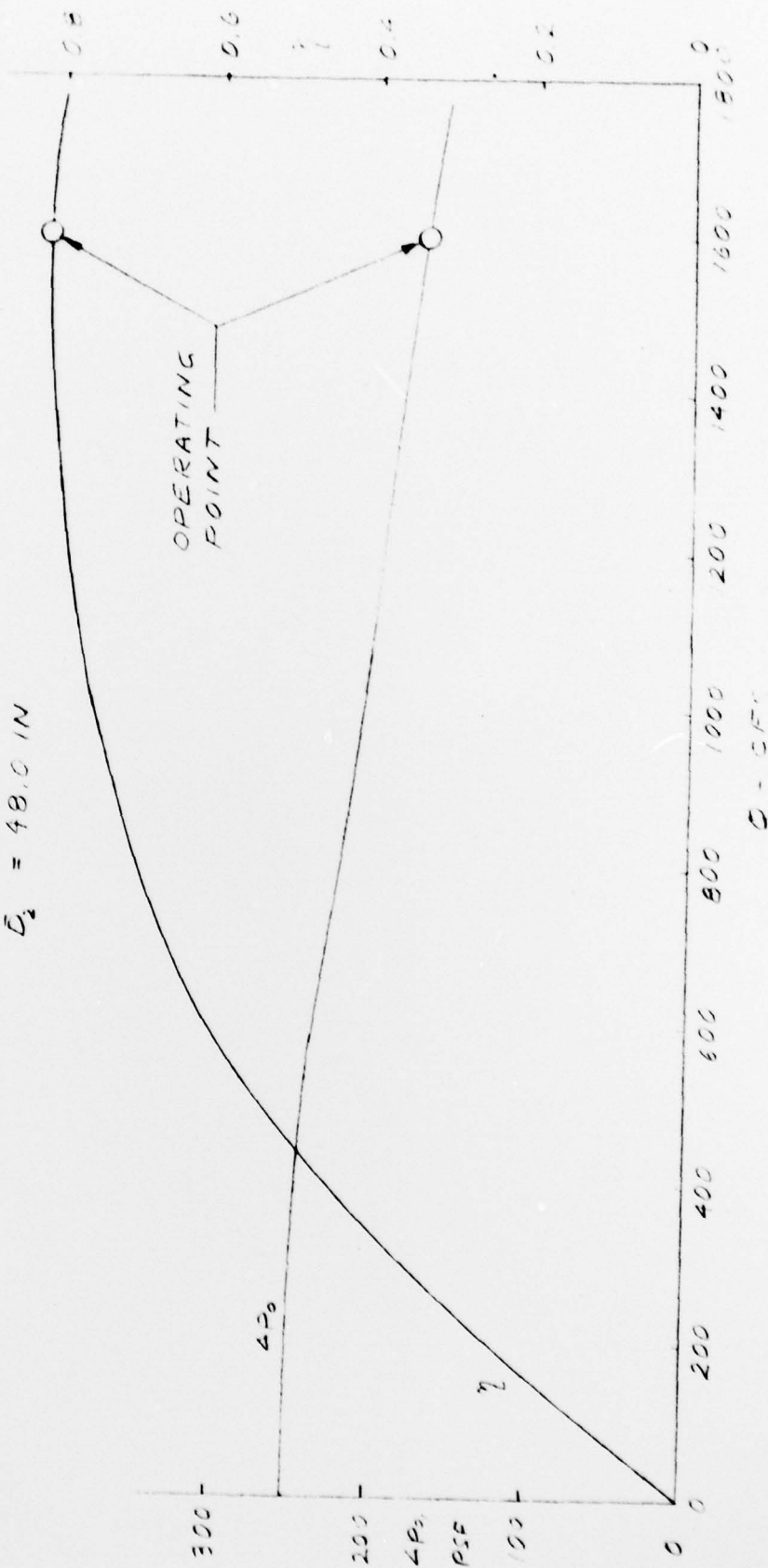


FIGURE 5.4-1

6. CONCLUSIONS

An experimental program was conducted for the purpose of improving the performance of a mixed flow lift fan for the JEFF(A) craft application. Conclusions regarding this investigation are as follows:

- 6.1 Rotor blade leading edge cut back can lead to an appreciable reduction of the fan peak efficiency.
- 6.2 Reduction of the rotor exit width reduced the fan efficiency at flow coefficients smaller than 0.28 and increased efficiency at higher flows. The head coefficient was higher over the entire flow range. Traverse data confirmed the presence of a wake near the outer shroud.
- 6.3 The rotor induces positive prerotation. At constant speed, positive prerotation is increased as the flow rate is reduced.
- 6.4 When guide vanes are placed in a neutral position, the prerotation is reduced and the incidence angle is increased.
- 6.5 Thick guide vanes produce wider variations in the tangential pre-whirl distribution than thin ones.
- 6.6 Fan performance is substantially the same with twisted guide vanes as with flat guide vanes.
- 6.7 An increase in housing axial width did not improve fan performance. The flow leaving the rotor follows the back wall and the increased housing volume is not fully utilized.
- 6.8 An increase of volute diameter from 13.6" to 15.1" improved fan efficiency by 4.2%.
- 6.9 Fan performance is drastically reduced when a plenum housing is substituted for a volute housing.

7. RECOMMENDED OPTIMUM FAN

The optimum mixed flow fan should have the following characteristics:

- 1) Zero incidence rotor blades.
- 2) Three-dimensional rotor blading designed to produce uniform pressure rise along all streamlines (twisted blades within structural limits).
- 3) Housing volute wrapped symmetrically around the rotor exit (not a rolled over volute).
- 4) Volute angle matched to the rotor exit absolute angle.
- 5) Three dimensional exit diffuser for maximum static pressure recovery.

8. REFERENCES

1. Aerodynamic Design and Model Testing of JEFF(A) Mixed-Flow Fan Rotor, Report Number 9752:0181, Contract N00024-71-C-0275, by S. A. Lorenc, Aerojet Liquid Rocket Company, Sacramento, California, March 1978.
2. JEFF(A) Scale Model Test Program - Lift Fan Performance Evaluation, Final Report, Report Number ALRC 9737-0621, by J. B. Stek, Aerojet Liquid Rocket Company, April 1977.
3. JEFF(A) Mixed Flow Model Lift Fan Performance Evaluation, Final Report, Report Number CDN 4357, Contract N00024-71-C-0275, by S. A. Lorenc, Aerojet Liquid Rocket Company, Sacramento, California, March 1978.
4. Fans, Design and Operation of Centrifugal, Axial-Flow and Cross-Flow Fans, by Dr.-Ing. Bruno Eck, Pergamon Press, 1972.

9. NOMENCLATURE

A	Area, Volute Diameter	IN ² , IN
B	Volute Axial Width	IN
b	Rotor Width	IN
D	Diameter	IN
g	Acceleration due to Gravity	FT/SEC ²
H	Head	FT
i	Incidence Angle	(o)
K	Housing Parameter = $\frac{\pi B}{4b_2} \left(\frac{A}{D_2} \right)^2$	
N	Rotational Speed	RPM
P	Pressure	PSF
ΔP	Pressure Rise	PSF
Q	Inlet Volume Flow	FT ³ /SEC
R	Radius	IN
R_e	Reynolds Number	-
T	Temperature	°F
U	Rotor Speed	FT/SEC
W	Relative Velocity	FT/SEC
α	Pre-whirl Angle (Measured from Axial Direction)	(o)
β	Blade Angle (Measured from Tangential Direction)	(o)
β'	Relative Flow Angle (Measured from Tangential Direction)	(o)
η	Total Efficiency	-
ϕ	Flow Coefficient, $144Q/A_2\bar{U}_2$	-
ψ	Head Coefficient, Hg/\bar{U}_2^2	-

SUBSCRIPTS

a	Atmospheric
T	Tip
0	Fan Inlet, Total Consitions
1	Rotor Inlet
2	Rotor Exit